

ENTATION PAGE

Form Approved
OMB No. 0704-0188

1a. REP UN		AD-A220 969		1b. RESTRICTIVE MARKINGS NONE	
2a. SEC		2b. DECLASSIFICATION/DOWNGRADING SCHEDULE		3. DISTRIBUTION/AVAILABILITY OF REPORT APPROVED FOR PUBLIC RELEASE; DISTRIBUTION UNLIMITED.	
4. PERFORMING ORGANIZATION REPORT NUMBER(S)		5. MONITORING ORGANIZATION REPORT NUMBER(S) AFIT/CI/CIA-90-003			
6a. NAME OF PERFORMING ORGANIZATION AFIT STUDENT AT University of Colorado		6b. OFFICE SYMBOL (If applicable)		7a. NAME OF MONITORING ORGANIZATION AFIT/CIA	
6c. ADDRESS (City, State, and ZIP Code)		7b. ADDRESS (City, State, and ZIP Code) Wright-Patterson AFB OH 45433-6583			
8a. NAME OF FUNDING/SPONSORING ORGANIZATION		8b. OFFICE SYMBOL (If applicable)		9. PROCUREMENT INSTRUMENT IDENTIFICATION NUMBER	
8c. ADDRESS (City, State, and ZIP Code)		10. SOURCE OF FUNDING NUMBERS			
		PROGRAM ELEMENT NO.		PROJECT NO.	TASK NO.
				WORK UNIT ACCESSION NO.	
11. TITLE (Include Security Classification) (UNCLASSIFIED) Understanding Troposcatter Propagation					
12. PERSONAL AUTHOR(S) Joseph J. Reynolds					
13a. TYPE OF REPORT THESIS/DISSERTATION		13b. TIME COVERED FROM TO		14. DATE OF REPORT (Year, Month, Day) 1990	
15. PAGE COUNT 245					
16. SUPPLEMENTARY NOTATION APPROVED FOR PUBLIC RELEASE IAW AFR 190-1 ERNEST A. HAYGOOD, 1st Lt, USAF Executive Officer, Civilian Institution Programs					
17. COSATI CODES			18. SUBJECT TERMS (Continue on reverse if necessary and identify by block number)		
FIELD	GROUP	SUB-GROUP			
19. ABSTRACT (Continue on reverse if necessary and identify by block number)					
<div style="text-align: center;">DTIC ELECTE APR 24 1990 S D D</div>					
90 04 23 070					
20. DISTRIBUTION/AVAILABILITY OF ABSTRACT <input checked="" type="checkbox"/> UNCLASSIFIED/UNLIMITED <input type="checkbox"/> SAME AS RPT. <input type="checkbox"/> DTIC USERS			21. ABSTRACT SECURITY CLASSIFICATION UNCLASSIFIED		
22a. NAME OF RESPONSIBLE INDIVIDUAL ERNEST A. HAYGOOD, 1st Lt, USAF			22b. TELEPHONE (Include Area Code) (513) 255-2259		22c. OFFICE SYMBOL AFIT/CI

UNDERSTANDING TROPOSCATTER PROPAGATION

by

JOSEPH HENDERSON REYNOLDS

B.S., United States Air Force Academy, 1982

A thesis submitted to the Faculty of the Graduate
School of the University of Colorado in partial
fulfillment of the requirements for the degree of
Master of Science

Program in Telecommunications

1990



Accession For	
NTIS CRA&I	
DTIC TAB	
Unannounced	
Justification	
By	
Distribution	
Avail	
Dist	
A-1	

RTOA: Capt Joseph H. Reynolds

14 Mar 1990

SUBJ: Thesis Abstract

TO: AFIT/CIRK (Capt Battles)

1. IAW AFITR 53-1 (1 Dec 1989), Para 7-7 the following is provided.

2. Abstract of thesis:

→ Although troposcatter communications systems suffer several shortcomings, this transmission scheme has found consistent use in several applications. This thesis discusses troposcatter propagation with emphasis on theory, characteristics, and prediction tools.

Theoretical understanding of the troposcatter propagation mechanism is rooted in atmospheric phenomena; specifically -- refractivity and turbulence. Two modes of transmission exist: *incoherent scatter*, if refractivity irregularities exist as turbulent blobs, and *quasi-coherent scatter*, if irregularities arrange themselves in layers. Frequency and meteorological parameters define the dominant mechanism.

One can expect received signal levels (RSL) to exhibit distance and frequency dependence; short and long-term fading; aperture-to-medium coupling loss; and diurnal, seasonal, climatic, and meteorological variations. Diversity techniques are indispensable in thwarting short-term fading. *Atmospheric multipath* is known to limit analog system bandwidths yet digital systems are prone to the related *delay spread* phenomenon which causes intersymbol interference (ISI). *Adaptive processing* is used to overcome this problem and can further improve digital performance through *implicit diversity*.

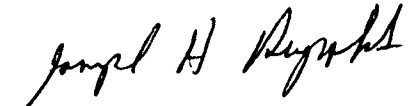
Most troposcatter prediction methods are rooted in empirical expressions. The laborious NBS Tech Note 101 method incorporates climatic variability and confidence measures. The CCIR methods offer simplicity as do the Yeh, Rider, Collins, and Bullington techniques. Unfortunately, all the methods suffer shortcomings with reliance on surface refractivity and incorrect coupling loss calculations topping the list. The computer based Parl method provides notable theoretical accuracy, yet cannot encompass a range of spectrum slope values. Accuracy can improve if tools such as the Parl or Radiometeorological Method effectively model gradient activity within the common volume.

3. Key information:

Author:	Joseph H. Reynolds
Thesis Title:	Understanding Troposcatter Propagation
Rank/Service Branch:	Capt, USAF
Date:	1990
Number of Pages:	245
Degree Awarded:	MS Telecommunications
University:	University of Colorado

90 04 23 070

4. See attachment 1 for an abbreviated bibliography; listed in attachment 1 are the sources used most often.


JOSEPH H. REYNOLDS, Capt, USAF
Student, AFIT/CIRK

ATTACHMENT 1: Abbreviated Bibliography

SPECIAL NOTE: The entire issue of *The Proceedings of the IRE*, vol. 43, no. 3 (March 1955) should be referenced.

Anthes, R.A., Cahir, J.J., Fraser A.B., and Panofsky, H.A. *The Atmosphere*. 3rd ed. Columbus, Ohio: Charles E. Merrill, 1981.

Boithias, L. *Radio Wave Propagation*. St. Louis: McGraw-Hill, 1987.

Booker, H.G., and Gordon, W.E. "A Theory of Radio Scattering in the Troposphere." *Proceedings of the IRE*, vol. 38, no. 4 (April 1950): 401-412.

Brauburger, G.H. Jr. (Capt, USAFR). "Meteorological Factors Affecting AN/TRC-97A Tropospheric Scatter Communications." Technical Report no. TACCA/XQT-TR-79-1, Langley AFB, Va, 1 August 1979.

CCIR. Volume V. *Propagation in Non-Ionized Media*. Dubrovnik, 1986.

Crane, R.K. "A Review of Transhorizon Propagation Phenomena." *Radio Science*, vol. 16, no. 5 (September-October 1981b): 649-669.

Crawford, A.B., Hogg, D.C., and Kummer W.H. "Studies in Tropospheric Propagation Beyond the Horizon." *The Bell System Technical Journal*, vol. 38, no. 5 (September 1959): 1067-1178.

du Castel, F. *Tropospheric Radiowave Propagation Beyond the Horizon*. New York: Pergamon, 1966.

Freeman, R.L. *Radio System Design for Telecommunications (1-100 GHz)*. New York: John Wiley & Sons, 1987.

Friis, H.T., Crawford, A.B., and Hogg, D.C. "A Reflection Theory for Propagation Beyond the Horizon." *The Bell System Technical Journal*, vol. XXXVI, no. 3 (May 1957): 627-644.

Hall, M.P.M. *Effects of the Troposphere on Radio Communication*. New York: Peter Peregrinus, 1979.

Military Handbook, Facility Design for Tropospheric Scatter (Transhorizon Microwave System Design). MIL-HDBK-417, Department of Defense, Washington, DC, 25 November, 1977. Available through Navy Publications and Forms Center, ATTN: NPODS, Office of Navy Publications, 5801 Tabor Avenue, Philadelphia, Pa., 19120-5094.

Monsen, P. "Fading Channel Communications." *IEEE Communications Magazine*, vol. 18, no. 1 (January 1980): 16-25.

- Monsen, P., Parl, S., Malaga, A., Tolman, S., and Fetteroll, J. *Digital Troposcatter Performance Model: Users Manual*. Lexington, Massachusetts: SIGNATRON, Inc. publication no. A288-15, November, 1983.
- Neiburger, M., Edinger, J.G., Bonner, W.D. *Understanding our Atmospheric Environment*. San Francisco: W.H. Freeman, 1973.
- Panter, P.F. *Communication Systems Design: Line-of-Sight and Tropo-Scatter Systems*. St. Louis: McGraw-Hill, 1972.
- Parl, S. A. "New Formulas for Tropospheric Scatter Path Loss." *Radio Science*, vol. 14, no. 1 (January-February 1979): 49-57.
- Rice, P.L., Longley, A.G., Norton, K.A., and Barsis, A.P. *Transmission Loss Predictions for Tropospheric Communication Circuits*. Vols. I and II. Rev. ed. U.S. Department of Commerce, National Bureau of Standards Technical Note 101. Washington: Superintendent of Documents, U.S. Government Printing Office, 1967.
- Roda, G. *Troposcatter Radio Links*. Norwood, Maine: Artech House, 1988.
- Sarkar, S.K., Dutta, H.N., and Reddy, B.M. "Development of a Prediction Technique for Tropo-Path Loss from Observed Transhorizon Propagation Characteristics over India." *Third International Conference on Antennas and Propagation (ICAP 83), Part 2: Propagation*, Institution of Electrical Engineers, London (1983): 229-232.

Memorandum: Estimated Thesis Expenses

Capt Joseph H. Reynolds
AFIT/CIRK
Student, University of Colorado
Telecommunications Program

The following is a conservative estimate of the money I used to complete my thesis "Understanding Troposcatter Propagation." I submit this in an effort to highlight the inadequate funding received during my program. I do not expect compensation; perhaps this can serve to justify future increases in allowances. Any item marked with an asterisk (*) indicates an estimate; in all cases, estimates are conservative.

Research Expenses

- Library Database Searches:	\$10.00*
- Travel (USAF Academy Library, US Dept of Commerce Library):	20.00*
- Copies of Journals/Publications:	70.00*
- Binders for Materials:	28.00
- Telephone Calls	36.00
- Postage	1.00

Preparation

- Computer Supplies (Paper, ribbons, floppys):	20.00
- Copies (drafts to committee, figures reduction):	60.00*
- MISC (softbinding, gluestick, staples, clips):	7.00

Defense

- Copies (Slide package):	4.00
- Transparencies (Overhead slides):	18.00
- Refreshments:	4.00

Submittal

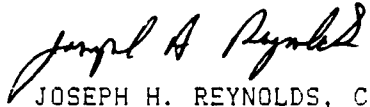
- Thesis Bond Paper:	44.00
- Copies	
-- On Thesis Bond (3 ea):	28.00
-- On Plain Bond (9 ea):	80.00
-- Binding	
--- Hardbound (2 ea):	34.00
--- Softbound (6 ea):	6.00
--- Ringed binder:	3.00
- Postage (4 copies distributed):	15.00*
- Graduate School Fees:	13.00

TOTAL COSTS

498.00

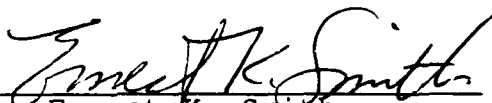
Again, I emphasize this as being quite conservative. Unfortunately I kept minimum records; regardless, I thought you might be interested. I estimate that about \$135 of the money spent could have been saved if I did not distribute copies to persons requesting them. However, since several of these persons provided substantial guidance, I felt

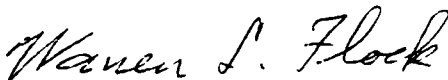
obligated. Notably, a similar breakout of book and supply costs would yield comparably high expenses.


A handwritten signature in cursive script, appearing to read "Joseph H. Reynolds".

JOSEPH H. REYNOLDS, Capt, USAF
AFIT/CIRK Student

This thesis for the Master of Science Degree by
Joseph Henderson Reynolds
has been approved for the
Program in
Telecommunications
by


Ernest K. Smith


Warren L. Flock


Samuel W. Maley

Date March 13, 1990

Reynolds, Joseph Henderson (M.S., Telecommunications)
Understanding Troposcatter Propagation
Thesis directed by Professor Ernest K. Smith

Early notions that troposcatter transmission could replace line-of-sight (LOS) communications links quickly diminished due to high costs, limited bandwidth, and the onset of satellite communications. Recently, however, digital processing schemes have reduced bandwidth concerns; furthermore, troposcatter systems have found consistent use in less developed countries and the military. This thesis discusses troposcatter propagation with emphasis on communications systems.

Theoretical understanding of the troposcatter propagation mechanism is rooted in atmospheric phenomena; specifically -- the index of refraction and turbulence. It is shown that turbulent eddies which encompass small-scale refractivity variations inhabit the *common volume*, an area defined by the intersection of antenna beamwidths. Further, these turbulent inhomogenities can arrange themselves as randomly disposed blobs or layers. This engenders the simultaneous existence of *incoherent scatter* and *quasi-coherent scatter* mechanisms, with the dominant mode contingent on frequency and meteorological

conditions. Additionally, diffraction may co-exist on shorter paths fostering multimode propagation.

One can expect received signal levels (RSL) to exhibit distance and frequency dependence; marked short and long-term fading; aperture-to-medium coupling loss; and diurnal, seasonal, climatic, and meteorological variations. Diversity techniques are indispensable in thwarting short-term fading.

Atmospheric multipath is known to limit analog system bandwidths yet digital systems are prone to the related *delay spread* phenomenon which causes intersymbol interference (ISI). *Adaptive processing* is used to overcome this problem and these processors also introduce *implicit diversity*, further improving digital performance.

Most troposcatter prediction methods are rooted in empirical expressions due to atmospheric unpredictability. The laborious NBS Tech Note 101 (TN 101) method, the standard for many years, incorporates climatic variability and confidence measures. The CCIR offers several simple techniques as do the methods of Yeh, Rider, Collins, and Bullington. Unfortunately, all the methods suffer shortcomings with reliance on surface refractivity and incorrect coupling loss calculations

topping the list. The computer based Parl method corrects these discrepancies, but cannot include known, real-time variations in the spectrum slope. Accuracy can improve if tools such as the Parl or Radiometeorological Method can effectively model gradient activity within the common volume.

CONTENTS

PREFACE	xv
CHAPTER	
1. INTRODUCTION	
1.1 A History of Troposcatter	
Propagation	1
1.2 A General Review of Troposcatter	
Systems	5
1.3 Path Geometry for Troposcatter	
Systems	13
1.4 Review of Thesis.	15
2. ATMOSPHERIC BASICS	
2.1 Introduction.	17
2.2 General Description of the	
Earth's Atmosphere.	18
2.2.1 The Composition of the	
Atmosphere.	21
2.2.2 The Structure of the Atmosphere .	24
2.3 The Radio Refractive Index.	28
2.3.1 Refractivity.	30
2.3.2 Refractivity Gradient	36
2.3.2.1 Effective Earth Radius.	36
2.3.2.2 Anomalous Propagation	38

2.3.3	Small Scale Changes in Refractivity.	42
2.3.4	Summary of Refraction	43
2.4	Turbulence.	44
2.4.1	The Causes of Turbulence.	45
2.4.2	A Refractivity Turbulence Model .	46
2.4.3	A Conclusion on Turbulence. . . .	47
2.5	Atmospheric Effects on Troposcatter Propagation.	48
2.5.1	Refraction.	51
2.5.2	Absorption.	54
2.5.3	Scattering.	59
2.5.4	Depolarization.	61
3.	TROPOSCATTER THEORY	
3.1	Introduction.	64
3.2	Turbulence Theories	67
3.3	Reflection Theories	72
3.4	Mode Theories	78
3.5	Other Theories.	81
3.6	Differentiating the Theories. . . .	83
3.7	Modern Theory	84
4.	CHARACTERISTICS OF TROPOSCATTER PROPAGATION	
4.1	Introduction.	92
4.2	Signal Level.	92
4.2.1	Distance Dependence	93

4.2.2	Frequency Dependence.	96
4.2.3	Fading.	100
4.2.3.1	Short-Term Fading	102
4.2.3.2	Long-Term Fading.	104
4.2.3.3	Frequency Selective Fading. . .	108
4.2.3.4	Diversity	109
4.2.4	Aperture-to-Medium Coupling Loss.	116
4.3	Multipath Delay Spread.	120
4.4	Bandwidth	129
4.5	Diurnal, Seasonal, Climatic, and Meteorological Variables.	134
4.5.1	Diurnal Variations.	136
4.5.2	Seasonal Variations	139
4.5.3	Meteorological Variations	142
4.5.3.1	Subrefraction	144
4.5.3.2	Super-Refraction.	145
5.	TROPOSCATTER PREDICTION TECHNIQUES	
5.1	Introduction.	149
5.2	Prediction Preparation.	150
5.3	Prediction Techniques	151
5.3.1	TN 101	154
5.3.2	CCIR Method I.	160
5.3.3	CCIR Method II	161
5.3.4	The CCIR Chinese Method.	163

5.3.5	The Radiometeorological Method .	164
5.3.6	The Parl Method.	166
5.3.7	The Yeh Method	170
5.3.8	The Rider Method	170
5.3.9	The Collins Method	171
5.3.10	The New Bullington Model	171
5.3.11	Digital Considerations	174
5.4	Comparisons of Methods.	176
5.5	Conclusions	183
BIBLIOGRAPHY.		185
APPENDIX		
A.	MULTIMODE PROPAGATION.	199
B.	THE SYSTEM EQUATION.	201
C.	THE SPECTRUM OF IRREGULARITIES	209
D.	DEPOLARIZATION	213
E.	THE REFLECTION COEFFICIENT	216
F.	CLIMATIC REGIONS	218

TABLES

Table

1. General Characteristics of a Troposcatter Communications System	8
2. Atmospheric Composition at Sea Level. . . .	23
3. Variation of N with Temperature and Relative Humidity (1000 mb)	33
4. Seasonal Variation Time Blocks.	140

FIGURES

Figure

1.	Troposcatter vs LOS	6
2.	Terrestrial transmission system domains . .	10
3.	Perspective of various transmission systems	11
4.	Transmission system bandwidth comparison. .	11
5.	Troposcatter path geometry.	13
6.	Pressure variations with altitude	20
7.	Atmospheric layers.	25
8.	Atmospheric temperature layers.	26
9.	Tropopause variations with latitude	27
10.	Refractivity profiles for model atmospheres	34
11.	World-wide values for N_0	35
12.	Ray bending at various K-factors.	37
13.	Refractive conditions leading to anomalous propagation events.	39
14.	Wave paths under various refractivity values for different earth models	39
15.	Spectrum of refractivity irregularities . .	46
16.	Troposcatter propagation causal framework .	49
17.	Effective earth radius factor, K, versus refractivity gradient	52

18.	Effective earth radius versus surface refractivity.	53
19.	Gaseous absorption.	56
20.	Combined oxygen and water vapor atmospheric absorption.	57
21.	Atmospheric absorption due to rain.	58
22.	Atmospheric absorption due to fog, mist and clouds.	58
23.	Absorption and scattering attenuation due to rain	58
24.	Single scatterer radiation pattern.	68
25.	Scattering by an individual blob.	69
26.	Scattering by a number of blobs	69
27.	Radiation pattern of a number of scatterers.	69
28.	du Castel's thin layer or feuillet.	74
29.	Specular and diffuse reflection within a feuillet.	76
30.	Radiation pattern for the reflection mechanism	76
31.	Mode theory propagation	79
32.	Various mode theory profiles matched with field data.	80
33.	Fading rates for UHF and SHF links over the same path	87
34.	Signal level variations for: (1) Coherent scatter, (2) Quasi-Coherent scatter, and (3) Incoherent scatter.	90
35.	Troposcatter loss with distance	93
36.	Scatter loss as a function of scattering angle	95

37.	The effect of frequency over similar paths	97
38.	Short-term effects of frequency	99
39.	Raleigh distribution showing short-term troposcatter fading amplitudes.	103
40.	RSL at different times for a 350 km, 300 MHz path.	106
41.	Log-normal density function for $\sigma = 8$ dB.	107
42.	Standard deviation, σ , varying with angular distance, θ	107
43.	Log-normal cumulative distribution function for various values of σ	108
44.	The diversity principle	110
45.	Diversity distribution curves	115
46.	Coupling loss	117
47.	Graphic method for coupling loss calculation	118
48.	Relative RSL comparison for antennas of different diameters for troposcatter links	120
49.	Delay scattering regions.	122
50.	Development of the delay power spectrum	123
51.	Delay spread profiles	128
52.	Useable bandwidth as a function of distance and antenna gain	130
53.	Distribution of bandwidths.	132
54.	Diurnal RSL and surface refractivity, N_s , variation	137
55.	Diurnal fading rates.	138
56.	Seasonal RSL, temperature, and surface refractivity variations	140

57.	Climate-variation factor as a function of effective distance and climate type	156
58.	Long term power fading for continental temperate climate	157
59.	The standard normal deviate	159
60.	Mean attenuation, overland path, temperate climate, 1 GHz.	162
61.	Collins method: Basic propagation loss at 1 GHz	172
62.	Collins method: Frequency correction curve	172
63.	Collins method: Horizon angle loss.	173
64.	Collins method: Coupling loss nomogram.	173
65.	Determination of BER for coherent BPSK and QPSK.	176
66.	Comparison of TN 101 (NBS) and the Parl (Turbulent Scatter) methods	182
67.	Comparison of the CCIR (1962 Data), TN 101 (Longley-Rice), and Bullington methods	182

PREFACE

When, as a Second Lieutenant in the U.S. Air Force, I arrived at my first duty assignment in a tactical communications unit, I entered during a difficult time. Not more than a week prior, the unit had failed an inspection; the cause -- failure of a troposcatter link to become operational. This unit had successfully installed this "tropo shot" on numerous occasions, but, during the inspection, the normally gentle Florida climate had turned cold. The unit, in turn, cited weather-oriented propagation effects as the culprit for substantially lower received signal levels (RSL) on this 50 mile, 5 GHz link. Additionally, it was noted that proximity to the coast, supplemented by several miles of overwater transmission, contributed to degraded performance. The inspection team did not buy this "excuse."

It was interesting to observe subsequent activity within the unit. As an unseasoned, unknowledgeable "contributor" I attempted to learn as much as I could about troposcatter since it provides the brunt of military, in-theater, tactical multichannel capability. Material was scarce; many

people I queried responded that "No one really knows how it works, but it works, and MIL-HNDBK 417 [*Military Handbook, Facility Design for Tropospheric Scatter*, 1977] is your tool in predicting performance." In the years following my 1982 commission I gained some familiarity with troposcatter, but the "No one really knows. . ." aspect remained unacceptable. Now, with the advantage of being a full-time graduate student under military funding, I am able to offer a condensed look at troposcatter, hopefully providing an understanding to anyone interested -- including Second Lieutenants.¹

This thesis discusses troposcatter propagation with emphasis on communications applications. A brief historical analysis along with a general description of troposcatter is provided in Chapter 1. Additionally, the rudiments of path geometry are given with emphasis on the *common volume* and *scattering angle*. Further discussion requires an understanding of atmospheric phenomena, especially

¹Concluding the story, during a delightfully mild week, my unit passed its follow-up inspection. The unit can take some consolation in the fact that weather can severely degrade propagation; however, from the inspector's point-of-view the mission was not accomplished, and a follow-up was necessary. Interestingly, my following assignment was to the same inspection team that had earlier failed my unit.

the *refractive index* and *turbulence*. As such, a quick tutorial covering these essentials is given in Chapter 2. With the basics established, discussion in the remaining chapters focuses on propagation theory, characteristics, and prediction.

By way of summary and to aid the reader in isolating areas of interest, the rest of this preface summarizes the essential areas of the remaining chapters.

Troposcatter systems allow intermediate range (40-500 mile), point-to-point, multichannel (commercial grade, 120 channels), high capacity (10 Mbps) communications. Although used for many years, an understanding of the mechanism causing propagation has only recently surfaced. Of the many theories presented in Chapter 3, the simultaneous occurrence of *incoherent scatter* and *quasi-coherent scatter* modes best explain the existence of the persistent, weak, beyond the horizon, troposcatter received fields. In addition, on shorter paths, diffraction becomes important and will exist in conjunction with the scatter mechanism in what is termed *multimode propagation*. Focusing on the scattering mechanism, the common volume is known to consist of turbulent refractive index irregularities which may arrange

themselves as randomly disposed blobs (incoherent scatter) or layers (quasi-coherent scatter) dependent on operating frequency or meteorological conditions.

Chapter 4 offers a lengthy discussion on the characteristics of troposcatter propagation. A quick synopsis of this chapter follows (with section numbers for easy reference):

- a. RSL VARIATIONS: (Section 4.2) Crucial in analog systems, the RSL predictably varies under the following conditions:
 - 1) Distance dependence (Section 4.2.1) is difficult to model due to the existence of several propagation mechanisms, generally 0.1 dB/km attenuation is used.
 - 2) Frequency dependence (Sections 4.2.2, 3.7) is known to obey an f^1 attenuation law up to about 3 GHz with greater attenuation beyond. Short-term attenuation variations may exhibit f^2 to $f^{-1/3}$ dependence.
 - 3) Short-Term Fading (Section 4.2.3.1), the "trademark" of troposcatter, is caused by atmospheric multipath and may occur at rates of a few per minute at VHF, 1 Hz at UHF, and several Hz at SHF. Amplitudes

closely follow a Raleigh distribution; losses of 8 dB can occur for 10% of the time.

- 4) Long-Term Fading (Section 4.2.3.2) due to gradient variations and changing mechanisms show log-normal amplitude distributions. Losses of 10 dB can occur for 10% of the time. Fading rates are discussed under SEASONAL and DIURNAL VARIATIONS.
- 5) Frequency Selective Fading (Sections 4.2.3.3, 4.3), not normally associated with RSL variations, will impact digital transmission schemes on analog subchannels if the correlation bandwidth is exceeded.
- 6) Diversity (Section 4.2.3.4) is an economical and essential approach to reducing the impact of short-term fading and may incorporate a variety of techniques. 7 dB gains, 50% of the time can be realized under *quad diversity*.
- 7) Aperture-to-Medium Coupling Loss (Section 4.2.4) occurs for high gain antennas when narrower beamwidths fail to encompass a

proportionate number of scatterers.

Losses of 6 dB are known to occur.

b. MULTIPATH DELAY SPREAD: (Section 4.3)

Provided a sufficient RSL is present, performance of digital troposcatter links is critically dependent on delay spread which may range in value from 50 to 370 ns. Due to atmospheric multipath, transmitted pulses will widen and this creates intersymbol interference. *Clever adaptive processing techniques exploit delay spread to realize implicit diversity.*

c. BANDWIDTH: (Section 4.4) Bandwidth is limited by atmospheric multipath which defines the correlation bandwidth in which uniform fading exists. A capacity of 4 MHz or 10 Mbps is typical. Narrow beam antennas will improve performance; however, coupling loss may offset this advantage. For digital systems using adaptive processing, bandwidth is less important than power (E_b/N_0) limitations.

d. DIURNAL, SEASONAL, CLIMATIC AND

METEOROLOGICAL VARIABLES: (Section 4.5)

Conditions may be such that case (a) the propagation mechanism changes, case (b) the

gradient changes slightly, or case (c) the gradient exhibits large-scale changes.

Diurnal and seasonal variations, with pronounced climatic dependency, or temporary meteorological conditions (weather) will foster such conditions. The result is either enhanced or degraded propagation.

- 1) Diurnal Variations (Section 4.5.1) can show daily 10 dB RSL swings in temperate zones. Fading rates are lowest in the afternoon; both case (a) and (b) situations are cited.
- 2) Seasonal Variations (Section 4.5.2) provide RSLs as much as 15 dB lower in the winter months for temperate climates; however, longer paths exhibit less seasonal influence. Case (b) situations, with emphasis on water vapor variability, are the cause.
- 3) Meteorological Variations (Section 4.5.3) are responsible for anomalous propagation events caused by case (c) conditions. Weather fronts, temperature inversions, subsidence, occlusions, and, sometimes, thunderstorms may signal the occurrence

of subrefraction, super-refraction, or ducting. Real-time prediction of RSL variation is difficult especially in areas where gradient data is unobtainable. Degradations may be short-lived, as with thunderstorms, or may persist for long (hours, days) periods if frontal movement is slow.

The final chapter, Chapter 5, briefly describes the tools available for troposcatter path predictions. A simple comparison is also offered. A summary follows:

a. PREDICTING RSLs: (Sections 5.2, 5.3, 5.4)

Assuming proper preparation, the engineer has a variety of prediction tools at his disposal; however, in nearly all cases, these techniques incorporate empirical, statistically-oriented data which injects some inaccuracy. Several methods take this into account through time availability and *service probability* confidence measures. The most commonly used methods, with descriptions, follow:

- 1) TN 101 (NBS Tech Note 101, Section 5.3.1)
is a lengthy, well-known document that

focuses on long term median path loss calculations for a variety of climates. Features include multimode calculations and confidence measures. The Longley-Rice method is a computerized version of this technique.

- 2) CCIR Methods (Sections 5.3.2, 5.3.3, 5.3.4) include Method I and the Chinese method (shortened versions of TN 101) and Method II, a graphical technique incorporating some climatic variability. All CCIR models are simple to use.
- 3) The Radiometeorological Method (Section 5.3.5) is an extremely accurate tool championed by Boithias and Battesti and well summarized in CCIR Reports 238-4 and 718-2. Despite great simplicity, it requires knowledge of the refractivity gradient within the common volume, a difficult to obtain parameter.
- 4) The Parl Method (Section 5.3.6) borrows from TN 101 yet offers more realistic predictions through computer flexibility. Whereas TN 101 is restricted to lower frequencies (less than 1 GHz), this

technique permits manipulation of the spectrum slope and climatic variables allowing application to virtually any configuration. Additionally, more accurate aperture-to-medium coupling loss calculations and analysis of digital modem performance is offered.

Unfortunately, modem analysis focuses on military systems only. The MITRE method, used for a specific military system, uses much of Parl's methodology.

- 5) Other Methods (Sections 5.3.7, 5.3.8, 5.3.9, 5.3.10) include those of Yeh, Rider, Collins, and Bullington.

Bullington's model is a new computerized version of Bullington's initial (1963) work in propagation theory. The remaining techniques are very simple with the Collins method providing surprising accuracy despite its totally graphical approach.

- 6) Digital Predictions (Section 5.3.11) will incorporate any discussed prediction tool for estimated path loss. In addition, calculation of delay spread and BER

performance is needed for complete
digital analysis

- b) SELECTING A PREDICTION TOOL: (Sections 5.4, 5.5) Every technique (excluding the Radiometeorological Method if accurate gradient data is available) admits to inaccuracy. Complete comparative analysis is unavailable; however, some techniques may appear more attractive due to simplicity. All CCIR methods, the Yeh, Rider, and Collins techniques provide this simplicity, yet computerized versions of TN 101, the Parl, and Bullington's models make the simplicity aspect less critical. With respect to conformity to theory, the Parl method stands out; TN 101 incorrectly emphasizes surface refractivity and a singular spectrum slope, CCIR Method I, the CCIR Chinese method, and Yeh and Rider's techniques also center on surface refractivity. The Collins method has limited application, CCIR Method II works best in temperate climates, and Bullington's treatment is untried and based, in part, on unaccepted mode theory. Finally, all methods calculating aperture-to-medium coupling loss

incorrectly assess this parameter with the exception of the Parl technique.

CHAPTER 1

INTRODUCTION

1.1 A History of Troposcatter Propagation

The discoveries of three different mechanisms for beyond the horizon propagation have prompted engineers to exploit associated capabilities and theorists to attempt explanations. Earth diffraction theory (ground wave), formulated in 1910, explained the suitability of MF and LF for intercontinental telegraphy systems. In 1927, cross-continent telephony at HF was accounted for by ionospheric reflection theory. Finally, since 1950, several hypotheses for the tropospheric forward scatter or *troposcatter* mechanism have endeavored to explain why transhorizon radio systems in the VHF, UHF, and SHF domains are possible [Sommerfeld, 1909; Boithias and Battesti, 1983, p. 657]. This thesis will explore the last mechanism, troposcatter.

It's probably no surprise that the first documented observance of unexpectedly high received signal levels beyond the horizon came from Guglielmo Marconi. In a series of experiments conducted

between 1928 and 1936, this radio pioneer "showed that microwaves could be reliably propagated to distances exceeding the optical range by two to three times" [Isted, 1958, p. 81]. His last paper (1933), "On the Propagation of Microwaves over Considerable Distances," summarized the results of one such experiment aboard the yacht *Elettra*. Marconi notes, "[t]he speculations that may arise from such results concern the entire theory of radio transmission over distances greater than the optical one" [Carroll 1956, p. 1057]. Earlier (1932), in a paper to the Royal Institution of Great Britain, he also observed:

In regard to the limited range of propagation of the microwaves, the last word has not yet been said. It has already been shown that they can round a portion of the earth's curvature, to distances greater than had been expected, and I cannot help reminding you that at the very moment when I first succeeded in proving that electric waves could be sent across the Atlantic Ocean in 1901, distinguished mathematicians were of the opinion that the distance of communications, by means of electric waves, would be limited to a distance of 165 miles [Wiesner, 1957, p. 46].

Unfortunately, several years passed before this phenomenon was further researched.

During the 1940's problems with high power UHF television and radar systems resurfaced Marconi's original observations; however, these unexpected signals were viewed more as a nuisance than a viable propagation method. TV frequency allocation plans,

based on Van Der Pol and Bremmer's 1937 smooth sphere predictions, proved inadequate due to interference caused by beyond the horizon propagation. This prompted the U.S. Government to "freeze" licensing of new television stations in 1949. Additionally, "[t]he advent of radar, which operated at higher frequencies and higher power, revealed the existence of reflections well beyond the horizon where the theory predicted that transmission was impossible" [Roda, 1988, p. 6]. This "nuisance factor" led several experimenters to further research short wave, transhorizon propagation.

Carroll [1952b, p. 7] delineates a few of the early experiments which highlighted short wave, beyond the horizon propagation research:

- a. Katzin's Caribbean experiments in 1945, performed to investigate ducting over water for wavelengths of 9 and 3 cm, also revealed unexpectedly high received signal levels beyond the horizon.
- b. In the Pacific (1946), the Naval Research Laboratory (NRL) group conducted tests similar to Katzin's and obtained similar results. A consequence of this endeavor was the first use of the term "scatter

region." Pekeris used this term to describe a distance of 30 miles beyond the horizon in which he concluded that propagation was due to a scattering mechanism.

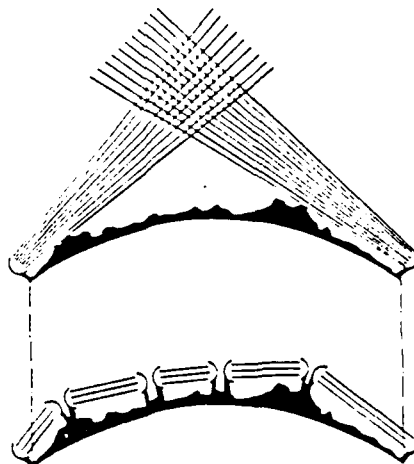
- c. During his 1949 experiment in Iowa, Gerks "reported measurements from a high power 400-mc transmitter at distances of around 100 miles, 50 db and more in excess of the $4/3$ -earth theoretical value." Conclusions again attributed the phenomenon to scatter.
- d. Megaw, the noted English researcher, made measurements of 10-cm received signals on a 370 mile link over the North Sea. He "interpreted the measurements as scattering by atmospheric turbulence."
- e. Finally, Bullington's 1950-51 tests at 500 and 3,700 mc in New Jersey showed consistent, useable signal levels over path lengths of several hundred miles. Bullington went further to predict available bandwidths of several megacycles fostering the idea of

reliable, short wave, beyond the horizon communications.

The benefits of this early research was far reaching. Experiments with troposcatter required high power transmitters, and, in conjunction with radar research, development of high power capabilities (klystrons) proceeded rapidly. Also, large, high gain antenna systems were needed, and engineers responded. A lot of credit for the initial development of troposcatter goes to the U.S. Air Force which, recognizing the benefits of troposcatter systems, provided the funding for the first active troposcatter system, *Polevault*, in 1952 [Gunther, 1966, p. 80]. These efforts also encouraged theoreticians to suggest a variety of explanations which dominated propagation research in the early 1950's. Theory will be discussed later; however, a general examination of troposcatter will justify the early enthusiasm for this new propagation mechanism.

1.2 A General Review of Troposcatter Systems

A quick glance at Figure 1 will help explain the initial excitement over troposcatter propagation. Simply, a troposcatter path is much longer than individual line of sight (LOS) radio paths. Roda [1988, p. 17] shows that this capability has several



Source: Rada, G. *Troposcatter Radio Links*.
Norwood, Maine: Artech House, 1988, p. 4.

Figure 1. Troposcatter vs LOS

advantages:

- a. The ability to "by-pass" inhospitable terrain to include mountains, jungles, bodies of water, marshes, swamps, and even politically sensitive regions.
- b. Reduction of the numbers of repeater sites.
- c. Lower overall costs in maintenance, buildings, access roads, spare parts, power access, and test equipment due to fewer sites.
- d. Frequency conservation due to fewer sites.
- e. Physical and information security enhancement. With less sites to defend, physical security is easier, and with

narrow antenna beams, the likelihood of signal interception is reduced.

Several applications of troposcatter systems logically follow [Aoda, 1988, p. 14; Freeman 1987, p. 139]:

- a. Connecting islands with one another and to the mainland.
- b. Military systems, both tactical (mobile systems in inhospitable terrain) and fixed (for example, a link into Berlin from West Germany).
- c. Connection to off-shore oil platforms.
- d. Commercial networking to sparsely populated areas where LOS repeater costs are unjustified.

Other, non-communications oriented applications of troposcatter propagation exist. For example, Barrow, et al. [1969] have used Rake techniques (a wideband signaling method used to reduce fading and resolve multipath effects) with troposcatter transmission to probe the scattering medium. Related applications are reported by Cox [1969, pp. 905, 916] to investigate atmospheric phenomena such as wind drift and random refractivity fluctuations. Finally, Crane [1981b, p. 649]

describes renewed interest in troposcatter for interference predictions (the "nuisance factor" remains); in light of the numerous transmission systems encompassing our world, all systems will encounter some scattering in the troposphere thus interfering with other systems.

Interest in troposcatter communications peaked in the early 1960's when satellite systems began to offer improved performance (mostly bandwidth and range) at less cost. Furthermore, individual troposcatter sites are more expensive than most alternatives while interference problems cannot (to a large degree) be constrained. The cost obstacle can best be explained by examining the general features of a troposcatter communications system as presented in Table 1.

Table 1. General Characteristics of a Troposcatter Communications System

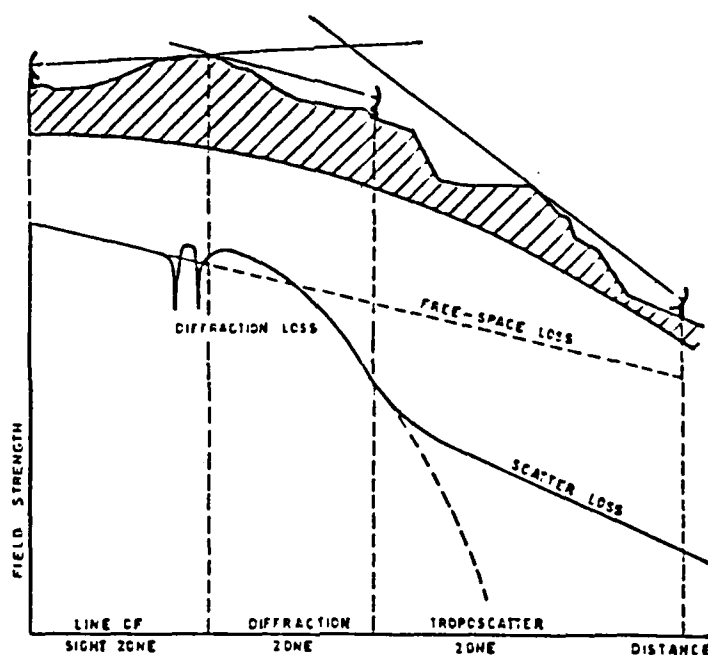
Very High Path Loss (180 - 260 dB)	
Very Sensitive Low Noise Receivers	
Severe Fading Effects	
VF Channels	< 120 (Commercial Grade)
Bit Rate	< 10 Mbps
Path Length	50 - 500 Miles
Transmit Power	100 - 50,000 Watts
Diversity	At Least Dual
Antenna Size/Gain	6 - 120 ft / 20 - 50 dB
Frequency Range	250 - 6,000 MHz

Adapted from *Freeman 1987, pp. 138; Roda, 1988 p. 8*

This table shows requirements for high power transmitters, large antennas (doubled if space diversity is used), and sensitive receivers all of which force extremely high costs. These costs, along with the emergence of satellite systems and insurmountable interference problems, thus engendered the demise of communications via troposcatter.

Several promising developments have, however, sparked some renewed interest in troposcatter communications. Adaptive signal processors on digital troposcatter systems have limited fading effects (multipath delay spread) to acceptable commercial quality. These modems, the "cornerstone" of digital troposcatter, have improved troposcatter capabilities to competitive levels; one such modem was tested on a military system with 15 MHz bandwidth at rates of 12.6 Mbps in 1980 [Monsen 1980, pp. 16,17]. Additionally, Crane [1988] demonstrated the feasibility of using higher frequencies (15 GHz) on troposcatter systems. While one might expect rain effects to limit capability, it was found that rain attenuation was insignificant while rain scatter actually improved performance. At these higher frequencies, required antenna sizes could be significantly reduced.

Aspects of troposcatter are summarized in Figures 2, 3, and 4. Figure 2 depicts the domains of



Source: Roda, G. *Troposcatter Radio Links*.
Norwood, Maine: Artech House, 1988, p. 3.

Figure 2. Terrestrial transmission system domains

the three terrestrial multichannel techniques: LOS, diffraction, and troposcatter. Interestingly, both diffraction and troposcatter can occur simultaneously in *multimode* propagation. This effect is explained further in Appendix A; however, while Figure 2 shows troposcatter loss significantly exceeding that of free space, useable signals are receivable. Figure 3 places troposcatter in perspective with other transmission modes (single hop), while Figure 4 provides bandwidth comparisons.

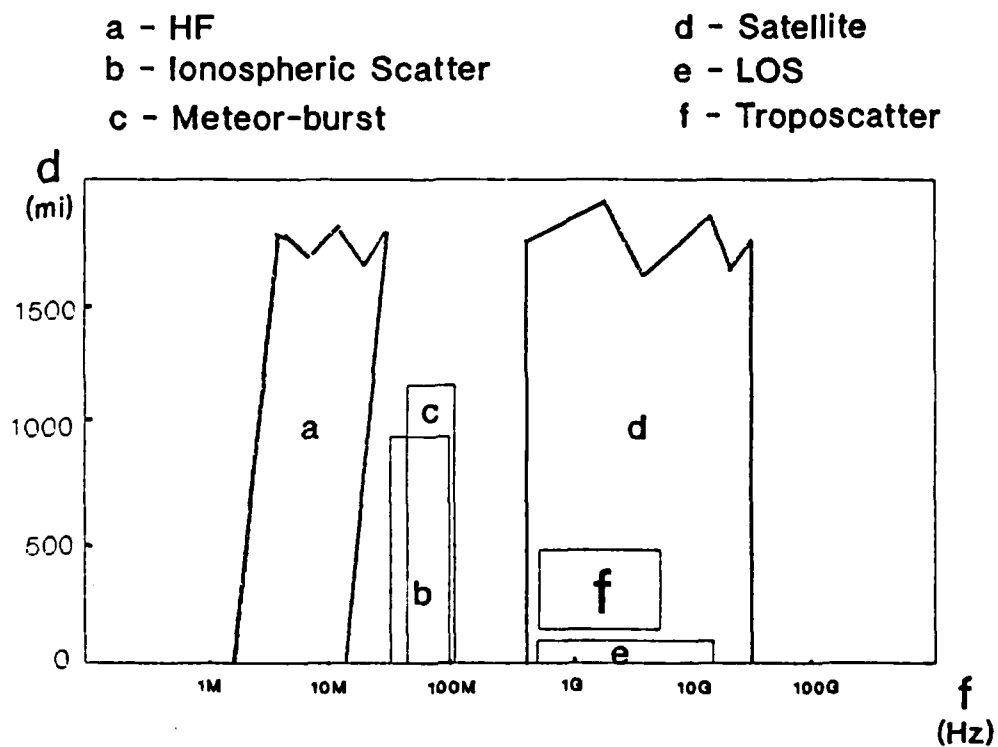


Figure 3. Perspective of various transmission systems

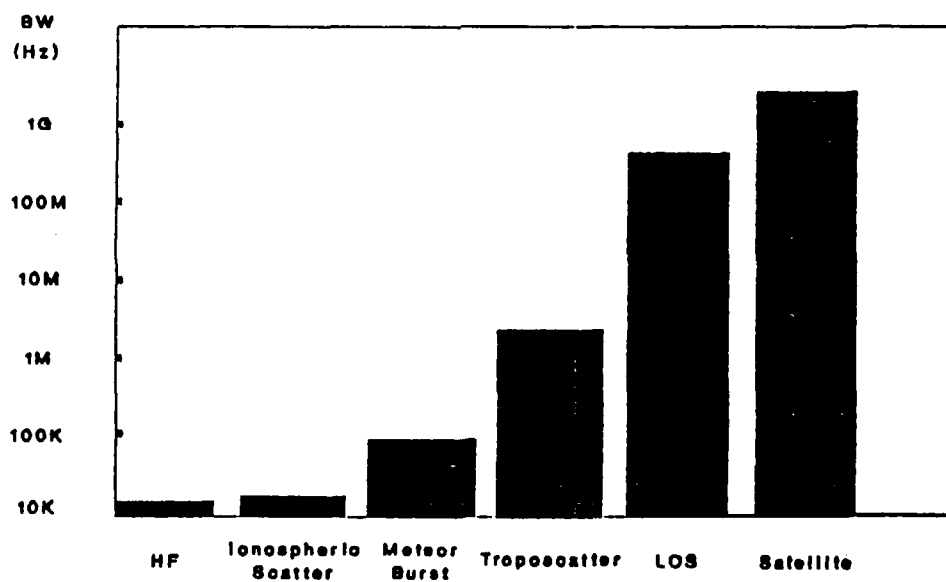


Figure 4. Transmission system bandwidth comparison

Satellite transmission offers clear advantages with respect to range, bandwidth, and area coverage (hence, not limited to point to point modes); however, costs can be prohibitive. Meteor-burst, riding on the crest of sophisticated digital technology, has experienced renewed interest, but erratic transmission bursts makes it unsuitable for voice transmission [Weitzen, 1988, p. 1813]. The nearly saturated spectrum, limited bandwidth, and aberrant performance of HF systems disqualify them as a steady, multichannel performer. Additionally, ionospheric scatter techniques suffer similar bandwidth and degradation characteristics. Finally, while offering high bandwidth, LOS systems incorporate numerous repeater sites fostering possibly higher overall costs.

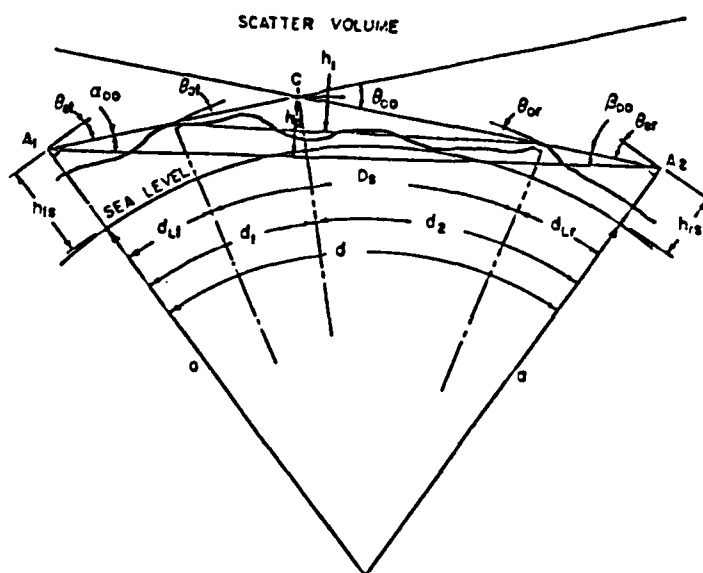
It can be seen, therefore, that troposcatter communications provides unique capabilities in certain situations. Military tactical networks still rely heavily on troposcatter due to its ability to circumvent inhospitable and/or hostile areas and as a means to conserve limited radio resources.¹ The oil

¹It should be noted that military tactical troposcatter provides connectivity within the theater of operation; however, connectivity to "the rest of the world" is achieved mostly through tactical multichannel SHF satellite terminals.

industry and less developed countries, which don't need extremely high capacity systems, also find troposcatter economically attractive. Undoubtedly, troposcatter will continue to occupy a necessary niche in transmission system selection, yet it is not the miracle transmission scheme as initially thought.

1.3 Path Geometry for Troposcatter Systems

An introduction to the path geometry for troposcatter systems will aid in later discussion. Figure 5 shows this geometry which can be broken down into a few key elements. Most critical is θ , angular



Source: Rice, P.L., Longley, A.G., Norton, K.A., and Baris, A.P. *Transmission Loss Predictions for Tropospheric Communication Circuits*. Vols. I and II. Rev. ed. U.S. Department of Commerce, National Bureau of Standards Technical Note 101. Washington: Superintendent of Documents, U.S. Government Printing Office, 1967, p. 6-8.

Figure 5. Troposcatter path geometry

distance, which is simply "the angle between horizon rays in the great circle plane, and is the minimum diffraction angle or scattering angle unless antenna beams are elevated" [Rice, P.L., et al., 1967, Vol 1, p. 6-5]. Relationships for θ follow:

$$\theta = \theta_{oo} = d/a + \theta_{et} + \theta_{er}, \quad (1-1)$$

where θ_{et} and θ_{er} are the transmitter's and receiver's horizon elevation angles respectively.

Also,

$$\theta_{oo} = D_s/a + \theta_{ot} + \theta_{or}, \quad (1-2)$$

with θ_{or} and θ_{ot} being "[t]he angular elevation of a horizon ray at the receiver or transmitter horizon" [Rice, P.L., et al., 1967, Vol 1, p. 12-10]. Note the influence of obstacles. A basic rule is that the smaller the scattering angle, the better the received signal; therefore, when performing path profiles, engineers choose sites (if that much flexibility is given) which avoid path obstacles. Otherwise, antenna elevations and, subsequently, scattering angle values will increase.

The other crucial element, the scatter or common volume, is related to the scattering angle. The smaller the scattering angle, the larger the

common volume. This region describes the location of the scattering mechanism which allows troposcatter propagation; logically, then, a large common volume contains more scatterers. Although larger common volumes typify enhanced signal levels, degraded bandwidth performance somewhat limits the benefits of large volumes. This characteristic, along with several others are discussed later.

1.4 Review of Thesis

The remainder of this treatment will focus on troposcatter propagation with emphasis on communications systems. (Attention will be on pure troposcatter; however, some discussion of multimode propagation is appropriate.) Specifically, the theory behind the propagation mechanism, the characteristics of troposcattered radiowaves, and the prediction tools used to assess troposcatter systems will be analyzed. The purpose is to provide a consolidated, simple description of radio communications via the troposcatter mode emphasizing "how it works" and "what one can expect" when using these systems.

The characteristics of the atmosphere are responsible for troposcatter propagation; therefore, Chapter 2 describes the earth's atmosphere and

analyzes its effects on radiowave propagation. Focus will be on the troposphere with emphasis on the refractive index and turbulence. Additionally, natural atmospheric phenomena ("causes") will be married with propagation phenomena ("effects") to describe the cause and effect ("causal") nature of the atmosphere on radiowave propagation.

In Chapter 3 an analysis of theory is offered. Provided are descriptions of the various theories developed over the past 40 years to explain the mechanism(s) behind consistent received signal levels far beyond the horizon at short waves.

The various characteristics of troposcatter transmissions are given in Chapter 4. Focus will be on performance parameters of interest to communications engineers that are directly influenced by propagation; equipment will be discussed when enhancements improve propagation performance.

Chapter 5, the final chapter, will describe the prediction tools available to determine the feasibility of planned links to support communications requirements. A comparison and criticism of the more common techniques will be provided.

CHAPTER 2

ATMOSPHERIC BASICS

2.1 Introduction

As radio technology continues to unveil remarkably sophisticated devices, no innovation has yet provided complete immunity to the effects of our atmosphere. Troposcatter systems are particularly susceptible to this uncontrollable medium, housed entirely in the most violent of atmospheric layers, the troposphere. While other external sources can influence radiowave propagation, "[p]oint-to-point transhorizon links are usually designed for high-gain antennas with relatively narrow beams, which are removed from terrain clutter by at least several wavelengths" [*Military Handbook*, 1977, p. 4-109]. The atmosphere then is the critical external parameter effecting troposcatter propagation; Appendix B further substantiates this assertion.

The atmosphere can be considered as simply a transmitting medium for radiowaves, much like a coaxial cable is the transmitting medium for cable TV.

An electromagnetic wave launched into a transmitting medium may change in intensity, phase, direction, or polarization in its passage. These changes are caused by and are characteristic of the medium through which the waves travel; media such as liquid, gases, solids, and aerosols produce a variety of effects [Derr, 1972, 9-1].

The above summary further highlights the need to understand our atmosphere when considering troposcatter systems. This chapter provides this basic understanding and further describes the atmosphere's general effects on radiowave propagation.

2.2 General Description of the Earth's Atmosphere

The parameters of the earth's atmosphere are determined through a variety of methods. The simplest are surface observations made by meteorologists. "By international agreement these observations are made simultaneously [synoptically], using procedures that meet uniform standards of accuracy" [Neiburger, Edinger, and Bonner, 1973, p. 10]. A more sophisticated method is the *radiosonde* which is a balloon launched instrument package containing pressure, temperature, and humidity sensors. A radio transmitter is also included to transmit information and provide tracking information for wind motion measurements. Radiosonde measurements are also made synoptically; however, the

cost of these packages inhibit worldwide coverage [Anthes, et al., 1981, p. 38].

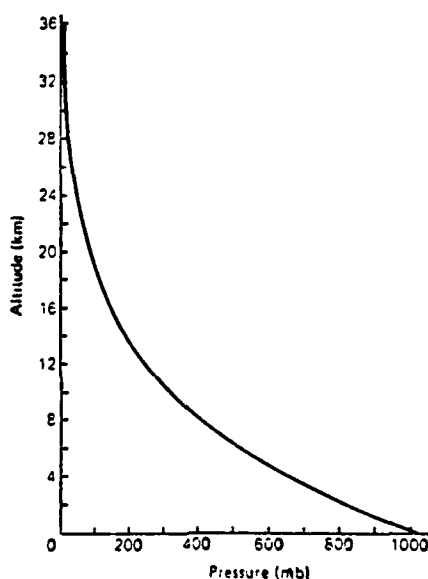
Ground and space-based remote sensors top the list of sophisticated atmospheric research tools, and can be operated in either passive or active modes. "[P]assive systems monitor radiation emitted by the atmosphere in the infrared, microwave, or visible portions of the spectrum" [Anthes, et al., 1981, p. 42]. These devices can measure, among other things, temperature layers and gaseous distributions. Active remote sensors emit electromagnetic energy for which the

direction of propagation is altered by the atmosphere. It may be scattered back toward the source (back scatter) or scattered ahead (forward scatter). In either case, the characteristics of the scattered signal provide information about the part of the atmosphere through which the signal is passing. This information may include the intensity of turbulence, the lapse rate, and the mean wind velocity [Anthes, et al., 1981, p. 40].

Lidar, radar, and sodar are the more common active remote sensors with lidar using laser beams, radar operating in the microwave range, and sodar using acoustic sounding techniques [Anthes, et al., 1981, pp. 40, 41].

Terminology commonly used to describe the atmosphere are temperature, pressure, and humidity. While temperature measurements are easily understood,

pressure measures the atmospheric force exerted per unit area on the surface of the earth. Units can be in inches of mercury (Hg) or millibars (mb) with 1 inch Hg equal to 33.86 mb [Anthes, et al., 1981, p. 29]. Figure 6 shows pressure variations with altitude. If expressed in miles, these variations



Source: Lutgens, F.K., and Tarbuck, E.J. *The Atmosphere: An Introduction to Meteorology*. 2nd ed. Englewood Cliffs, New Jersey: Prentice-Hall, 1982, p. 13.

Figure 6. Pressure variations with altitude

follow a general rule up to about 60 miles: 1000 mb at sea level, 100 mb at 10 miles, 10 mb at 20 miles, etc [Anthes, et al., 1981, p. 55].

Humidity measures the water vapor content in air and comes in a variety of forms:

Absolute humidity is stated as the weight of water vapor in a given volume of air [g/m^3].

Specific humidity is expressed as the weight of water vapor per weight of a chosen mass of air [g/kg]. *[R]elative humidity* is the ratio of the air's water vapor content to its water vapor capacity at a given temperature [%] [Lutgens and Tarbuck, 1982, pp. 75,76; italics not mine].

Of the three humidity measures, relative humidity is probably the most familiar, yet is easily misunderstood.

Relative humidity reaches 100% when the air is saturated. Saturation occurs at a particular temperature when water vapor content is the maximum that a parcel of air can support. If the relative humidity is less than 100%, the *dew point* "is the temperature to which a parcel of air would have to be cooled in order to reach saturation" [Lutgens and Tarbuck, 1982, p. 77]. Additionally, if rain occurs in an unsaturated region, the air cools as energy is used to evaporate the rain. The *wet-bulb temperature* occurs when evaporation ceases and the air is saturated (100% relative humidity) [Anthes, et al., 1981, p. 29].

2.2.1 The Composition of the Atmosphere

The culmination of atmospheric measurements provides an understanding of the structure and composition of the atmosphere. In general terms, the atmosphere is a thin, gaseous envelope that surrounds the earth and is held in place by gravity. Its

density decreases with height; 90% of its mass is contained in approximately the first 20 km of height while 99.9% resides within the 50 km level [Iribarne and Cho, 1980, p. 1].

Table 2 shows the composition of clean, dry air at sea level. Interestingly, up to about 100 km, this composition is nearly the same anywhere in the world [Neiburger, Edinger and Bonner, 1973, p. 24]. Additionally, the region below about 100 km is called the *homosphere* since its chemical composition remains virtually constant, while the *heterosphere*, above 100 km, exhibits varying composition [Iribarne and Cho, 1980, p.5].

Items marked with cross on Table 2 are

variable constituents introduced by biological activities and industrial processes. . . . [which have] deleterious effects even when present in concentrations as low as one part per million or less [Neiburger, Edinger and Bonner, 1973, p. 26].

Notably, there is some alarm concerning several of these variables. Khalil and Rasmussen [1988] report doubled CO concentrations since pre-industrial times and warn of increased tropospheric O₃ leading to detrimental climate changes. Volz and Kley [1988] and Penkett [1988] substantiate the increase of tropospheric O₃. Other potential disturbances such as depletion of the critical UV blocking ozone layer

Table 2. Atmospheric Composition at Sea Level

Constituent gas and formula	Content, percent by volume	Content variable relative to its normal	Molecular weight*
Nitrogen (N ₂)	78.084	—	28.0134
Oxygen (O ₂)	20.9476	—	31.9988
Argon (Ar)	0.934	—	39.948
Carbon dioxide (CO ₂)	0.0314	†	44.00995
Neon (Ne)	0.001818	—	20.183
Helium (He)	0.000524	—	4.0026
Krypton (Kr)	0.000114	—	83.80
Xenon (Xe)	0.0000087	—	131.30
Hydrogen (H ₂)	0.00005	?	2.01594
Methane (CH ₄)	0.0002	†	16.04303
Nitrous oxide (N ₂ O)	0.00005	—	44.0128
Ozone (O ₃)	Summer: 0 to 0.000007	†	47.9982
	Winter: 0 to 0.000002	†	47.9982
Sulfur dioxide (SO ₂)	0 to 0.0001	†	64.0628
Nitrogen dioxide (NO ₂)	0 to 0.000002	†	46.0055
Ammonia (NH ₃)	0 to trace	†	17.03061
Carbon monoxide (CO)	0 to trace	†	28.01055
Iodine (I ₂)	0 to 0.000001	†	253.8088

* The content of the gases marked with an asterisk may undergo significant variations from time to time or from place to place relative to the normal indicated for those gases.
From the U.S. Standard Atmosphere, 1962

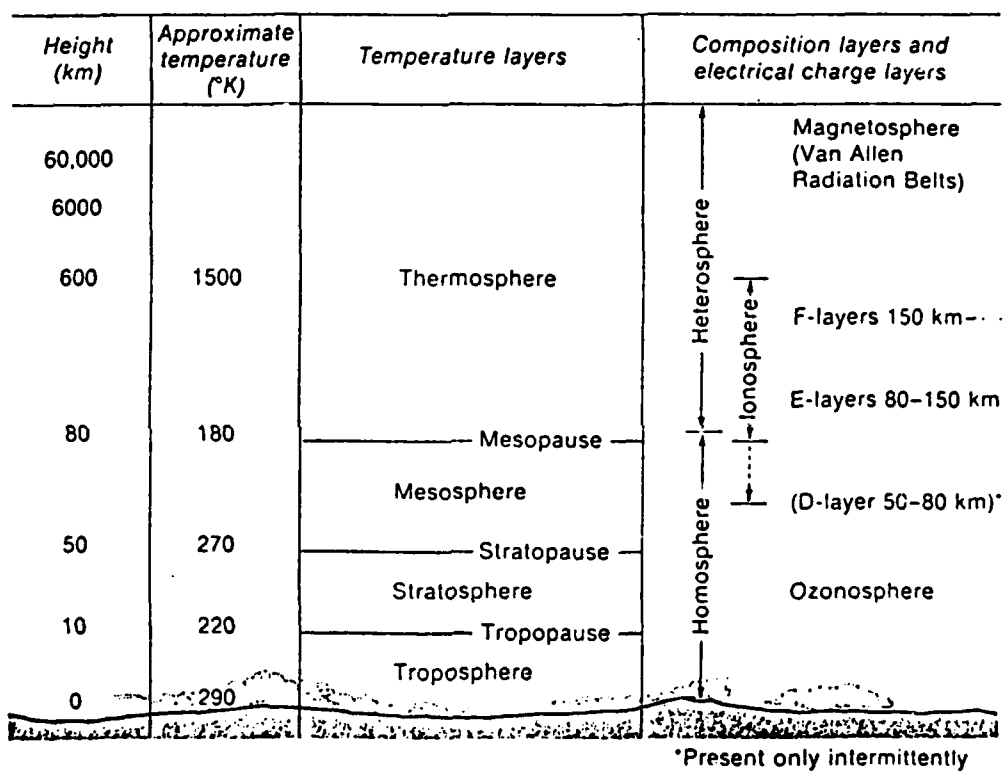
Source: Derr, V.E. *Remote Sensing of the Troposphere*. U.S. Department of Commerce, National Oceanic and Atmospheric Administration, Environmental Research Laboratories, and the University of Colorado. Washington: Superintendent of Documents, U.S. Government Printing Office, August 15, 1972, p. 1-2.

as well as acid rain have been noted; furthermore, "modification of the radiative properties of the atmosphere" justify consideration from a wide spectrum of professions [*Global Tropospheric Chemistry*, 1984, p. 8].

Derr [1972, pp. 1-2, 1-3] notes that not listed in Table 2, yet meriting mention, are water vapor, hydrometeor, and aerosol constituents. Water vapor's absolute humidity rarely exceeds about 25 g/m³ compared to normal dry air density of 1000 g/m³. However, while small in contribution, water vapor is the most important and most variable atmospheric component. Its ability to change states within the atmosphere (gas to liquid) produces *hydrometeors* (hail, snow, and rain). Finally, "[a]erosols are particulate matter suspended or slowly falling in the gaseous mixture of the atmosphere" [Derr, 1972, p. 1-3]. Aerosols are differentiated from hydrometeors in both content and size. Examples of aerosols include haze, clouds, and smoke all whose droplet radius sizes are less than 1 micron.

2.2.2 The Structure of the Atmosphere

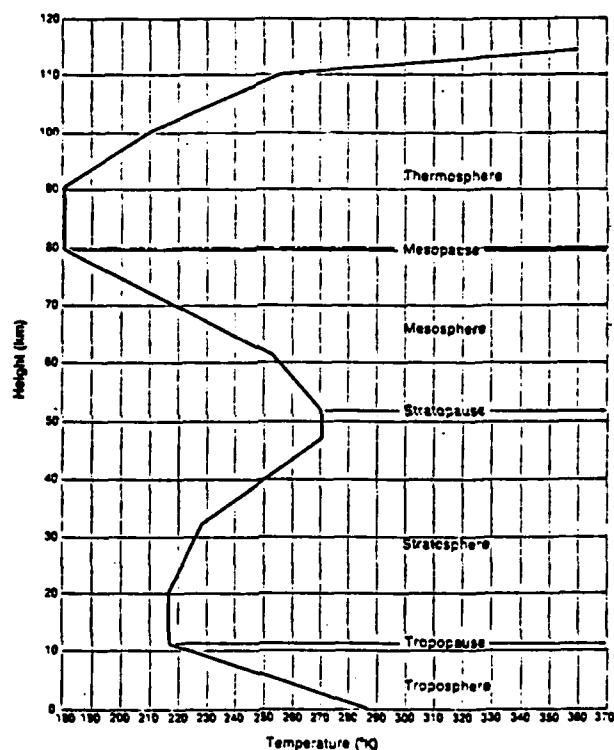
The atmosphere's structure, Figure 7, is layered to reflect its physical characteristics. The homosphere and heterosphere, mentioned earlier,



Source: Neiburger, M., Edinger, J.G., Bonner, W.D.
Understanding our Atmospheric Environment. San Francisco: W.H. Freeman,
 1973, p. 28.

Figure 7. Atmospheric layers

divide chemical composition features. The ionosphere is layered to show significant levels of electron content. Finally, temperature layers, more accurately depicted in Figure 8, relate significant temperature transitions (transitions occur at layers ending in -pause). One might expect steadily



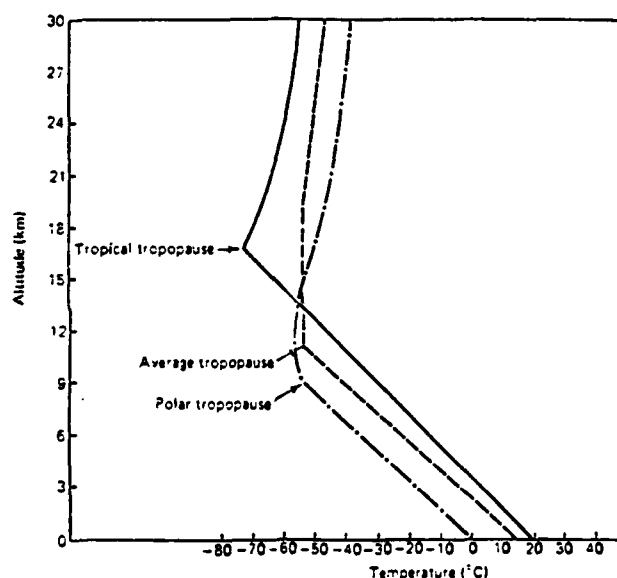
Sources: Neiburger, M., Edinger, J.G., Bonner, W.D.
Understanding our Atmospheric Environment. San Francisco W.H. Freeman,
 1973, p. 39.

Figure 8. Atmospheric temperature layers

decreasing temperatures with height; however, this is obviously not the case. The stratosphere experiences temperature increases due to solar absorption by ozone, while the thermosphere shows increases due to

oxygen and nitrogen solar absorption [Smith, E.K., 1968, p.14; Lutgens and Tarbuck, 1982, p. 17]. While other atmospheric division schemes exist (Smith, E.K., 1968 p. 14 mentions division by processes), the temperature layer scheme is the most common.

Attention is focused on the troposphere which, as shown in Figure 9, varies in height (about 7 to 17 km) depending on latitude. Knowledge of the



Sources: Lutgens, F.K., and Tarbuck, E.J. *The Atmosphere: An Introduction to Meteorology*, 2nd ed. Englewood Cliffs, New Jersey: Prentice-Hall, 1982, p. 17.

Figure 9. Tropopause variations with latitude

troposphere is extensive since it contains about 80% of all air mass and originates most weather phenomena [Iribarne and Cho, 1980, p. 7]. Weather is described as follows:

The forces that control the physical state of air are sunlight, surface and air temperatures, water

vapor concentration, and cloud cover. Since all four agents influence one another, the feedback interactions are complicated. Cause becomes effect, and vice versa. This never-ending activity is known as *weather* [Lynch, 1980, p. 3, italics not mine].

The term "troposphere," first used by Treisserenc de Bort in 1908, "literally means the region where air 'turns over,' a reference to the appreciable vertical mixing of air in this lowermost zone" [Lutgens and Tarbuck, 1982, p. 15]. The steady temperature decrease with height or lapse rate of the troposphere is significant. Although it can vary considerably, the troposphere has a normal lapse rate of 6.5 K/km which, according to Derr [1972, p. 1-9], indicates large amounts of mixing. This mixing is both convective and mechanical and ceases at stratospheric levels. "Thus, the troposphere is a well-defined thermodynamic environment that does not interact much with the overlying layer of stable air, or stratosphere" [Lynch, 1980, p. 3].

2.3 The Radio Refractive Index

Elementary optics describes the process of refraction as the bending of a light beam as it travels between different media. Similarly, since the troposphere generally decreases in density, temperature, water vapor content, and pressure with height, radio waves traveling upward, through the

troposphere, will be refracted as the medium changes. Simplistically, under normal tropospheric conditions, radiowaves will bend downward as "the portion of the wave in the thinner air starts traveling faster than the lower portion which is still in dense air"

[*Evaluation of FDM and FM Systems*, 1983, p. 12-7].

Note that horizontal variations can also occur.

Propagation engineering focuses on the radio refractive index, n , to quantize refraction. It is defined as "the ratio of the phase velocity of an electromagnetic wave in a vacuum [(the speed of light, c)] to phase velocity [v_p] of the wave in the medium" [Flock, 1979, p. 141]. Mathematically,

$$n = c/v_p. \quad (2-1)$$

Livingston [1970, p. 7] shows v_p as equal to $1/\sqrt{\mu\epsilon}$ with μ , the magnetic permeability, remaining essentially constant in the atmosphere at $4\pi/10^7$. ϵ , the dielectric constant, varies, however, forcing n to also vary. No single parameter approaches the radio refractive index in significance concerning propagation; among others, effective earth radius, anomalous propagation, and radiowave scattering calculations rely heavily on the refractive index.

The radio refractive index can typically be measured in two ways. Direct measure is obtained through the *refractometer*, an airborne device developed independently in the early 1950's by Birnbaum (National Bureau of Standards) and Crain (University of Texas). This device consists of a resonating cavity which directly measures the air's dielectric constant, and, through autocorrelation analysis, provides refraction measurements [Gordon, 1955, p. 23; Crain, 1955, p. 1405]. Early work using the refractometer is described by Crain and Gerhardt [1952] and Birnbaum and Bussey [1955]. Additionally, McGavin [1962] provides a good narration of some of the earlier versions of the refractometer. The second way to measure the radio refractive index is through surface observations applied to equation (2-3) as described in the next section.

2.3.1 Refractivity

The refractive index can range from 1.000240 to 1.000400 at sea level, but is commonly converted to *refractivity* (N) [Panter, 1972, p. 342]:

$$N = (n - 1)10^6. \quad (2-2)$$

N therefore ranges from 240 to 400 N units at sea level. Refractivity gains complexity as one

considers the variety of random combinations (temperature, pressure, and water vapor content) characterizing the atmosphere. Supporting this, consider

$$N = 77.6/T(p + 4810e/T) \quad (2-3)$$

where

p = total pressure in millibars

e = partial pressure of water vapor in millibars

T = absolute temperature [K] [Smith and Weintraub, 1953, p. 1035].

A variation of expression (2-3) is

$$N = 77.6p/T + (3.73 \times 10^5)e/T^2. \quad (2-4)$$

While still other equations for N exist, CCIR [1986] Report 563-3 chooses equation (2-4) as the recommended expression for refractivity. Hall [1979, p. 14] adds that this formula

is correct to within 0.5% for atmospheric pressure between 200 and 1100 mb, air temperatures between 240 and 310 K, water vapor pressures less than 30 mb and for radio frequencies less than 30 GHz.

Expression (2-4) can be thought of as containing two terms: $N_{\text{dry}} = (77.6p/T)$ and $N_{\text{wet}} = (3.73 \times 10^5 e/T)$. Bean [1956, p. 32] notes that the

dry term varies with atmospheric density and the wet term varies primarily due to water vapor pressure.

Further, as Table 3 shows,

[a]t very low temperatures N_{wet} becomes very small even for saturated air, and so N is almost independent of relative humidity. As the temperature rises, there is a slow decrease in N_{dry} but a rapid increase in the saturated value of $N_{\text{wet max}}$. At high temperatures $N_{\text{wet max}}$ can become somewhat larger than N_{dry} and so N varies considerably with relative humidity. At high temperatures and high relative humidity, N is very sensitive to small changes in temperature and relative humidity [Hall, 1979, p. 15].

Refractivity variations are therefore attributed principally to humidity changes; consequently, the radio refractive index varies more in hot, humid areas than in colder, dry regions.

Of particular interest is the value of refractivity in the first km of height where most troposcatter links propagate. In this case, CCIR Report 563-3 [1986, p. 108] recommends use of the average exponential model given by

$$N(h) = N_A \times \exp(-b_A h) \quad (2-5)$$

where

$N(h)$ is refractivity at height (h) in km,

$N_A = 315$ N units,

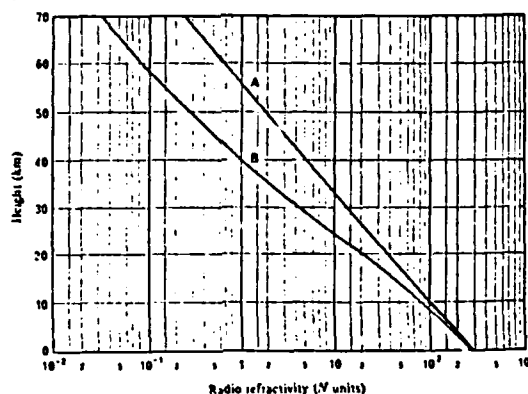
$b_A = 0.136 \text{ km}^{-1}$.

Table 3. Variation of N with Temperature and Relative Humidity (1000 mb)

t°C	H%						Maximum value of N_{wet}	e_s mb
	0	20	40	60	80	100		
N_{dry}								
-30	319.3	320.0	320.7	321.4	322.1	322.7	3.4	0.5
-28	316.7	317.5	318.3	319.1	319.9	320.7	4.0	0.6
-26	314.2	315.1	316.1	317.0	317.9	318.9	4.7	0.8
-24	311.6	312.8	313.9	315.0	316.1	317.2	5.5	0.9
-22	309.2	310.5	311.7	313.0	314.3	315.6	6.5	1.1
-20	306.7	308.2	309.7	311.2	312.7	314.2	7.5	1.3
-18	304.3	306.1	307.8	309.6	311.3	313.1	8.8	1.5
-16	301.9	304.0	306.0	308.0	310.1	312.1	10.2	1.8
-14	299.6	302.0	304.3	306.7	309.0	311.4	11.7	2.1
-12	297.3	300.0	302.7	305.5	308.2	310.9	13.6	2.5
-10	295.1	298.2	301.3	304.4	307.5	310.7	15.6	2.9
-8	292.8	296.4	300.0	303.6	307.2	310.8	17.9	3.4
-6	290.6	294.8	298.9	303.0	307.1	311.2	20.6	3.9
-4	288.5	293.2	297.9	302.6	307.3	312.0	23.5	4.6
-2	286.3	291.7	297.1	302.5	307.8	313.2	26.9	5.3
0	284.2	290.4	296.5	302.6	308.7	314.9	30.6	6.1
2	282.2	289.1	296.1	303.1	310.0	317.0	34.8	7.0
4	280.1	288.0	295.9	303.8	311.7	319.6	39.5	8.1
6	278.1	287.1	296.0	305.0	313.9	322.9	44.7	9.3
8	276.2	286.3	296.4	306.5	316.6	326.7	50.6	10.7
10	274.2	285.6	297.0	308.4	319.9	331.3	57.1	12.2
12	272.3	285.1	298.0	310.9	323.7	336.6	64.3	14.0
14	270.4	284.8	299.3	313.8	328.2	342.7	72.3	15.9
16	268.5	284.7	301.0	317.2	333.4	349.7	81.1	18.1
18	266.7	284.9	303.0	321.2	339.4	357.6	90.9	20.6
20	264.8	285.2	305.5	325.9	346.2	366.6	101.7	23.4
22	263.1	285.8	308.5	331.2	354.0	376.7	113.6	26.5
24	261.3	286.6	312.0	337.3	362.7	388.0	126.7	29.9
26	259.5	287.8	316.0	344.2	372.4	400.6	141.1	33.8
28	257.8	289.2	320.6	351.9	383.3	414.7	156.9	38.1
30	256.1	290.9	325.8	360.6	395.4	430.3	174.2	42.8
32	254.4	293.0	331.7	370.3	408.9	447.5	193.1	48.1
34	252.8	295.5	338.3	381.0	423.7	466.5	213.7	53.9
36	251.1	298.4	345.6	392.9	440.1	487.4	236.2	60.4
38	249.5	301.7	353.8	406.0	458.1	510.3	260.8	67.5
40	247.9	305.4	362.9	420.4	477.9	535.4	287.5	75.4

Source: Hall, M.P.M. *Effects of the Troposphere on Radio Communication*. New York: Peter Peregrinus, 1979, p. 16, 17.

Expression (2-5) is plotted along with an average profile at mid-latitude on Figure 10 (A and B plots respectively).



Source: CCIR, Volume V, *Propagation in Non-Ionized Media*, Geneva, 1982, p. 97.

Figure 10. Refractivity profiles for model atmospheres

Frequently the terms N_s and N_0 are used to provide refractivity values where N_s is the value at any surface location and N_0 is the value at sea level [Panter, 1972, p. 342]. In this instance, CCIR Report 563-3 [1986, p. 109] provides

$$N_s = N_0 \times \exp(-b_A h_s). \quad (2-6)$$

Values for N_0 vary world-wide and are provided in Figure 11 for February (top) and August (bottom). The surface height above that of sea level is used for h_s . As N_s is more easily determined (from an economical standpoint) it is often used in analyzing refractive effects on troposcatter propagation. For

example, Fitzsimons [1968] reports correlations between N_s and signal levels on an 87 km, 4.7 GHz, 1 kW troposcatter link in Cyprus.

2.3.2 Refractivity gradient

As shown in Figure 10, refractivity models establish a decrease in refractivity with height. This decrease is quantified through the refractivity gradient, $\Delta N/\Delta h$, and is "approximated by the difference between the refractivity values of the surface and 1 km above the surface" [*Military Handbook*, 1977, p. 4-84]. In the troposphere, parameters normally decrease with height:

pressure p by about 1 mm (1.3 mb) per 11 m,
temperature by about 1 degree C per 200 m,
humidity by about 1 mb per 300 m [*David and Voge*, 1969, p. 122].

Under these conditions $\Delta N/\Delta h$ equals about -40 N units/km. More specific values are obtainable [*Military Handbook*, 1977, p. 4-87]:

$$\Delta N/\Delta h = -7.32 \exp(0.00557N_s) \quad \text{for the U.S.,} \quad (2-7a)$$

$$\Delta N/\Delta h = -9.30 \exp(0.004565N_s) \quad \text{for Germany} \quad (2-7b)$$

$$\Delta N/\Delta h = -3.95 \exp(0.0072N_s) \quad \text{for the U.K.} \quad (2-7c)$$

2.3.2.1 Effective Earth Radius

The "decrease of N with height bends rays towards the earth but not sufficiently to overcome the curvature of the earth" [*Hall and Barclay*, 1989,

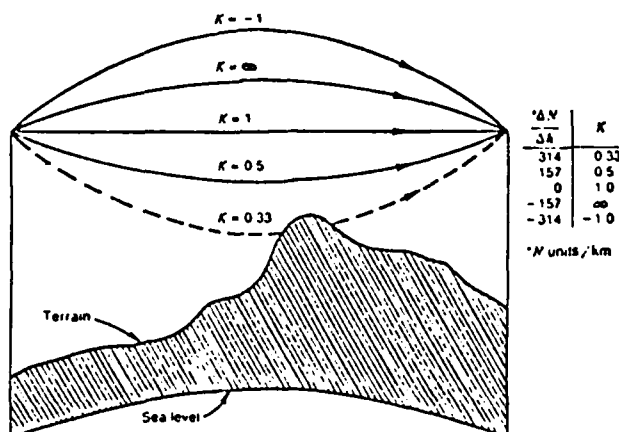
152]. The earth's curvature is $1/a_0$ (a_0 being the earth's radius, about 6370 km), but refractivity gives cause to use a modified earth curvature through the *K-factor*, K , to produce the *effective earth radius*, a :

$$K = a/a_0. \quad (2-8)$$

Freeman [1987, p.6] further shows that:

$$K \approx \{1 + (\Delta N/\Delta h)/157\}^{-1} \quad (2-9)$$

Figure 12 shows the different curvatures for various *K*-factors.



Source: Freeman, R.L. *Radio System Design for Telecommunications (1-100 GHz)*. New York: John Wiley & Sons, 1987, p. 5.

Figure 12. Ray bending at various *K*-factors

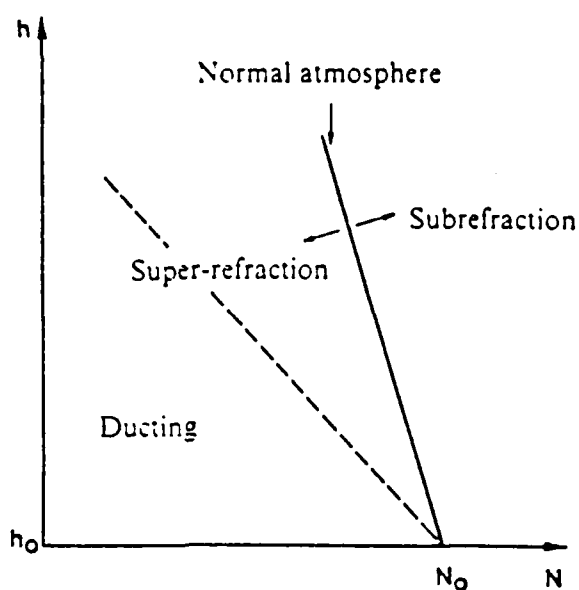
Essentially, the effective radius allows engineers to assume "an atmosphere of constant refractive index" [Boithias, 1987, p. 91]. Using $\Delta N/\Delta h = -40$ N units for the first km of height (often

termed "standard refraction"), K will be about 1.33. This leads to the common $4/3$ effective earth radius figure used in special planning charts for troposcatter path profiles.¹ Realistically, however, the troposphere is not so predictable and $\Delta N/\Delta h$ actually decreases with height. For example, Sarkar, Dutta, and Reddy [1983] show daily K -factors ranging from 1.4 to 2.2 on a 240 km, 2 GHz link in India. Furthermore, extreme variations in the refractivity gradient (and, hence, the K -factor) can lead to serious propagation problems, termed, for simplicity, *anomalous propagation*.

2.3.2.2 Anomalous Propagation

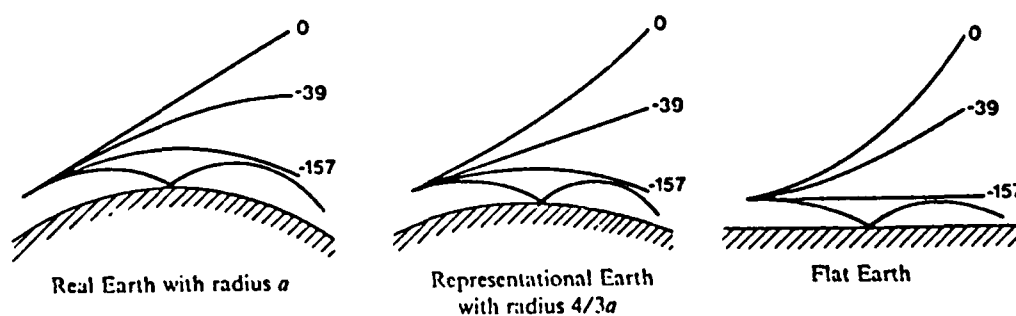
Three types of anomalous propagation can degrade troposcatter system performance significantly. Figures 13 and 14 will aid in this discussion (note Figure 14's use of -39 N units/km for standard refraction). Gradients exceeding -40 N units produce the first anomalous propagation event, *subrefraction*. In this case, paths are less curved; furthermore, a gradient of zero produces straight

¹ $4/3$ earth radius charts are but one of several tools available. $2/3$ charts are used under worst case conditions. Also, flat earth charts are available but are more difficult to use. Flat earth models use M , modified refractivity, instead on N [Hall and Barclay, 1989, p. 153].



Source: Boithias, L. *Radio Wave Propagation*.
St. Louis: McGraw-Hill, 1987, p. 92.

Figure 13. Refractive conditions leading to anomalous propagation events



Source: Boithias, L. *Radio Wave Propagation*.
St. Louis: McGraw-Hill, 1987, p. 93.

Figure 14. Wave paths under various refractivity values for different earth models

lines (real earth model) while positive gradients bend waves upwards [Boithias, 1987, p. 92]. This event will redefine the common volume of a troposcatter link and can lead to signal fading. Surface conditions that can invoke subrefraction typically occur in two forms: Type A - surface temperatures exceeding 30° C and relative humidity below 40%, and Type B - surface temperatures between 10° and 30° C and relative humidity more than 60%. Brauburger [1979, pp. 26,27] explains that Type A and Type B conditions lead to density increases with height, chiefly in water vapor content, resulting in subrefraction.

A second anomalous propagation phenomenon, *super-refraction*, occurs at gradients less than -40 N units. Basically, super-refraction results in more bending, and can, in some instances, obliterate communications as the bent wave never reaches the receiver. Super-refractive conditions normally accompany modified temperature gradients brought on by the passage of cold fronts, subsidence (vertical, downward movement of air), or even night time cooling on the ground [Boithias, 1987, pp. 85,86; Brauburger, 1979, pp. 24,25].

Ducting, the final example of anomalous propagation, is a well documented event and likened to propagation in a waveguide. Two types of ducts can occur. In a *surface duct*, extreme super-refraction bends the radiowave into the earth and the earth reflects the bent wave back into the atmosphere. Conditions permitting (continued, extreme super-refraction over a reflecting earth), this process can be repeated over great distances. Surface ducts are

fairly common over water, especially in the tropics. For instance it is not unusual to propagate signals over a distance of 1500 km in such areas as the Arabian Sea [Staniforth, 1972, pp. 206,207].

Elevated ducts, the second type, never return to the earth's surface. They appear under the unique condition of simultaneous super and subrefractive conditions at different altitudes. A wave launched through a subrefractive layer will be bent upward and later bent downward as it travels to a higher altitude super-refractive layer. Hall and Barclay [1989, pp. 155-161] add that refractivity values less than -157 N units can cause either ducting condition and further show advection, evaporation, subsidence, temperature inversions, and weather fronts as conditions fostering duct creation.

2.3.3 Small Scale Changes in Refractivity

To this point, discussion of refractivity has focused on large-scale variations with height. Refractivity also exhibits localized, fine-scale variations in both space and time that are crucial in understanding troposcatter theory.

Therefore equal-index surfaces are not perfect spheres concentric to the earth [as previous discussion may suggest], but may take a variety of forms. Some may even constitute closed surfaces in which the internal refractive index may be slightly higher (or lower) than external values [Boithias and Battesti, 1983, p. 657].

Typically, irregularities have amplitudes of a few N units above or below the surrounding median; however, they decrease in both number and amplitude with height.

Localized temperature and humidity deviations cause these irregularities. Eklund and Wickerts [1968] cite humidity as the chief determinant, and describe refractive index fields as consisting of sharply bounded air volumes containing excess humidity. Further,

[i]nteraction between wet and dry air causes refractive index fluctuations. Through the turbulence, the strong gradient will be broken down into a spectrum of fluctuations [Eklund and Wickerts, 1968, p. 1071].

Section 2.4 describes turbulence and the spectrum model; however, while it is agreed that this fine-

scale structure can cause scattering and scintillation effects, its precise modeling eludes theoreticians.

2.3.4 Summary of Refraction

Under normal atmospheric conditions, the decrease in the radio refractive index causes electromagnetic waves to experience velocity increases at higher altitudes in the troposphere. Consequently, these waves are bent downward with curvatures defined through the refractivity gradient. This gradient, as well as the radio refractive index, is contingent on temperature, pressure, and water vapor content with the latter displaying the most influence. Abnormal deviations in the gradient result in the anomalous propagation events of subrefraction, super-refraction, and ducting. Finally, gradient models focus on large-scale variations refractivity with height; however, small-scale variations, critically important in troposcatter, also exist. It bears mentioning that challenges to the general models used in refractivity profiles exist. Carroll and Ring [1955] and Crain and Levy [1987] highlight several objections.

2.4 Turbulence

Much of the theory surrounding troposcatter propagation stems from turbulence theory applicable to the small-scale refractivity variations mentioned in Section 2.3.3. This is because "the atmospheric turbulence behaves like a source of inhomogeneities which produce scattering" [Tatarski, 1961, p. vii].

Surely turbulence entered propagation theory with a vengeance in 1949. The troposphere was pictured as an inhomogeneous medium, that is, one which could be pictured as instantaneously containing more or less spherical blobs of air whose index of refraction differed from that of the surrounding air by an amount of the order of one millionth [Carroll, 1952b, p. 8].

Unfortunately, in many respects, atmospheric turbulence remains "one of the great unsolved areas of science and engineering" [Derr, 1972, p. 4-1]. Difficulties root themselves in the large numbers of variables inherent in governing equations which are, in themselves, quite complex. A sampling of these variables include geographical dependence and weather on the large scale, and the small-scale influences of wind, solar heating, and surface roughness [Derr, 1972, p. 4-1]. This section will cite the causes of turbulence and relate a model that attempts to describe small-scale refractivity variations.

2.4.1 The Causes of Turbulence

Anthes [1981, pp. 70,122,326] begins that turbulent eddies or blobs have dimensions of hundreds of meters to a centimeter, with a time scale ranging from a few minutes to a second. These eddies are produced either through *thermal* or *mechanical* mechanisms. Thermal turbulence begins with surface heating and leads to rising air columns or *convection currents* (described by Crain and Gerhardt [1952] as *buoyancy forces*). Mechanical turbulence occurs close to the surface with air flows interrupted by the stationary ground. This produces horizontal *wind shear*. Additional mechanical turbulence is produced by frictional forces between either thermally or mechanically created eddies. Both wind shear and convection currents can rise to higher altitudes and, here, are larger in scale.

Hopefully, the above description of turbulence is confusing since turbulence itself is a random, chaotic event. A typical model of turbulence therefore shows eddies produced through thermal or mechanical processes which interact ("mix") to produced refractivity fluctuations [Crain and Gerhardt, 1952, p. 51].

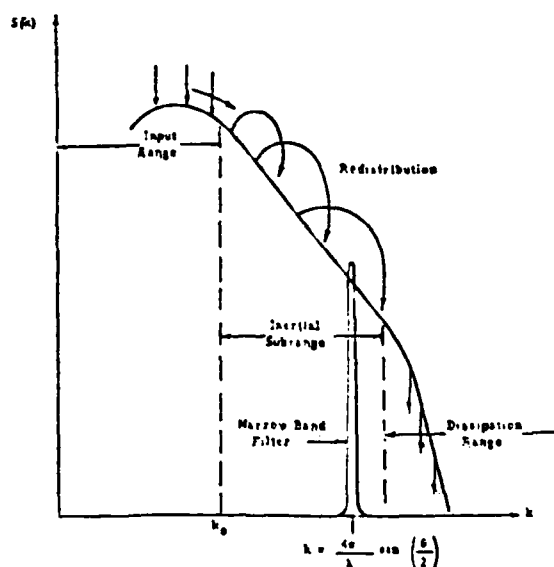
2.4.2 A Refractivity Turbulence Model

As turbulent eddies mix with one another,
both their size and intensity change. L.F.

Richardson aptly describes this process:

Big whirls have little whirls,
That feed on their velocity;
And little whirls have lesser whirls--
And so onto viscosity [Megaw, 1957, p. 444].

Figure 15, which shows the spectrum of refractivity irregularities, $S(k)$, plotted as a function of wavenumber (k), is useful in modeling this process.



Source: Wheelon, A.D. "Radio Scattering by Tropospheric Irregularities." *Journal of Atmospheric and Terrestrial Physics*, vol. 15, nos. 3/4 (October 1959), p. 188.

Figure 15. Spectrum of refractivity irregularities

Blobs created in the input range spawn smaller structures by the cascading process described above and eventually the irregularities are dissipated when their scale size falls below about 1 mm. These very small structures are dominated by the influence of viscosity and diffusion and cannot sustain turbulent activity [Hall and Barclay, 1999, p. 169].

From Figure 15, three distinct areas are evident. In the *input range*, large eddies with low wavenumbers are inserted. They maintain a certain energy level derived from winds and internal pressure or temperature gradients. Entering the second region, the *inertial subrange*, energy is expended through creation of smaller eddies and viscous friction. It is within this region that controversy about the form of the irregularities' spectrum resides. Finally, in the *dissipation range*, the irregularities are lost through heat conversion [Picquenard, 1974, pp. 33,34; Ortwein, Hopkins, Pohl, 1961, p. 790].

Gerlach [1984] mentions that eddy sizes of 1 m to 1 km are of most interest, and are in the inertial subrange. Theories describing irregularities within this domain include Obukhov's mixing theory and the mixing-in-gradient theory. Wheelon [1959], Staras and Wheelon [1959], and du Castel [1966] provide general descriptions of both. Additionally, Appendix C further discusses the spectrum of irregularities.

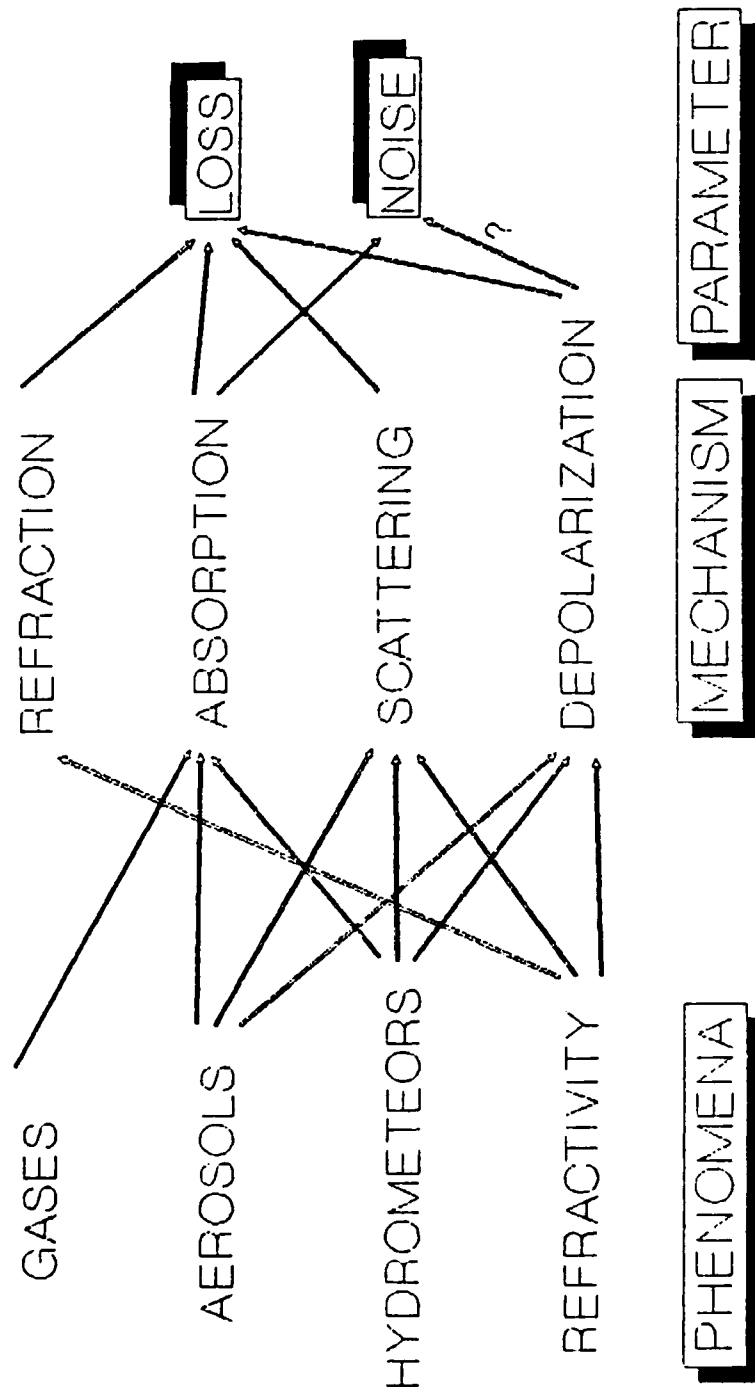
2.4.3 A Conclusion on Turbulence

Turbulence is easily observed in the twinkling of stars or the unsettling feeling of a

bumpy airplane ride. Unfortunately, it is perhaps the least predictable of atmospheric parameters impacting troposcatter propagation. Without it, however, small-scale refractivity gradients would not exist and, therefore, neither would troposcatter. While thought of as a boon in this instance, turbulence will cause scintillation (described later); furthermore, the turbulence model, as outlined above, is the foundation of scattering loss theory. The turbulence of refractivity centers around the portion of the spectrum function contained in the inertial subrange. Equations for this spectrum (Appendix C) exhibit some speculation as do the theories describing eddy activities within this region.

2.5 Atmospheric Effects on Troposcatter Propagation

This concluding section is meant to embrace previous discussion while introducing some of the more pertinent atmospheric effects on radiowave propagation. Figure 16 charts the course this section will take. *Natural phenomena*, on the extreme left includes the observable yet uncontrollable events characterizing the troposphere. For lack of a better term, the refractivity event includes both large and small-scale refractivity changes as



Adapted From: Ippolito, L.J. Jr. Radiowave
 Propagation in Satellite Communications. New York:
 Van Nostrand Reinhold Co., 1986, p. 20.

Figure 16. Troposcatter propagation causal framework

described earlier. Crane [1981a] and Bean, Horn, and Riggs [1962] loosely bundle gases and aerosols under macroscale (100-1000 km) variations; hydrometeors within mesoscale (10-100 km) and cloud (1-10 km) motions; and refractive index fluctuations among microscale (1 mm to 1 km) changes. Note that dust and sand constituents, which may occasionally enter the atmosphere, are not included. CCIR [1986] Report 563-3 mentions that dust and sand propagation degradations need further research, while Report 721-1 adds that these contributions appear negligible.

In the center of Figure 16 are *mechanisms*. These are the effects of natural phenomena on troposcatter propagation. Finally, on the far right are *system parameters*. Appendix B shows external noise and propagation loss as the only variable parameters in the system equation; therefore, all atmospheric effects on troposcatter propagation are reflected within either or both parameters. (Noise due to depolarization is manifested through crosstalk; however, Figure 16 shows a question mark, "?", here as no source listed this as a noise contributor.) In essence, then, the effects of the atmosphere on troposcatter propagation can be viewed from a *causal framework*: natural phenomena cause

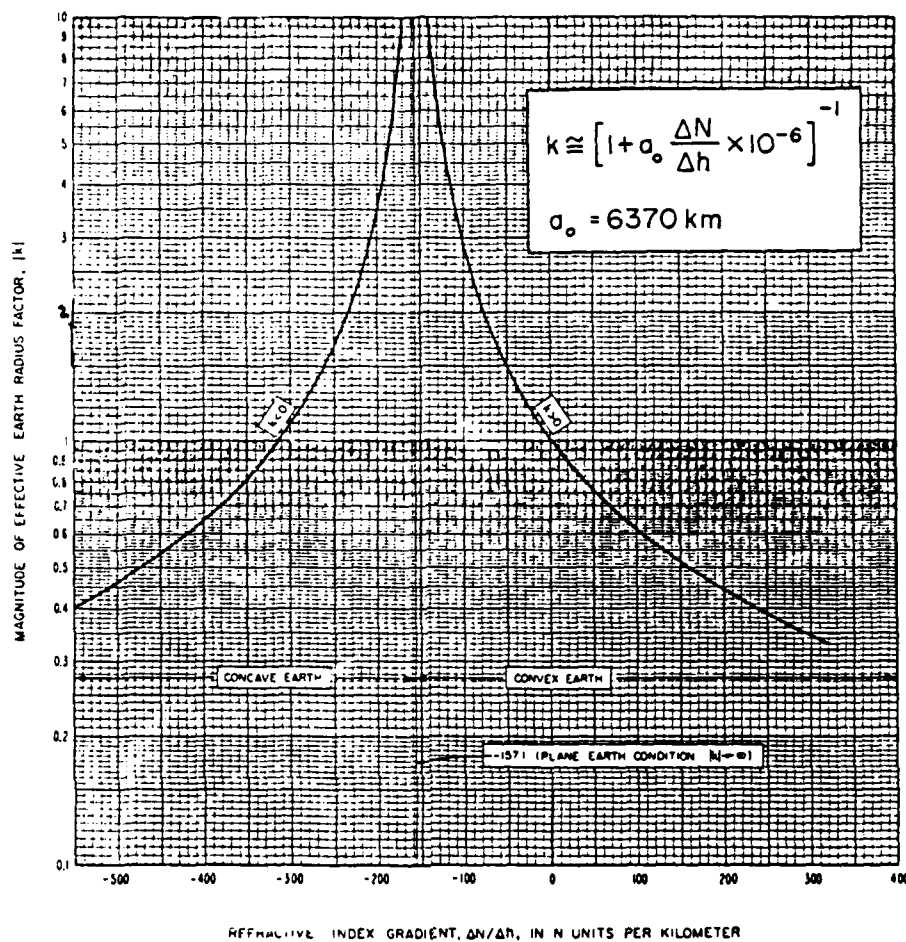
degrading propagation mechanisms which cause changes in system parameters.

While various approaches describing these relationships are possible, this section will focus on the mechanisms. Note should be made that although Figure 16 neatly categorizes the causal nature of the atmosphere on radiowave propagation, the entire process is very complex. Therefore, this treatment is intended to be more introductory than rigorous. The multitude of texts devoted to radiowave propagation confirm this assertion.

2.5.1 Refraction

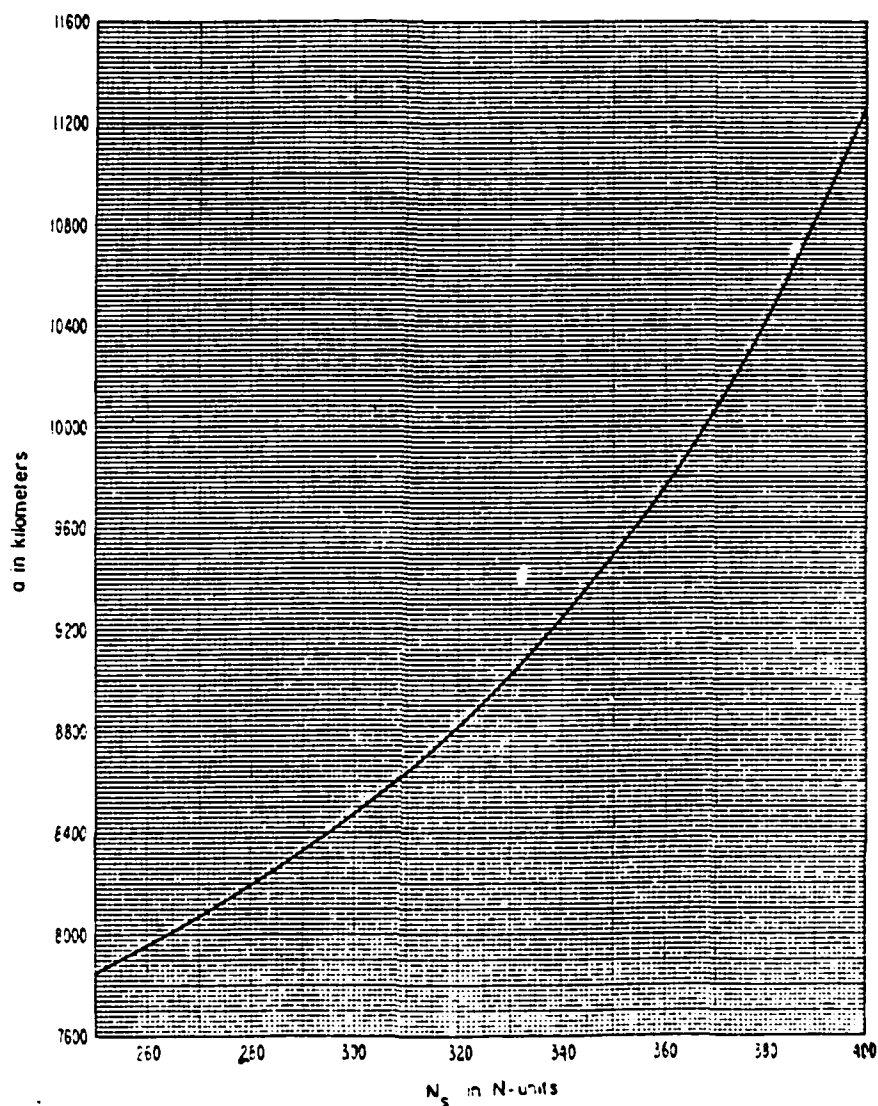
The ability of the atmosphere to refract or bend radiowaves was treated earlier in Section 2.3. Considerations of refractivity therefore include effective earth radius adjustments and allowances for anomalous propagation. Figures 17 and 18 can be used to determine the effective earth radius if either the gradient of refractivity ($\Delta N/\Delta h$) or the surface refractivity (N_s) are known respectively. Clavier [1956, p. 112] notes that effective earth radius K-factor variations of 4/3 to 0.7 should be expected due to large-scale refractivity changes.

Anomalous propagation events (subrefraction, super-refraction, or ducting) can enhance or degrade



Source: Military Handbook, Facility Design for Tropospheric Scatter (Transhorizon Microwave System Design). MIL-HDBK-417, Department of Defense, Washington, DC, 25 November, 1977, p. 4-86.

Figure 17. Effective earth radius factor, K, versus refractivity gradient



Source: *Military Handbook, Facility Design for Tropospheric Scatter (Transhorizon Microwave System Design)*. MIL-HDBK-417, Department of Defense, Washington, DC, 25 November, 1977. Available through Navy Publications and Forms Center, ATTN: NPODS, Office of Navy Publications, 5801 Tabor Avenue, Philadelphia, Pa., 19120-5094, p. 4-90.

Figure 18. Effective earth radius versus surface refractivity

received signal levels. In rare circumstances, a surface duct will engender long periods of abnormally good propagation. More often, however, under extreme super-refraction (much less than -40 N units), radiowaves are bent towards the earth surface and signal blackouts occur as the surface duct "skips" over the intended receiver. Elevated ducts can also cause complete signal loss. Roda [1988, p. 147] concludes that instances of these extreme events subscribe to no definite rules; therefore, experience in site specific situations provides the best prediction tool. He notes an example of ducts over the North Sea lasting several hours yet occurring only 0.7% of the year.

More often, however, deviations from standard refraction (-40 N units) fosters slow signal fades [Clavier, 1956, p. 112; Roda, 1988, p. 68]. Engineers recognize the inevitability of such attenuations and include them in the system equation of Appendix B. This fading is discussed more in depth in Chapter 4.

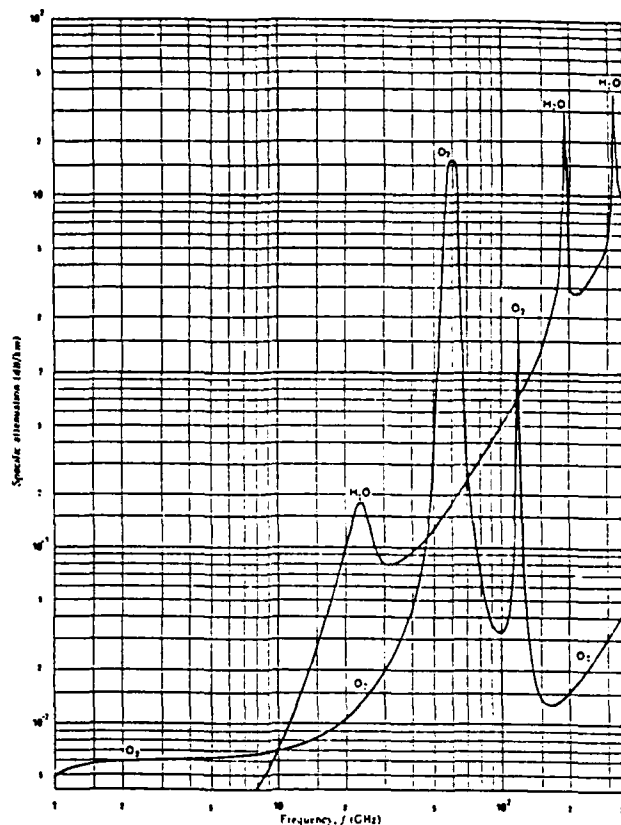
2.5.2 Absorption

Electromagnetic energy can be partially converted into thermal energy through absorption [Flock, 1979, p. 174]. Signal loss as well as

increases in noise result from this process. Figure 16 shows gases, aerosols, and hydrometeors as the events leading to absorption. For simplicity, aerosols will be grouped with hydrometeors although Derr [1972, pp. 1-3 to 1-5] notes physical dissimilarities between the two events.

Of the gaseous elements listed in Table 2, only oxygen exhibits significant absorptive qualities. This is because it possesses "a small magnetic moment" which, under the influence of a magnetic field (an electromagnetic wave), causes it to "rotate end over end or to oscillate in many other possible ways" [Livingston, 1970, p. 10; Kerr, 1987, p. 25]. Furthermore, at certain frequencies, oxygen will resonate, and absorption peaks to significant levels. Figure 19 depicts these critical frequencies, 60 and 119 GHz, and further shows water vapor absorption which displays similar characteristics at 22, 183, and 325 GHz. Water vapor differs from oxygen since it has an electric dipole moment, yet the absorption process is very similar.

Comparing the attenuation contributions of oxygen and water vapor, one notes oxygen's dominance at lower frequencies, about 0.007 dB/km between 2 and 12 GHz, while water vapor remains under 0.005 dB/km

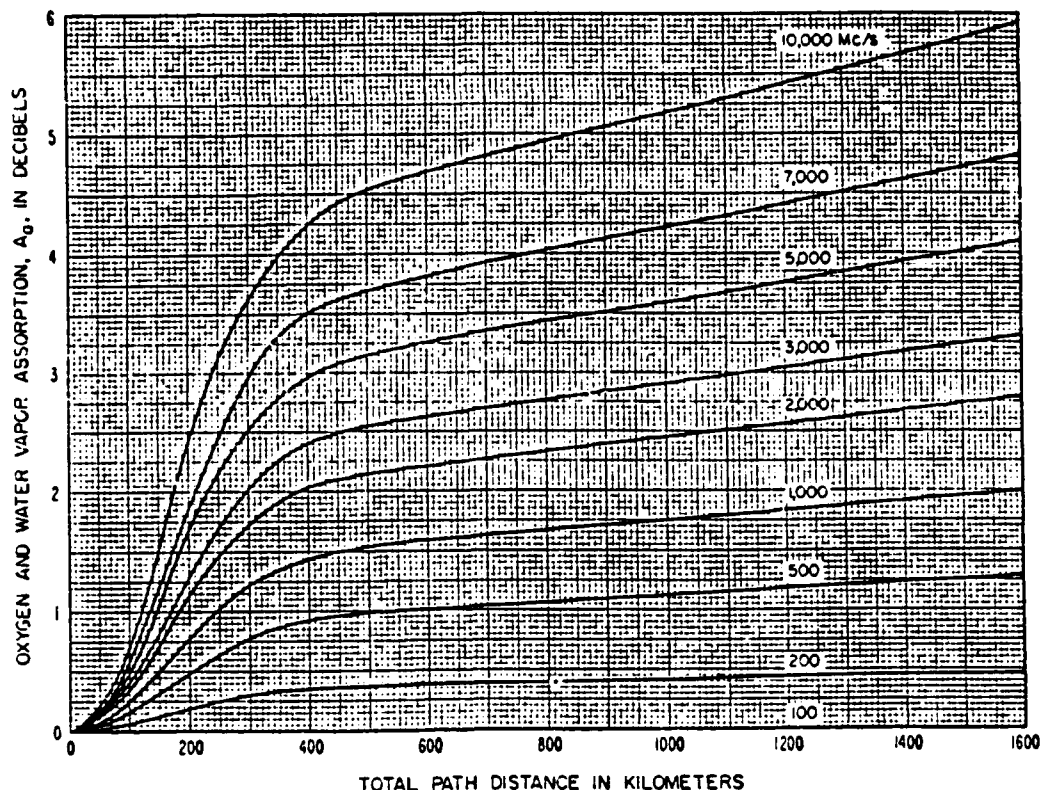


Source: CCIR. Volume V. *Propagation in Non-Ionized Media*. Geneva, 1982, p. 141.

Figure 19. Gaseous absorption

below 8 GHz. Beyond 12 GHz water vapor contributions match, then, for the most part, exceed those of oxygen [Engineering Considerations, 1972, p. 50]. Figure 20 provides a consolidated look at oxygen and water vapor absorption attenuations for typical troposcatter frequencies and path lengths.

Normally, hydrometeor attenuation calculations, particularly rain, include absorption and scattering, the sum of which is termed extinction. In an attempt to differentiate the two mechanisms, Flock [1979, p. 175] reports that "the



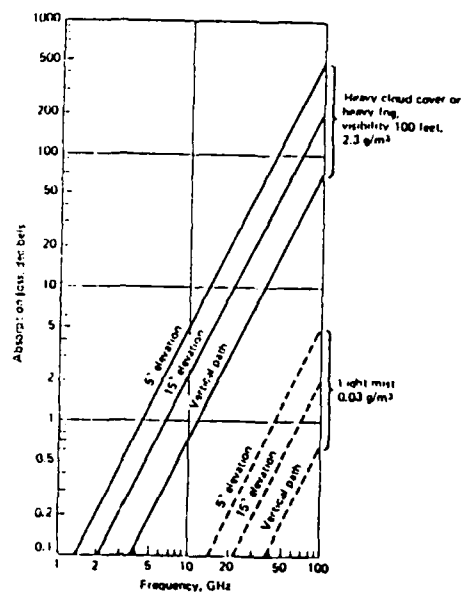
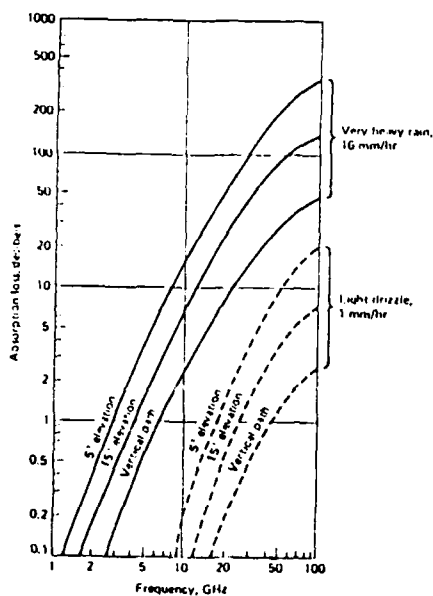
Source: *Military Handbook, Facility Design for Tropospheric Scatter (Transhorizon Microwave System Design)*. MIL-HDBK-417, Department of Defense, Washington, DC, 25 November, 1977. Available through Navy Publications and Forms Center, ATTN: NPODS, Office of Navy Publications, 5801 Tabor Avenue, Philadelphia, Pa., 19120-5094, p. 4-91.

Figure 20. Combined oxygen and water vapor atmospheric absorption

effect of small, lossy water droplets at microwave frequencies is primarily one of absorption."

For wavelengths which are long compared with the drop size, i.e. in the SHF band, attenuation due to absorption will be greater than that due to scatter. Conversely, for wavelengths which are short in relation to drop size, i.e. in and above the EHF band, scatter will predominate [Hall, 1979, p. 47].

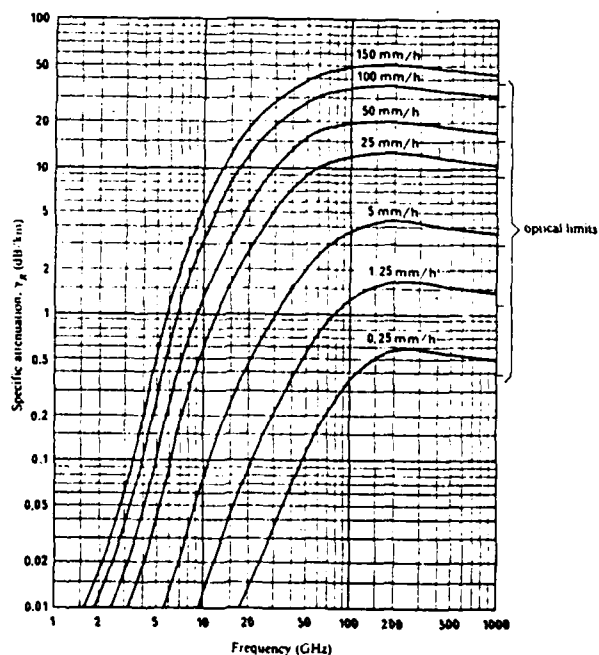
Figures 21 and 22 show hydrometeor absorption for earth-space paths traversing the entire troposphere. Figure 23, more applicable for troposcatter, depicts



Source: Martin, J. *Communications Satellite Systems*. Englewood Cliffs, N.J.: Prentice-Hall, Inc., p. 115.

Figure 21 (Left). Atmospheric absorption due to rain

Figure 22 (Right). Atmospheric absorption due to fog, mist and clouds



Source: CCIR. Volume V. *Propagation in Non-Ionized Media*. Geneva, 1982, p. 168.

Figure 23. Absorption and scattering attenuation due to rain

cumulative absorption and scatter attenuation in dB per km. Note in all instances the insignificance of hydrometeor absorption at troposcatter frequencies.

2.5.3 Scattering

Scattering is essentially the re-radiation of portions of the electromagnetic energy in directions deviating from that intended. Obviously, those signals re-routed from the intended direction contribute to propagation loss. As mentioned, hydrometeors are a scattering source; additionally, small-scale refractivity variations will cause scattering thus making troposcatter propagation possible. Radar systems profit from this process since airplanes scatter signals, and, finally, scattering is a source of interference among different transmission systems [Lane, 1968, p. 4].

Scattering theory emphasizes particle size and number. Simplistically, at troposcatter wavelengths, scatter attenuation due to hydrometeors increases with drop size (with respect to a certain wavelength) and the number of drops [Staniforth, 1972, p. 208]. Flock [1979, p. 175] further shows that the Rayleigh scattering model applies at

troposcatter wavelengths.² However,

[i]t must be stressed that there is at present no single model for drop size distributions which is generally accepted as representing physical reality - even as a statistical mean over many rain events [Hall and Barclay, 1989, p. 176].

Crane [1981a, p. 200] contends that the scattering properties of "the more complex shapes actually assumed by water drops . . . can be approximated only after long and tedious numerical analysis." However, he concludes, scattering attenuation can be estimated through simple models.

As mentioned, hydrometeor effects on radiowave propagation conventionally include both scatter and absorption. Again, Figure 23 is referenced, and the combined attenuation due to hydrometeors (specifically, rain) is seen as insignificant at troposcatter frequencies. Hall and Dowling [1974] offer the same conclusion, but add that "rain may cause significant changes in the mean direction of arrival of the scatter signal" in a troposcatter system. Crane [1988] and Doherty and Stone [1960] further report enhanced median signal levels during rain, but Doherty and Stone [1960] add that fading rates will increase.

²The Rayleigh scatter model is used when scatterer size is small compared to wavelength. Raindrops range from 0.05 to 0.65 cm, at 6 GHz wavelength is 5.0 cm; thus, Rayleigh scatter applies.

The final discussion on scattering highlights small-scale refractivity changes. These variations are responsible for the troposcatter propagation mechanism and also "cause random independent bending of the antenna beams both horizontally and vertically" [Roda, 1988, p. 68]. This action results in rapid fluctuations of received signal levels termed *scintillation* [Crane, 1981a, p. 202]. While small in amplitude, system equation margins must allow for scintillation induced by scattering. Boithias [1987, p. 108] expresses scintillation amplitudes through the structure constant, C_N^2 , as described in Appendix C.

2.5.4 Depolarization

The final mechanism encountered by radiowaves propagating through the troposphere is *depolarization* which may also be termed *transpolarization* or *cross polarization*. This mechanism results in portions of the propagating energy reappearing orthogonally to the intended polarization as discussed in Appendix D. The causes of depolarization, as illustrated in Figure 16, are aerosols, hydrometeors, and refractivity (again, aerosols will be lumped with hydrometeors). It should be noted that this mechanism arises from a mix of other mechanisms

(scatter and refraction) and is difficult to differentiate; however, its effect is unique, meriting separate treatment.

Depolarization due to both large and small-scale refractivity variations is routinely associated with *multipath*. Multipath, described in more detail in Chapter 4, results from a variety of sources such as scattering, terrain and atmospheric reflection, as well as refraction. Simplistically, depolarization due to multipath results from the simultaneous arrival of the wanted, transmitted wave and an unwanted, orthogonally polarized wave created under multipath conditions [*Ippolito, 1986, p. 116; Boithias, 1987, p. 110*].

Hydrometeor (rain) depolarization greatly depends on drop shape. These shapes change from spherical to oblate spheroids as drop size increases. Depolarization, then,

is caused by the individual drops falling as oblate spheroids and producing different attenuation and phase shift for waves polarised [sic] parallel or perpendicular to the major axes of the drops [*Hall, 1979, p. 112*].

More specifically, if the radiowave's electric field

is not parallel to the axis of the equatorial plane of the drops, it gives rise, by scatter, to a wave with orthogonal polarization to that of the incident wave. The relative level of this orthogonal wave depends on many factors such as the angle of incidence of the wave, the canting

angle of the drops, the intensity of rainfall, the distribution of drop diameter, frequency, etc [Boithias, 1987, p. 138].

Rain depolarization is further discussed in Appendix D. At troposcatter frequencies, depolarization is considered unimportant; however, as higher frequencies are used (see Crane, 1988) it may become significant [Military Handbook, 1977, p. 4-173].

CHAPTER 3

TROPOSCATTER THEORY

Long experience has . . . taught me not always to believe in the limitations indicated by purely theoretical considerations, or even calculations. These--as we all know--are often based on insufficient knowledge of all the relevant factors. I believe, in spite of adverse forecasts, in trying new lines of research, however unpromising they may seem at first sight [Carrol, 1956, p. 1057].

- Guglielmo Marconi, 1932

3.1 Introduction

In the late 1940's, new theories attempting to explain high signal levels received beyond the horizon at short wavelengths first appeared. Prior to these, classical diffraction theory was modified to include atmospheric refractivity and ducting to account for this peculiarity. Success was marginal as experiments showed consistent signal levels many decibels greater than those predicted by these modified theories [Bullington, 1953, p. 132; Ortusi, 1955, p. 87]. Investigators realized that nature had conveniently provided some sort of low altitude passive reflector, yet were baffled by its nature.

Accepted beyond the horizon theory was rooted in Van Der Pol and Bremmer's 1937 smooth sphere diffraction predictions which indicated "an exponential decrease in signal strength at a rapid rate at and beyond the radio horizon" [*Radio Transmission*, 1960, p. 30]. With a predicted decay of about 1 dB/km at 500 MHz and 2 dB/km at 5 GHz, long range propagation at and beyond VHF was thought impossible. Experimentation showed these figures as somewhat pessimistic, and large-scale refraction was included which extended the radio horizon through allowance for an effective earth radius $4/3$ greater than actual [*Lane*, 1968, p. 2]. However, even this modification could not adequately explain all observed data.

After WWII, both radar and television systems highlighted circumstances where transmission ranges exceeded classical predictions.

It was also pointed out that the median signal received at points far beyond the horizon could not be explained by modifying the effective earth radius since the data could not be fitted to an exponential law [*Bullington*, 1955, p. 1176].

Anomalous propagation events such as super-refraction and ducting as well as ionospheric influences were then incorporated. However, these conditions were sporadic and again could not clarify the persistency

of observed beyond the horizon fields [Radio Transmission, 1960, p. 30].

Sources contend that even today the mechanism behind troposcatter propagation is not completely understood [McKay, 1989, p. 220; Roda, 1988, p. 2]. However, what is known can be briefly summarized in Figure 2.

The only mechanisms for radio propagation beyond the horizon which occur permanently for frequencies greater than 30 MHz are those of diffraction at the Earth's surface and scatter from atmospheric irregularities. Attenuation for diffracted signals increases very rapidly with distance and with frequency, and eventually the principal mechanism is that of tropospheric scatter [CCIR, 1986, p. 367].

In short, troposcatter propagation exists, and is reliable enough to use for beyond the horizon communications.

While both diffraction and scatter can simultaneously exist as multimode, transhorizon propagation (see Appendix A), this section will examine pure troposcatter theory only, ignoring diffraction. Gjessing and Irgens [1964] group troposcatter theories under "turbulence", "reflection", or "mode" classifications; this treatment will do the same. Discussion will avoid technical analysis, but will provide a physical understanding of the proposed mechanisms.

3.2 Turbulence Theories

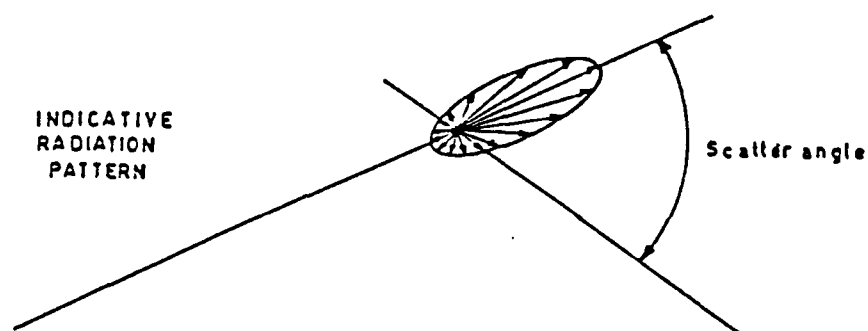
Concerning theories on troposcatter propagation, no single citation is referenced more than Booker and Gordon's 1950 *IRE* article, "A Theory of Radio Scattering in the Troposphere." However, their suggestion that constant, beyond the horizon fields are due to scattering from small turbulent blobs was initially forwarded by Pekeris [1947] [Johnson, 1958, p. 166]. Additionally, at about the same time as Booker and Gordon, Megaw [1950] independently published a similar theory. A summary of turbulence theory proponents is offered by du Castel [1966, p. 12].

Simplistically, turbulence theory purports that within the common volume, portions of transmitted energy are scattered by small-scale refractive variations "much as fog or moisture seems to scatter a searchlight on a dark night" [Freeman, 1975, p. 265]. Tatarski summarizes the problem:

A plane monochromatic electromagnetic wave is incident on a volume V of a turbulent medium; because of turbulent mixing within the volume V , there appear irregular refractive index fluctuations, which scatter the incident electromagnetic wave. It is required to find the mean density of the energy scattered in a given direction [Tatarski 1961, p. 59].

Booker and Gordon pictured the atmosphere as consisting of a collection of spherical blobs of

diameter l (the scale of turbulence) with each blob having a refractive index slightly different from that of the mean. "Incident waves cause polarization of the elementary volumes, converting them to electric dipoles, which in turn radiate energy" [Picquenard, 1974, p. 32]. Figure 24 depicts a scatterer's radiation pattern which decreases very rapidly from the transmission beam's axis.¹

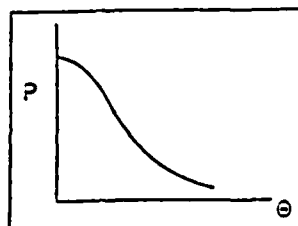


Source: Roda, G. *Troposcatter Radio Links*. Norwood, Maine: Artech House, 1988, p. 63.

Figure 24. Single scatterer radiation pattern

Individual blob scattering is plotted as scattered power (P) versus scattering angle (θ) on Figure 25. When all blobs within the common volume are considered, the plot becomes smeared as in Figure 26 and the radiation pattern resembles Figure 27.

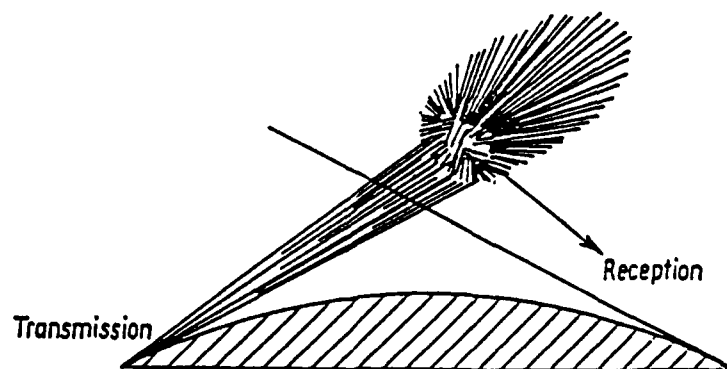
¹This, along with the fact that more scatterers are located in the lower portion of the troposphere, explains the need for a small scatter angle.



Source: Gordon, W.E. "A Simple Picture of Tropospheric Radio Scattering." *IRE Transactions on Communications Systems*, vol. CS-4, no.1 (March 1956), p. 98.

Figure 25 (Top). Scattering power by an individual blob

Figure 26 (Bottom). Scattering power by a number of blobs



Source: du Castel, F. *Tropospheric Radiowave Propagation Beyond the Horizon*. New York: Pergamon, 1966, p. 48.

Figure 27. Radiation pattern of a number of scatterers

Although most power is radiated in the forward direction ($\theta=0$), the receiver is located at ($\theta>0$); therefore, Booker and Gordon assert that the mathematical expression of Figure 26, the scattering coefficient or the scattering cross section (σ), is critical.

The scattering coefficient answers Tatarksi's question by giving the scattered power per unit solid angle, per unit incident power density, per unit volume [Picquenard, 1974, p. 32]. When integrated over the scattering volume, it provides the power scattered to the receiver [Gordon, 1955, p. 98]. A number of references provide different expressions for σ ; however, these will not be provided due to the complexity involved.² Regardless, the crucial parameter in expressions for σ relates to turbulence modeling. Wheelon [1959, p. 193] gives two equations for σ using either the spectrum of irregularities, $S(k)$, as described in Appendix C, or the spacial correlation function $C(r)$.

Booker and Gordon used an exponential $C(r)$ model [Picquenard, 1974, p. 31]:

$$C(r) = \exp(-r/l) \quad (3-1)$$

²See Booker and Gordon [1950]; Gordon [1955]; Wheelon [1959]; and du Castel [1966] for example.

The scale of turbulence l is considered to be the distance at which the cross correlation between the two sets of simultaneous refractive index fluctuation falls to $1/e$ of the value obtained at zero separation [Crain and Gerhardt, 1952, p. 50].

Thus the correlation function falls between unity ($r=0$) and zero ($r=\infty$). However, this choice was somewhat speculative as the ability to measure small-scale atmospheric refractivity variations was, at that time, marginal [Chisholm, 1956, p. 8; Picquenard, 1974, p. 33]. Later, after the development of the refractometer, other models were developed with the Bessel model, described by Staras and Wheelon [1959, p. 81], providing better agreement with experimental data.

Another adjustment to Booker and Gordon's work is due to their disregard for the time variations of refractive index irregularities. Emphasis in turbulence theory shifted to the spectrum function, $S(k)$, which is especially suited to depict these temporal fluctuations [Staras and Wheelon, 1959, p. 80]. This function, described in Appendix C, "is the Fourier decomposition of the space correlation function" [Wheelon, 1959, p. 186]. Ortwein, Hopkins, and Pohl [1961] and Staras and Wheelon [1959] summarize both spacial correlation and spectrum methods in modeling turbulence.

While the above description of turbulence theory does not provide rigorous treatment, a few important conclusions are evident. Primarily, turbulence theory attributes persistent, beyond the horizon fields to scattering from spherical blobs whose refractive indexes slightly differ from the mean. Received fields are calculated through integration of the scattering coefficient over the critical common volume. Crucial in this theory is the modeling of turbulence which has undergone numerous revisions and exhibits several variations (see Appendix C).

3.3 Reflection Theories

The idea that beyond the horizon fields at short wavelengths are caused by reflections from tropospheric layers was first suggested by Norton [1948]. Later, Feinstein [1951, 1952a, 1952b], launched a similar investigation but his ideas were adapted to subsequent mode theories (discussed later). Serious endeavors include the work of Friis, Crawford, and Hogg [1957] and French researchers led by du Castel [1966, p. 12].

In general, proponents assert that layers within the troposphere are formed by relatively sharp gradients in the refractive index. These layers are

numerous in number, display limited yet varying dimensions, and present random position and orientation.

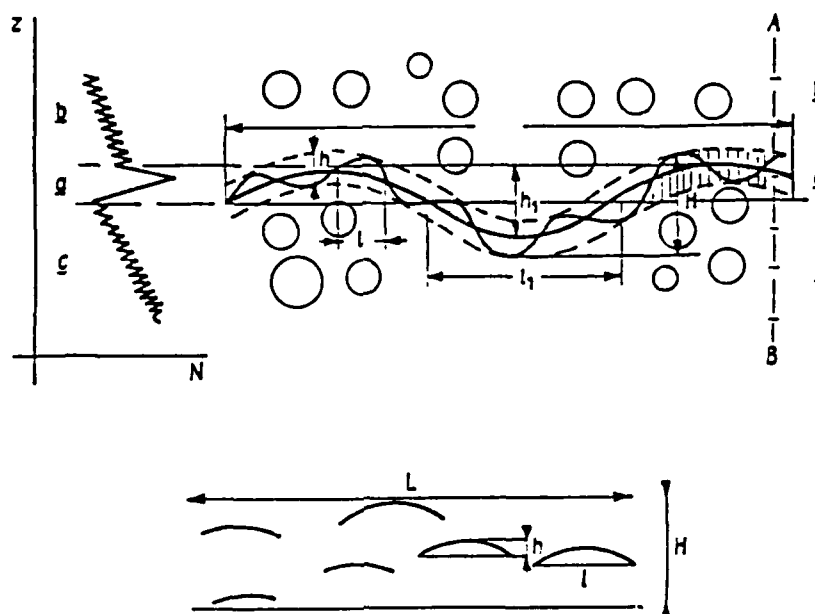
The number and size of the reflecting layers, as well as the magnitude of the discontinuities in the gradient of dielectric constant which form them, influence the received power [Friis, Crawford, and Hogg, 1957, p. 628].

An understanding of the character of a layer aids received power calculations.

When Friis, Crawford and Hogg first postulated their theory, refractometer data substantiated the existence of steep variations in the refractive gradient. However, the actual shape of the layers formed by these variations remained speculative. In short, then, calculations were performed for three general cases: large, small, and intermediate size layers with respect to Fresnel zone dimensions.³ Later, du Castel [1966] offered a more thorough, and, quite elegant, description of these layers.

Figure 28 displays du Castel's layer or *feuillet*. This thin, stable layer forms when laminar air flow "within a layer produces a change in the

³Fresnel zones may be viewed as three-dimensional ellipsoids encompassing radiated energy, and dimensionally dependent on wavelength. Boithias [1987], Livingston [1970], and Kerr [1987] further describe this basic concept.



Source: du Castel, F. *Tropospheric Radiowave Propagation Beyond the Horizon*. New York: Pergamon, 1966, p. 154.

Figure 28. du Castel's thin layer or feuillet

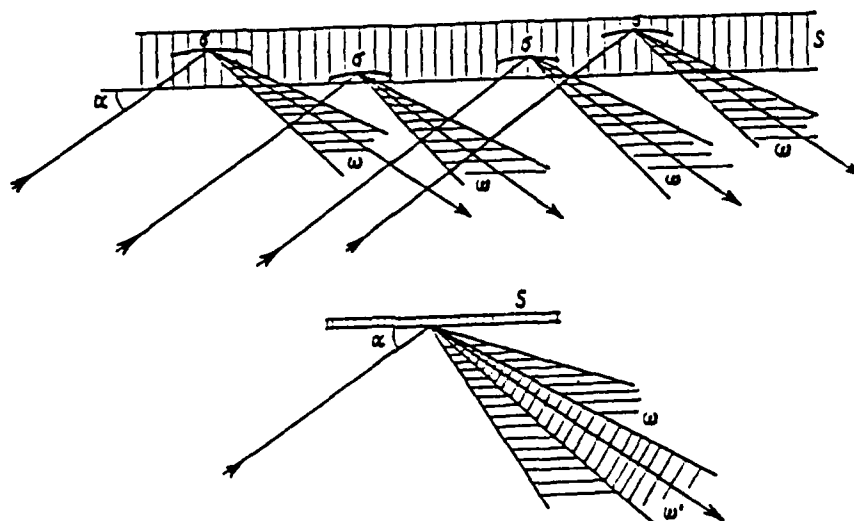
mean refractive index across its thickness" [du Castel, 1966, p. 26]. As shown on the left of Figure 28, the refractivity gradient contains a discontinuity; therefore, within the layer, the refractive index differs slightly from that above and below the layer. The surface has primary irregularities, l and h , both on the order of tens of meters, and secondary irregularities, l_1 and h_1 , several kilometers and a few hundreds of meters respectively. Activity within an irregularity may be likened to that of a turbulent blob described earlier; however, although turbulent irregularities

are crucial in layer formation, in this instance the existence of a layer is more critical than individual blobs. A simplified layer model, consisting of numerous irregularities, is of size L and thickness H and is shown at the bottom of Figure 28 [du Castel, 1966, pp. 154,155].

A feuillet's reflection mechanism is easily understood through application of elementary optics. While the main flow of transmitted energy propagates (refracts) through the layer, a portion is reflected, hence, *partial reflection* occurs as predicted in Snell's law for mediums of differing dielectric constants. Furthermore, depending on the nature of the reflecting layer, either *specular* or *diffuse* reflection occurs [Barton, 1962, p. 335].⁴ Figure 29 shows a number of elements, σ (not to be confused with the scattering coefficient described under turbulence theory), within a surface, S , with transmitted energy incident at a *grazing angle* α .

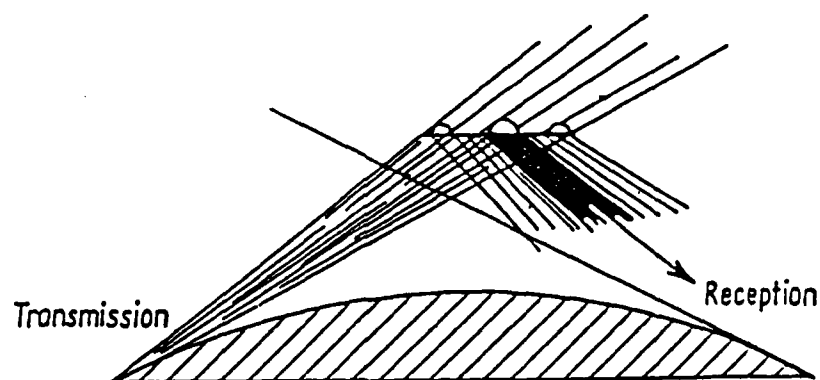
The primary reflections at the surface elements σ within a solid angle ω , add together in phase to give specular reflection in a smaller solid angle ω' , or add randomly to give diffuse reflection in a solid angle ω [du Castel, 1966, p. 159].

⁴Boithias [1987, p. 49] simplistically differentiates between specular and diffuse reflection.



Source: du Castel, F. *Tropospheric Radiowave Propagation Beyond the Horizon*. New York: Pergamon, 1966, p. 159.

Figure 29. Specular and diffuse reflection within a feuillet



Source: du Castel, F. *Tropospheric Radiowave Propagation Beyond the Horizon*. New York: Pergamon, 1966, p. 48.

Figure 30. Radiation pattern for the reflection mechanism

Figure 30 gives a general look at troposcatter propagation via specular and/or diffuse partial reflection.

Calculations for the received field rely exclusively on evaluation of the *reflection coefficient, ρ* . Appendix E discusses ρ in greater detail. However, while determination of reflected power is a basic exercise, the complexities introduced by "the spatial distribution of layers, in size and intensity distributions, and in distributions of curvature for nonflat layers" make computations more statistically oriented [Cox, 1969, p. 907]. Thus, a simple calculation (see Friis, Crawford and Hogg [1957]), is again made difficult due to the unpredictability of the atmosphere.

Recapitulating, when the normally smooth refractivity profile exhibits sharp discontinuities, layers consisting of turbulent irregularities are likely to form. These layers act as partial mirrors, reflecting a portion of the transmitted power. Normally basic calculations for received power are complicated by a reflection coefficient that must consider the complexities of the variable shapes and motions of atmospheric reflecting layers (see Appendix E).

3.4 Mode Theories

When Bremmer [1949] mentioned that 4/3 earth curvature theory ignored the reflected component, partial coherent internal reflection or *mode theory* took root.⁵ Feinstein [1951, 1952a, 1952b], Carroll [1952a, 1952b, 1952c], and Carroll and Ring [1955] were enthusiastic (most notably, Carroll) of this idea which challenged classical notions.

Initially, one will find some similarities between mode and reflection theories. Both incorporate Snell's law of reflection and refraction; however, mode theory introduces no "new" concepts, such as turbulent irregularities. Instead, it focuses on large-scale refractivity noting that not only a refracted (see Section 2.3) but a series of *reflected waves* must be produced due to the refractivity gradient [Feinstein, 1951, p. 1292]. This in turn causes various modes of propagation similar to surface ducts, the distinction being that only the reflected, not the refracted, wave is considered. Figure 31 simplistically depicts one ray for several modes; however, it should be noted that each mode will exhibit a family of such rays, and these rays will experience reflection (external), and

⁵For the earth's atmosphere, an upgoing wave reflects an internal wave, and a downcoming wave reflects externally [Carroll, 1952b, p. 9, 10].



Source: Katzin, M. "Tropospheric Propagation Beyond the Horizon." *Transactions of the IRE, Professional Group on Antennas and Propagation*, PGAP-3 (August 1952a), p. 116.

Figure 31. Mode theory propagation

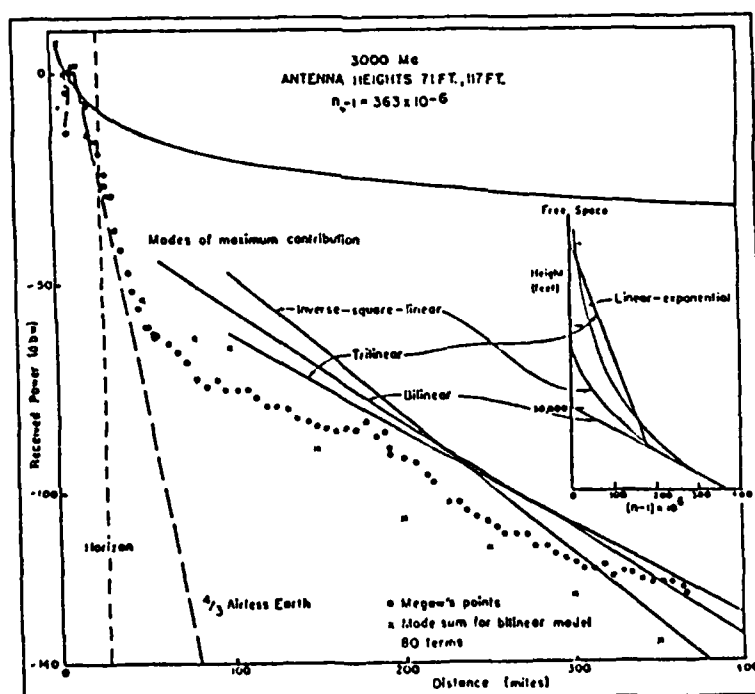
therefore attenuation, as they propagate downward [Katzin, 1952a, pp. 112,113].

The object of the internal reflection hypothesis is to relate the average received field to the rate of decrease in atmospheric density, and hence to eliminate some of the arbitrary parameters required by the scattering concepts [Bullington, 1963, p. 2850].

Mode theory proponents were particularly critical of then accepted refractive index profiles which showed "decreases linearly with height indefinitely . . . [causing] the index of refraction to become less than 1 or even negative at sufficiently large heights" [Carroll, 1952c, p. 93]. Initially, then, a bilinear model was introduced which showed linear refractivity decreases to 30,000 feet and, above this sharp break in gradient, the index was assumed to be unity. Determining the received field involved an infinite summation of mode

contributions from successive layer reflections using Fresnel's summation rules. This eventually gave a reflected field "equivalent to half the reflection from the half-wave layer of maximum contribution" [Carroll, 1952c, p. 84]. Although proponents admit nonrigorous calculations, close theoretical agreement with experimentation was provided by Colwell and Anderson [1952].

Attempts to provide a better fit with field data (Megaw's points) included use of trilinear and inverse square profiles as depicted in Figure 32.



Source: Chisholm, J. H. "Progress of Tropospheric Propagation Research Related to Communications Beyond the Horizon." *IRE Transactions on Communications Systems*, vol. CS-4, no. 1 (March 1956), p. 10.

Figure 32. Various mode theory profiles matched with field data

However, Chisholm [1956, p. 8] and du Castel [1966, p. 132] point out that the mode of maximum contribution occurs at the gradient discontinuities of the bilinear and trilinear models and that such discontinuities do not exist in nature. Further, the inverse square and a subsequent parabolic profile yield poor results [Picquenard 1974, pp. 52,53].

These "hit or miss" endeavors contradict Bullington's assertion that mode theory offers less arbitrary parameters, and provides the first criticism of mode theory. Other objections exist. Turbulence, which is known to persist, is not incorporated. Carroll and Ring [1955] admit to this shortcoming and use it as a possible explanation for high troposcatter fading rates. Saxton [1956] is critical of mode theory's nonrigorous approach, and Katzin [1952a, 1952b] shows the internally reflected component to be of negligible magnitude. Finally, du Castel [1966, p. 132] notes an absence of frequency dependence which contradicts experimentation.

3.5 Other Theories

While turbulence, reflection, and mode theories represent the brunt of ideas explaining the troposcatter mechanism, other perceptions have been published. Most notable is that of Bullington [1963]

which incorporates the "best" of all three theories while eliminating inherent arbitrary factors.⁶ In essence, Bullington's approach assumes an exponential refractivity profile on which turbulent fluctuations are superimposed. The primary mechanism is that of partial internal reflection with the statistical fluctuations explaining both fading and frequency dependence. Turbulent irregularities are analyzed through long-term empirical data, and the reflection coefficient is related to the variance of this turbulent activity. Christopher and Debroux [1987] have found Bullington's predictions both suitable and simple. However, due probably to the use of mode theory, sources do not mention further work in this direction.

Attempts were also made to explain beyond the horizon fields through terrain irregularities. In fact, Bullington [1947, 1953] pointed out that surface roughness could, in some instances, produce enhanced fields, yet troposcatter paths over smooth paths such as water were known to exist [Jowett, 1958, p. 92]. Thus, *pure diffraction theory*, as

⁶Bullington considers scatter and reflection theories as basically the same; however, his use of the reflection coefficient favors reflection theory. This hesitancy to differentiate the two is explained in Section 3.6.

championed by Ortusi [1955], never amounted to much. A similar fate befell de Belatini [1959] who envisioned turbulent toroidal shapes, a few kilometers in diameter, which acted as weak lenses. These atmospheric lenses were said to cause vertical divergence of transmitted waves which allowed beyond the horizon propagation.

3.6 Differentiating the Theories

Judging from presented criticisms and the quantity of supportive sources, two theories, turbulence and reflection, best seem to explain the troposcatter propagation mechanism. At this time it's productive to further distinguish the two, since, as mentioned earlier, there is some difficulty differentiating them. Scattering may be thought of in two ways. Normally, one thinks of scattering as a random spread of energy from some source through space. If, however, some coherence is evident, then the terms reflection, forward scatter, and focusing may be used [Rice, et al., 1967, vol. 2, p. IV-1; Bullington, 1959].

Turbulence theory therefore refers to the random spread of transmitted energy *from a single irregularity or blob*. Although Booker and Gordon originally assumed isotropic scattering, turbulence

theory backers admit anisotropy. The summation of power scattered by the numerous blobs within the common volume are purported to add *incoherently*. Conversely, reflection theory is essentially scattering *from a layer consisting of numerous turbulent irregularities*. Due to specular and diffuse components, power in this case is said to add in a *quasi-coherent* fashion. Therefore, while both theories recognize "scattering" as the propagation mechanism, the scattering source, individual blobs or collective layers, is in question. Taken one step further, the question does not center on turbulence since turbulence is known to exist; rather, the question is whether turbulent irregularities exist as single, randomly disposed entities or arrange themselves into layers. Finally, following Waterman [1970] and the above discussion, **turbulence theory will henceforth be termed incoherent scattering while reflection theory is called quasi-coherent scattering.**

3.7 Modern Theory

Although early work presented two dominant theories, a few cautious individuals like Saxton [1956], M. A. Johnson [*Discussion on Tropospheric Propagation-I*, 1958], and even Carroll [1952b]

acknowledged the possibility of several concurrent mechanisms. Indeed, both incoherent and quasi-coherent scattering will occur simultaneously with dominance related to operating frequency. However, this now accepted conclusion took many years to prove and arrived mostly through assorted experiments and theoretical "adjustments" designed to strengthen proposed theories.

After development of the refractometer, incoherent scatter promoters saw the need to alter Booker and Gordon's original proposal since the scale of turbulence was larger than initially thought. Gordon [1955] and Booker and deBettencourt [1955] incorporated this change in modified theories; furthermore, the latter provided experimental results verifying their ideas. Later, however, de Belatini [1959], Bolgiano [1958], and Rice, et al. [1967, vol.2] challenged incoherent scatter based on uncorrelated theoretical versus experimentally derived wavelength dependencies (discussed in Chapter 4).

Evidence supporting quasi-coherent scatter includes a sizable effort from Crawford, Hogg, and Kummer [1959]. Of particular note are the wavelength dependence results [p. 1092] which, for intermediate

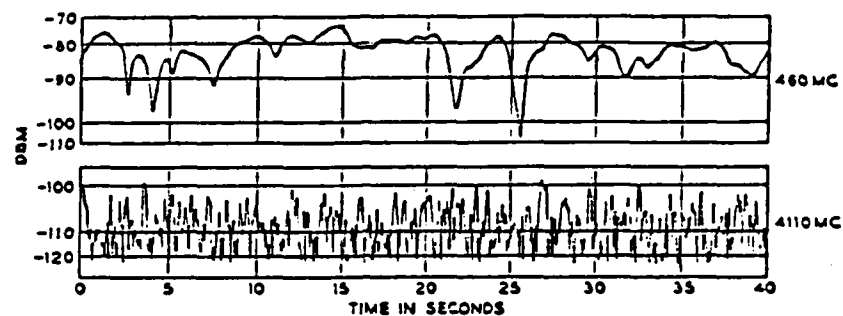
size layers, closely match theory to data, while small layers, likened to single blobs, show poor correlation. Additionally, with respect to fading rates (Figure 33), these researchers show rather smooth signal levels at UHF -- a difficult result for incoherent scatter to explain, but causing no problem in quasi-coherence. Yet, as Appendix E demonstrates, quasi-coherent scatter (a reflection theory) is insignificant beyond UHF since reflection coefficients reduce substantially. Further, the uncertainties of layer size, orientation, and motion inject considerable guesswork in calculations.

Of scatter concepts as a whole, then, Bullington asserts that they are

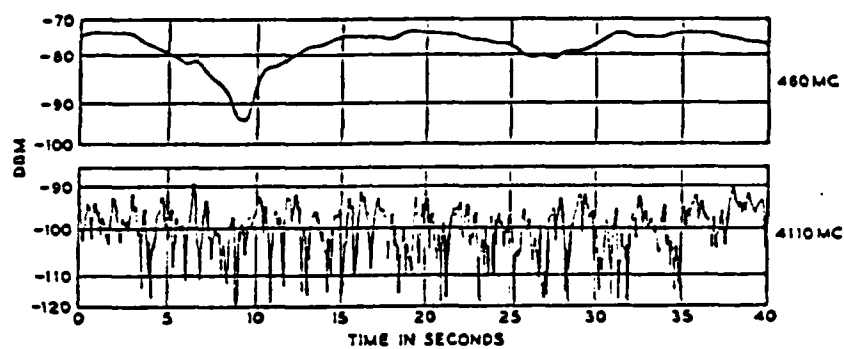
a statistical framework that can be adjusted by arbitrary parameters to fit almost any consistent experimental data and, in fact, the values of the parameters have been changed significantly when the need to accommodate unexpected experimental results has arisen [Bullington, 1963, p. 2849].

Additionally, in a superb review of troposcatter field tests, Cox [1969] provides several conclusions:

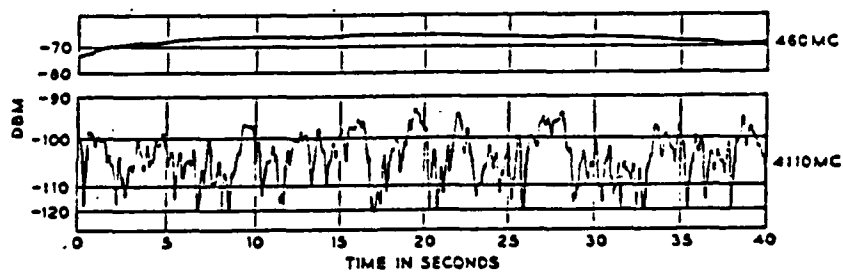
1. The most striking feature observed in all the experiments is the wide range of variation in the measured parameters for different time periods, regardless of what the parameters are.
2. [S]imilar measurements were interpreted in different ways.
3. [D]uring some time periods the atmosphere appears to be in a state of nearly isotropic, homogeneous, nonchanging (stationary) turbulence,



(a) RAPID FADING



(b) SLOW FADING



(c) VERY SLOW FADING

Source: Crawford, A.B., Hogg, D.C., and Kummer W.H. "Studies in Tropospheric Propagation Beyond the Horizon." *The Bell System Technical Journal*, vol. 38, no. 5 (September 1959), p. 1119.

Figure 33. Fading rates for UHF and SHF links over the same path

. . . but during other time periods the turbulence may be anisotropic and/or inhomogeneous and/or changing with time. During still other time periods (often at night) the atmosphere may tend toward a stable state with the major irregularities being caused by stratified layers having different characteristics [Cox, 1969, p. 921].

In short, then, two shortcomings are noted. First, experimenters are "guilty" of partiality to their theory, and, second, the source of scattering is of such unpredictability that complete theoretical agreement is currently impossible. Ignoring the first accusation, a closer look at the scattering source is desirable.

Certainly the atmosphere is unpredictable. In fact, in his recent (1988) book, *Troposcatter Radio Links*, Roda is satisfied in concluding that two types of discontinuities coexist within a sufficiently large common volume: turbulent motion comprising blobs, vortices, or eddies; and laminar motion composed of feuillets or small reflecting surfaces [p. 63]. Physical evidence supporting small-scale turbulent motion is found in voluminous refractometer profiles conducted over many years. Furthermore, Hooke and Hardy [1975] have detected thin, wavelike disturbances produced through gravity waves, and Crane [1981] adds that newer radar systems enable direct observation of such layers. Finally,

indirect evidence of dual discontinuities occurred as far back as 1961 in Ortwein, Hopkins and Pohl's multi-frequency measurements. Undoubtedly, then, both incoherent scatter and quasi-coherent scatter explain short wave, beyond the horizon propagation.

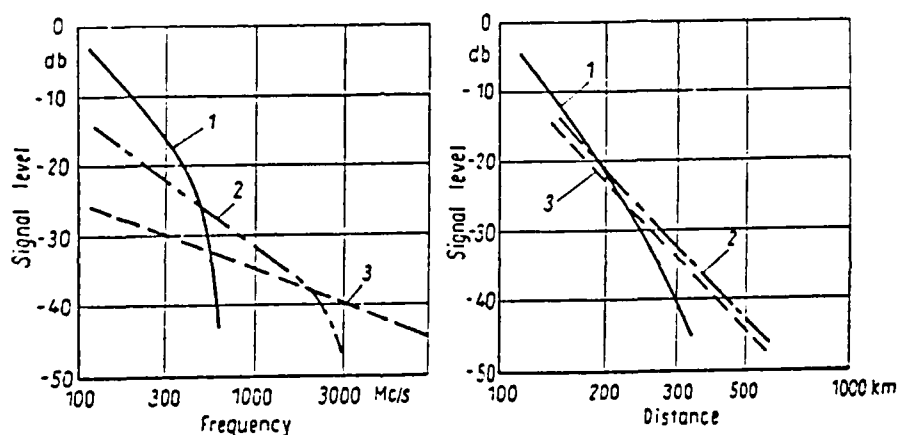
What remains is determination of the dominant propagation mechanism. Waterman [1970] uses generalized meteorological conditions to differentiate the two. Sarkar, Dutta and Reddy [1983] experimentally prove that the spectral slope (m , see Appendix C), refractivity gradient, or wavelength can be used as discriminators. Most sources use frequency (wavelength) as the differentiator; above a certain operating frequency incoherent scatter will dominate. Crane [1981, p. 656] shows the transition wavelength as

$$\lambda = 2L_{OV}\sin(\theta/2) \quad (3-2)$$

where L_{OV} , the *outer scale of turbulence*, dimensionally describes the largest eddies entering the inertial subrange of Figure 15. Again, then, uncertainty enters the picture as L_{OV} will vary depending on atmospheric conditions. Eklund and Wickerts' [1968] tests place the transition between 1

and 3 GHz, while Monsen, et al. [1983] use a 1 GHz cutoff.

By way of summary, Figure 34 shows signal level variations versus frequency and distance for (1) coherent scatter, (2) diffuse scatter, and (3) incoherent scatter. (Coherent and diffuse scatter add to give quasi-coherent scattering.)



Source: du Castel, F. *Tropospheric Radiowave Propagation Beyond the Horizon*. New York: Pergamon, 1966, p. 171.

Figure 34. Signal level variations for: (1) Coherent scatter, (2) Diffuse scatter, and (3) Incoherent scatter

Three conclusions may be drawn. First, the transition frequency resides between 1 and 3 GHz contingent on atmospheric conditions. Second, both mechanisms have similar ranges. Finally, as will be explained in Chapter 5, predictions would benefit

from using incoherent scatter received power calculations as it provides a worst case approach.

Thus, uncertainty induced by the atmosphere continues although great progress has transpired. For some, years of theoretical work has been fruitful; however, many sources state the need for theoreticians to cease pursuit of a universal approach, instead focusing on practical measures. Some may argue that the methods offered in Chapter 5 supply such vehicles; however, until atmospheric phenomena is completely determinable, it is likely that some effort will persist.

CHAPTER 4

CHARACTERISTICS OF TROPOSCATTER PROPAGATION

4.1 Introduction

Although a complete understanding of troposcatter remains elusive, this transmission technique continues to enjoy world-wide use. Chapter 1 surveyed these applications; an excellent summary of early troposcatter systems is provided by Gunther [1966]. This chapter will summarize pertinent characteristics of troposcatter transmission systems, emphasizing those parameters directly influenced by propagation. Specifically, it will highlight attributes of interest to communications engineers, providing typical values while describing expected performance. Equipment will be discussed only when enhancements, designed to reduce the effects of degraded propagation, are possible.

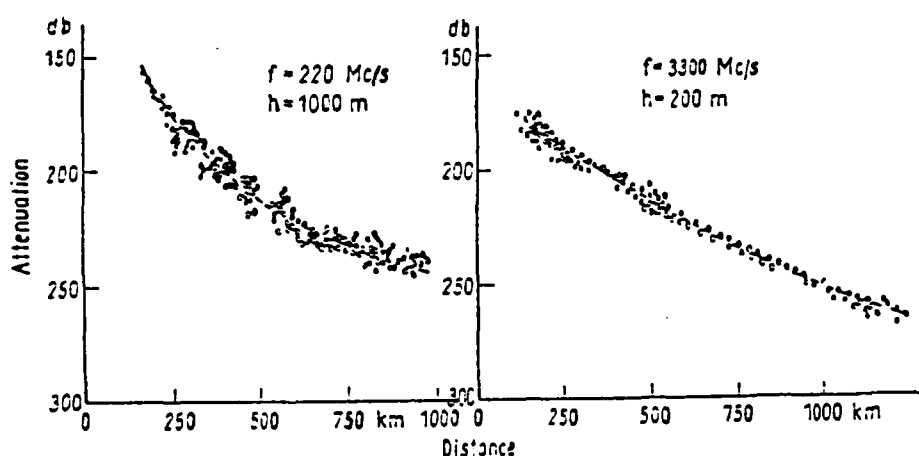
4.2 Signal Level

Critical in evaluating the feasibility of a transmission system to support communications requirements is the received signal level (RSL). Appendix B and Chapter 5 analyze RSL calculation.

This section looks at the distance and frequency dependence, fading characteristics, and aperture-to-medium coupling loss of troposcatter received signals. Since the RSL is expressed as a statistical median, this section will not emphasize the "temporary" effects of diurnal, seasonal and climatological influences. These events are covered elsewhere in this treatment; however, their influence cannot be understated.

4.2.1 Distance Dependence

Figure 35, derived experimentally, more accurately depicts attenuation for the scatter loss portion of Figure 2.¹ It can be construed,



Source: du Castel, F. *Tropospheric Radiowave Propagation Beyond the Horizon*. New York: Pergamon, 1966, p. 64.

Figure 35. Troposcatter loss with distance

¹The term "scatter loss" describes the loss exceeding that of a free space, line-of-sight link; it is more commonly used as attenuation relative to free space.

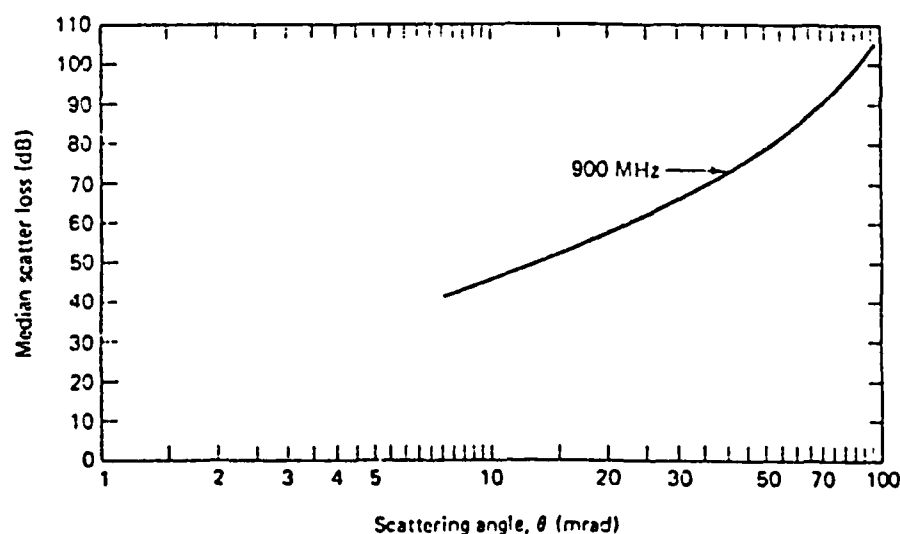
therefore, that troposcatter links exhibit distance dependence with losses ranging from 150 to 250 dB. This dependence is difficult to express in simple mathematical terms since different losses per unit distance occur for different link ranges [Boithias and Battesti, 1983, p. 658].² For example, in 1960 the Joint Technical Advisory Committee (JTAC) reported a 20 dB/100 statute miles loss for links of 100 to 300 miles, and 11 to 12 dB/100 miles in the subsequent 200 to 300 miles ["Radio Transmission," 1960, p. 35]. Most sources generalize to an inverse power relationship such as the d^{-4} law (d , distance) giving about 0.1 dB/km [David and Voge, 1969, p. 148].

Other estimates are available. For links covering 150 to 300 km, $d^{-5.5}$ may suffice for antennas at zero degree elevation; however, an additional loss following h^{-2} , where h is the height of the common volume, is included for antenna beams above the horizon [Picquenard, 1974, p. 41]. Surprisingly, Sarkar, Dutta and Reddy [1983] found distance exponents ranging from -7 to -13 for a 240 km, 2 Ghz link in India (median value not given).

²Explainable by multimode and/or simultaneous incoherent and quasi-coherent scatter propagation.

This unexpected variability is attributed to changing refractivity gradients.

Another method which uses angular distance (θ , the scatter angle) to predict loss was introduced by Norton, Rice and Vogler [1955]; however, in some instances (most notably, the influence of terrain) calculations are unsatisfactory [du Castel, 1966, p. 67]. Regardless, Parl [1979] relates ranges of θ^{-2} to θ^{-6} , and Flock [1979] provides Figure 36 showing scatter loss as a function of angular distance for 900 MHz links. A correction factor, $10 \log (f_2/900)$,



Source: Flock, W.L. *Electromagnetics and the Environment: Remote Sensing and Telecommunications*. Englewood Cliffs, New Jersey: Prentice-Hall, 1979, p. 190.

Figure 36. Scatter loss as a function of scattering angle

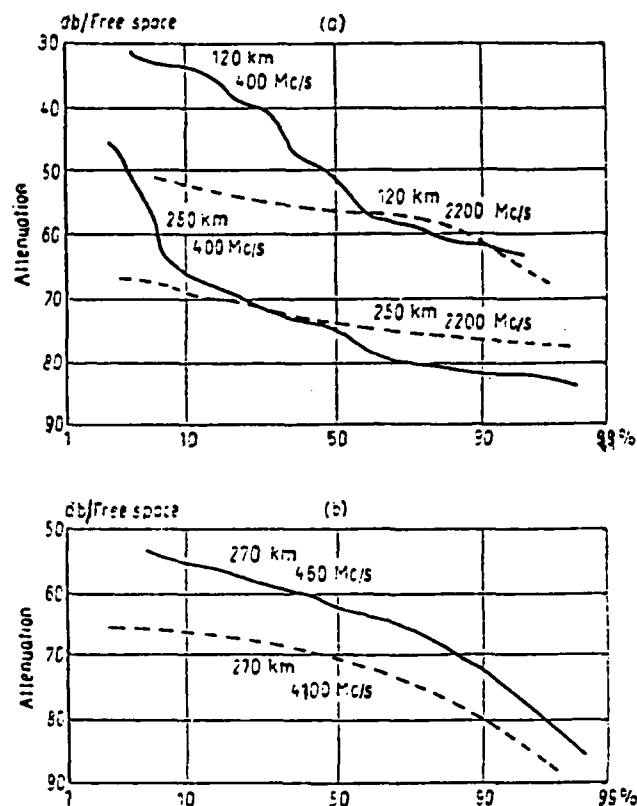
provides additional loss in dB for any frequency, f_2 , other than 900 MHz. Finally, note should be made

that for short links where smooth earth diffraction can dominate (multimode), an exponential law may be appropriate.

The mentioned high loss of troposcatter links requires exceptionally precise antenna siting to avoid attenuating obstructions while keeping elevation angles at an absolute minimum. In addition, compared to typical line-of-sight systems, troposcatter links necessarily use 30 to 50 dB more transmission power, receivers with nearly 12 dB more sensitivity, and much larger antennas with aperture diameters of up to 120 feet [Azurza, 1975, pp. 18,20].

4.2.2 Frequency Dependence

Troposcatter links normally operate in the 250 to 6,000 MHz range (see Table 1). This domain is limited by antenna size on the low end and absorption and depolarization on the upper, although Crane [1988] recently showed the feasibility of higher operating frequencies [Hall and Barclay, 1989, p. 207]. Concerning the effect of frequency on signal levels, it was shown above (through the correction factor for angular distance dependence) and on Figure 34 that loss increases (RSL decreases) as frequency increases. However, as Figure 37 discloses, this



Source: du Castel, F. *Tropospheric Radiowave Propagation Beyond the Horizon*. New York: Pergamon, 1966, p. 69.

Figure 37. The effect of frequency over similar paths

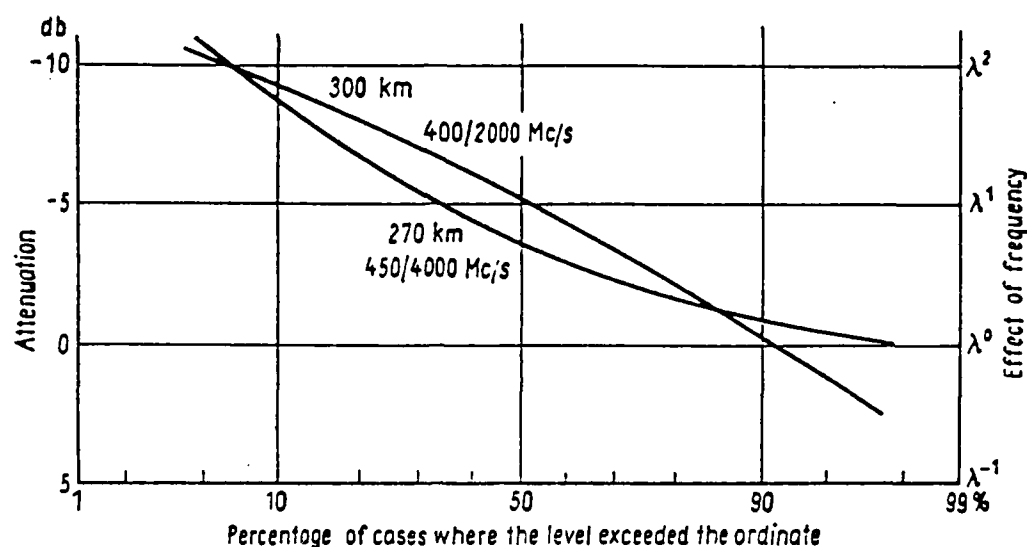
increase is subtle at lower frequencies (below 2.2 GHz in this instance). CCIR Report 238-5 [1986, pp. 377, 381] notes that troposcatter path attenuation relative to free space generally obeys an f^{-1} law up to 3 GHz.³ Expressions for higher frequencies were not found.

³Similarly, the ratio of power received (including scatter loss) to the power one should receive after free space loss only, P_r/P_{fs} , is proportional to f^{-1} . One should be aware that the exponent's sign will change when expressing this ratio as signal level versus attenuation; discussion uses attenuation relative to free space only.

Short-term variations of this general law are known to exist, however, and Report 238-5 notes such instances. As an example, two links in France operating at 460 and 2220 MHz, observed f^2 , 1% of the time and f^1 , 99% of the time for the longer (325 km) link. The shorter link (165 km) had a dependence of $f^{1.5}$, 1% of the time and $f^{0.5}$, 99% of the time. In addition, Eklund and Wickerts [1968, p. 1068, their Figure 3] revealed short-term frequency dependences ranging from f^2 to $f^{-1/3}$ for a 259 km path at 1 and 3 GHz. Figure 38 clarifies short-term frequency dependences by showing distributions for the attenuation ratio of two frequencies traversing the same path; agreement with Eklund and Wickerts is notable.⁴

As mentioned in Chapter 3, conflicts between theoretical and experimentally derived frequency dependence values (specifically, the exponent "n" of f^n) were an early source of controversy among theoreticians. Depending on the turbulence model used for incoherent scatter theories, attenuation

⁴Again, confusion may develop. In Figure 38 the attenuation ratio used corresponds to differences in RECEIVED POWER between opposing frequencies. Cited values by Eklund and Wickerts show ATTENUATION WITH RESPECT TO FREE SPACE; hence, the exponents of λ on the far right of Figure 38, in Eklund and Wickerts' terms, would change sign.



Source: du Castel, F. *Tropospheric Radiowave Propagation Beyond the Horizon*. New York: Pergamon, 1966, p. 70.

Figure 38. Short-term effects of frequency. The received power ratios 200/2000 Mc/s and 450/4000 Mc/s with their subsequent attenuation coefficients are shown. In terms applicable to discussion, a frequency dependence range of about $f^{-1/3}$ to f^2 is depicted.

relative to free space was predicted to obey either $f^{1/3}$ or f^1 laws [du Castel, 1966, p. 147; Rice, et al., 1967, p. IV-7]. Likewise, quasi-coherent scatter theory predicts exponent (n) values of either 2 or 4, although in the particular case of diffuse reflection from intermediate size layers a value of 1 is obtainable [Eklund and Wickerts, 1968, p. 1067; Crawford, Hogg, and Kummer, 1959, p. 1092]. Further, when short-term variations, as discussed

above, were noted, evidence mounted against a single, dominant propagation mechanism.

Once both theories were incorporated and theoreticians recognized the variability of turbulence, these short-term fluctuations were understandable. Consequently, the results of Sarkar, Dutta, and Reddy's [1983] experiments on a 240 km link in India are explainable. For a single frequency (2 GHz), they report exponent values ranging from -2.1 to -0.9 under mostly turbulent conditions, and 0.4 to 2.5 during layered situations (median values were not provided). Regardless, as one can deduce from Figure 37 (attenuation relative to free space), the long-term effect of frequency on signal level will be generally small below 3 GHz, but becomes important at higher frequencies.

4.2.3 Fading

Probably the most distinguishing parameter of troposcatter propagation is the extreme fading observed in the RSL. As discussed earlier, scattering within the common volume directs portions of energy toward the receiver; furthermore, the nature of these scatterers is quite variable. As a result, received signals, which are the sum of these numerous reradiations, exhibit variations directly

related to the activity within the common volume. As will be discussed, the RSL is then characterized by short and long-term fluctuations about a median value, and, in some instances, frequency selectivity is observed. Fading is a critical concern for analog communications systems; however, as discussed later (Section 4.3), digital systems are troubled more by a different parameter.

Due to the unpredictability of the atmospheric phenomena responsible for fading, expressions for these variations are rooted in statistics. Common techniques depict cumulative amplitude distributions over hourly periods while stating the median value as that level equaled or exceeded 50% of the time [*"Radio Transmission,"* 1960, p. 34]. Many RSL prediction techniques, detailed in Chapter 5, heavily rely on these statistical distributions. Additionally, while short and long-term amplitude variations exhibit Rayleigh and log-normal distributions respectively, the actual instantaneous signal level is difficult to express mathematically but may be presented graphically as described in Panter [1972, pp. 365-369].

Generally speaking, short-term fading rates will increase with frequency (see, for example,

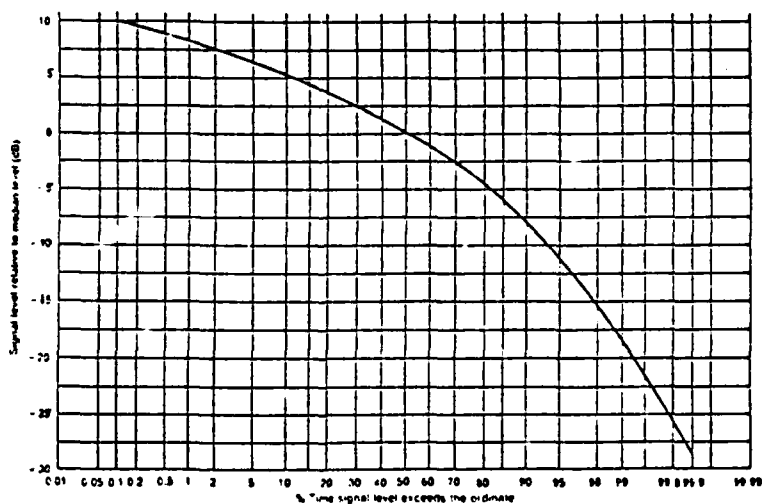
Figure 33); however, this can be reduced by using antennas with narrow beamwidths. Further, as later highlighted in Section 4.5, long-term fading will show diurnal, seasonal, and climatological dependency [du Castel, 1966, p. 86; Crawford, Hogg, and Kummer, 1959, p. 1118]. Since fading can, at times, severely impact transmission quality, techniques to improve performance are essential. Among these, diversity reception offers the greatest utility.

4.2.3.1 Short-Term Fading

Persistent short-term fades, much like scintillation mentioned in Section 2.5.3, are the "trademark" of troposcatter propagation. Fading rates of a few per minute at VHF, 1 Hz at UHF, and several (up to 20) Hz at SHF are not uncommon. Studies of fading rates use statistical formats by which the mean fading frequency has been shown to vary "between 0.044 (exceeded for 99% of the time) and 4.3 (exceeded for 1% of the time) times its median value" [Hall, 1979, p. 142]. Additionally, CCIR Report 238-5 shows that short-term fading rate distributions vary as the hourly median RSL itself changes (a long-term fade). In short, when the median RSL falls above or below its median, fading

either decreases or increases respectively [CCIR, 1986, p. 384].

The amplitudes of short-term troposcatter fades will closely conform to a Raleigh distribution. This follows logically when one examines the cause of rapid troposcatter fades. The numerous scatterers within the common volume each provide individual contributions which, upon arrival at the receiver, add constructively or destructively to the RSL. In this way, *atmospheric multipath* emerges, and due to the randomness of the individual phase contributions, a Raleigh distribution, as provided in Figure 39, is established [Livingston, 1970, p. 121].⁵ Typically,



Source: Freeman, R.L. *Radio System Design for Telecommunications (1-100 GHz)*. New York: John Wiley & Sons, 1967, p. 141.

Figure 39. Raleigh distribution showing short-term troposcatter fading amplitudes

⁵Often, the term *phase interference fading* is used instead of short-term or Raleigh fading; this explains why [Peterson, et al., 1966, p. 5].

one can expect short-term fading amplitudes to exceed the median by 5 dB, 10% of the time, while 90% of the time the fade will not fall below 8 dB of the median; 30 dB fades are shown to occur less than 0.1% of the time [Saxton, 1956, p. 588].

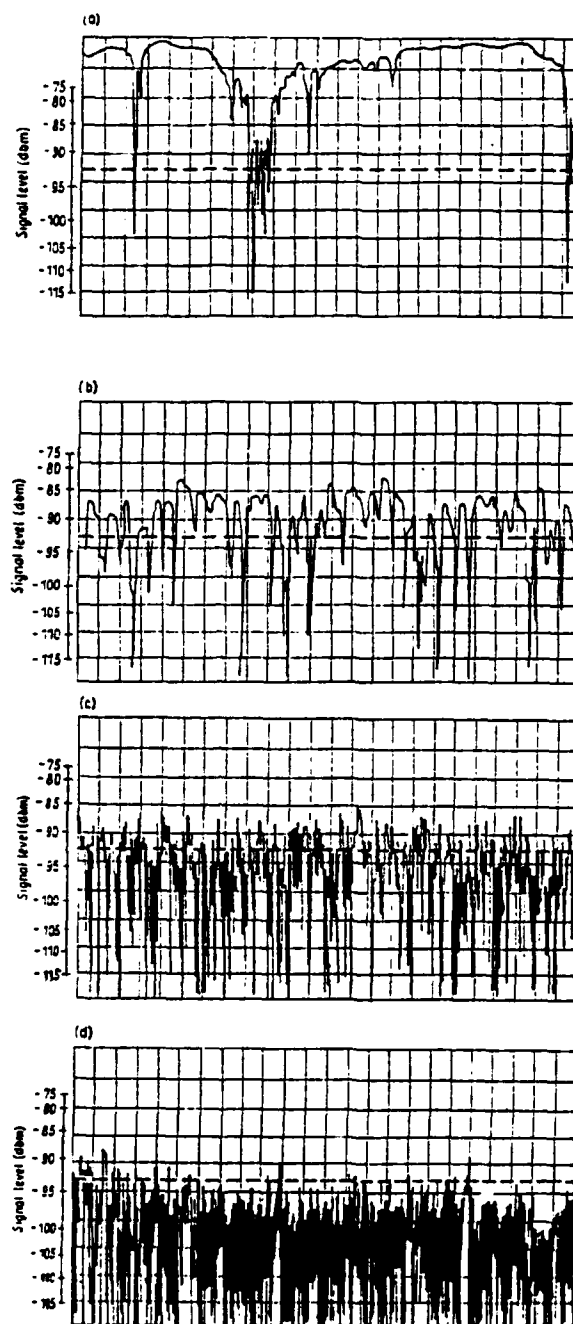
4.2.3.2 Long-Term Fading

Short-term fades are superimposed on long-term or *power fades* which feature cyclic changes on the order of hours, days, and even seasons. The primary cause is variations in the refractivity gradient which will show high climatological dependence, while operating frequency provides little influence [Hall, 1979, pp. 139,140; Livingston, 1970, p. 120; Bullington, 1955, p. 1179]. As the gradient changes, bending will essentially redefine the common volume; hence, the number of scattering sources will change. In addition, gradient fluctuations will influence the intensity of individual scatterers (related by the structure constant, C_N^2 , in Appendix C), and both situations will cause RSL deviations. An additional cause of power fading is that propagation mechanisms (multimode, incoherent scatter, and quasi-coherent scatter) can change

[Rice, et al., 1967, vol. 1, p. 10-1].⁶ Figure 40 provides evidence of mechanism changes on a 350 km, 300 MHz path.

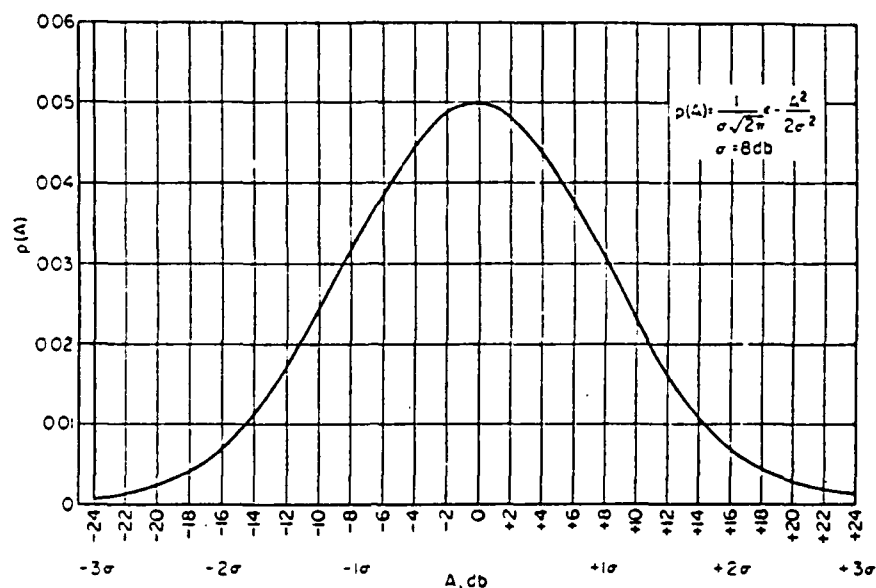
Long-term fading is usually expressed as an hourly median which is derived from a "distribution of the hourly medians over a period of at least one full year" [Panter, 1972, p. 353]. When plotted on a decibel scale, the hourly median loss (that is, the value exceeding the long-term median) will display a log-normal density function [Saxton, 1956, p. 588]. Figure 41 shows this function for a standard deviation, σ , of 8 dB. Hall [1979, p. 140] notes that depending on path length and climate, σ typically varies between 4 and 8 dB. This variation is depicted with respect to angular distance, θ , in Figure 42. Figure 43 provides the cumulative distribution for several values of σ . Interpreting, for a standard deviation of 8 dB, the hourly median value will exceed the long term median by 10 dB 10% of the time, while 90% of the time it will not drop below 10 dB of the same long term median.

⁶Explaining mechanism changes, gradient variations will cause bending that may enhance the diffraction mechanism (multimode). Atmospheric conditions may foster extensive stratification (quasi-coherent scatter) or extreme turbulence (incoherent scatter) [Watterman, 1970].



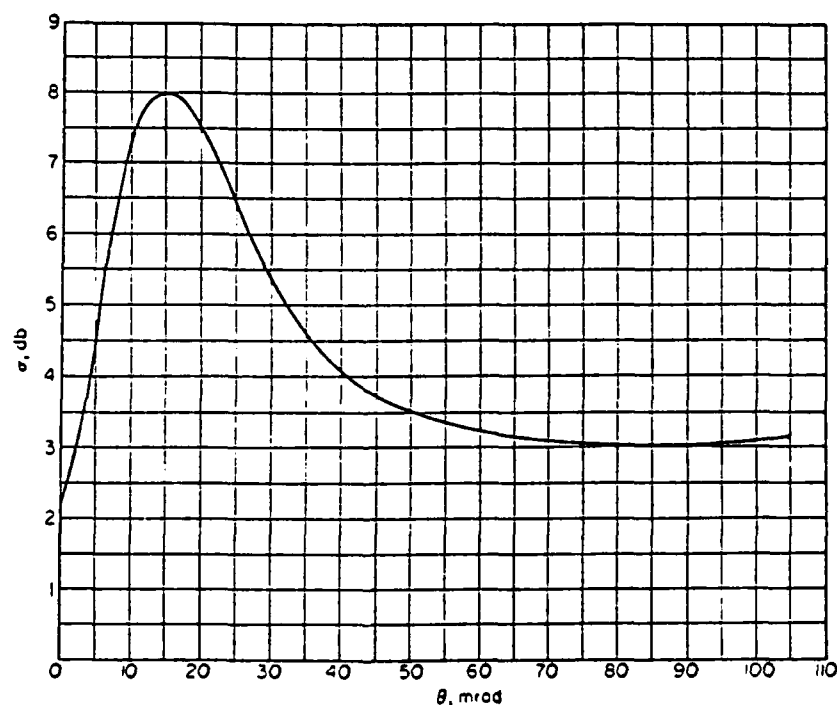
Source: du Castel, F. *Tropospheric Radiowave Propagation Beyond the Horizon*. New York: Pergamon, 1966, pp. 82, 83.

Figure 40. RSL at different times for a 350 km, 300 MHz path. (a) Specular dominant, quasi-coherent scatter; (b) and (c) Diffuse dominant, quasi-coherent scatter; and (d) Incoherent scatter.



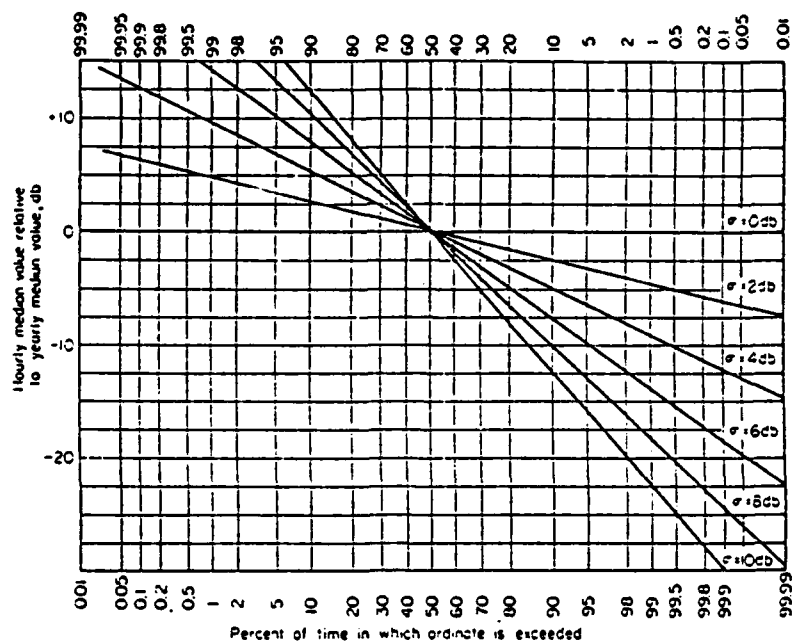
Source: Panter, P.F. *Communication Systems Design: Line-of-Sight and Tropo-Scatter Systems*. St. Louis: McGraw-Hill, 1972, p. 355.

Figure 41. Log-normal density function for $\sigma = 8$ dB



Source: Panter, P.F. *Communication Systems Design: Line-of-Sight and Tropo-Scatter Systems*. St. Louis: McGraw-Hill, 1972, p. 358.

Figure 42. Standard deviation, σ , varying with angular distance, θ



Source: Panter, P.F. *Communication Systems Design: Line-of-Sight and Tropo-Scatter Systems*. St. Louis: McGraw-Hill, 1972, p. 357.

Figure 43. Log-normal cumulative distribution function for various values of σ

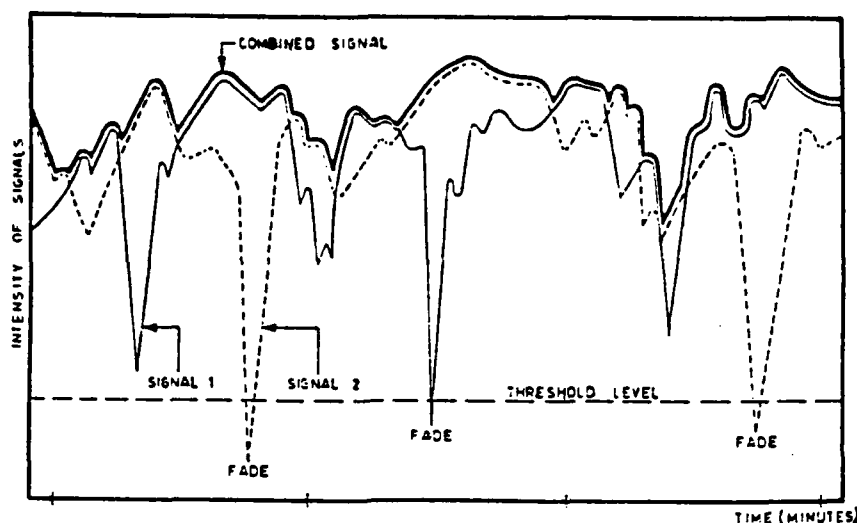
4.2.3.3 Frequency Selective Fading

For troposcatter FDM-FM schemes (which still comprise a sizable portion of in-use systems), performance is also related to frequency selective fading characteristics. Essentially, the transfer function of a troposcatter channel, showing amplitude with respect to frequency, reveals random variations within the transmitted, RF, bandwidth. Although close correlation among adjacent frequencies is typical (the so-called "correlation bandwidth"), independent fading occurs for frequencies sufficiently separated.

Due to this independent fading, certain subchannels may fade and intermodulation noise on the baseband signal results. As a result, while not cited as critical in analog techniques, digital data transmitted on individual subchannels via low rate modems will experience an error rate that cannot be reduced. Bello [1969a, 1969b] and Bello and Ehrman [1969] should be referenced for detailed information; additionally, Section 4.3 further discusses frequency selective fading.

4.2.3.4 Diversity

While an obvious method to combat the effects of fading would be to build in large power margins, a more economical and less detrimental (more power increases chances for interference) solution is *diversity reception*. This well documented technique provides substantial improvement with respect to short-term and, to a lesser degree, frequency selective fading. While several parameters are available, the diversity principle remains the same: separate signals over virtually the same path will exhibit different short-term variations although their mean levels are nearly identical [Boithias, 1987, p. 208]. The combination of the best of these distinct signals results in improved overall



Source: Roda, G. *Troposcatter Radio Links*.
Norwood, Maine: Artech House, 1988, p. 84.

Figure 44. The diversity principle

performance as Figure 44 illustrates.

Clearly, the true value of diversity lies not in the median gain (of a few decibels), but in the fact that it flattens out the no-diversity Rayleigh distribution. With diversity, short-term signal fluctuations are greatly reduced, leaving only long-term variations to be contended with [Panter, 1972, pp. 351, 352].

Diversity reception is an indispensable tool for troposcatter communications systems.

Diversity techniques may be physically visible, termed *explicit diversity*, or inherent in the channel itself, termed *implicit diversity* [Monsen, 1980, p. 18]. Analysis will focus on explicit techniques; Section 4.3 discusses implicit diversity. Single, explicit techniques (often called *dual diversity*) consist of the following:

- a. When two or more antennas are sufficiently separated, space diversity is established and advantage is taken of the different signals produced by slightly different common volumes [*"Evaluation of FDM and FM Systems," 1983, pp. 12-11, 12-12*].
- b. Frequency diversity uses different frequencies which cause scatterers to reradiate at differing phases [*"Evaluation of FDM and FM Systems," 1983, pp. 12-11, 12-12*].
- c. Polarization diversity, which uses separate polarizations (horizontal and vertical), provides limited improvement unless used in conjunction with space diversity [*Monsen, et al., 1983*].
- d. Angular diversity incorporates separate feedhorns on a single antenna; however, "the upper beam from the antenna generally receives a slightly lower mean level" [*Boithias, 1988, p. 209*].
- e. Finally, time diversity may be of benefit if real-time transmission is not essential [*Hall, 1979, p. 147*].

The use of two techniques simultaneously is termed *quad diversity*.

While each technique offers both benefits and shortcomings, space and frequency diversity are most often used. Both techniques add certain equipment (receivers, duplexers, combiners, waveguide, etc) to the transmission system; however, space diversity costs are generally higher due to the additional antenna(s). Conversely, frequency diversity may be difficult as it increases spectrum use. Regardless of whether space or frequency diversity is used, adequate parameter separation is essential. Formulas to derive this separation stem from correlation analysis.⁷ Correlation coefficients describing the degree of independent signal fades with respect to one another will range from 1 (fully correlated) to 0 (no correlation). While sources disagree over expected values, acceptable diversity occurs at values as high as 0.6 [*Engineering Considerations*, 1972, p. 57; Roda, 1988, p. 85].

From the correlation coefficient, a scale length, l in meters, is derived. Horizontal separation distances for troposcatter space diversity antennas are then given by

$$\Delta_h = 0.36\{D^2 + 4(l)^2\}^{1/2} \quad (4-1)$$

⁷A superb example is found in Monsen, et, al. [1983] for a quad diversity (dual space, dual polarization) tactical military system.

where D is the antenna diameter in meters.

Typically, l , for horizontal space diversity, will be about 20 m. For frequency diversity,

$$\Delta f = (1.44f/\theta d) (D^2 + l^2)^{1/2} \quad (4-2)$$

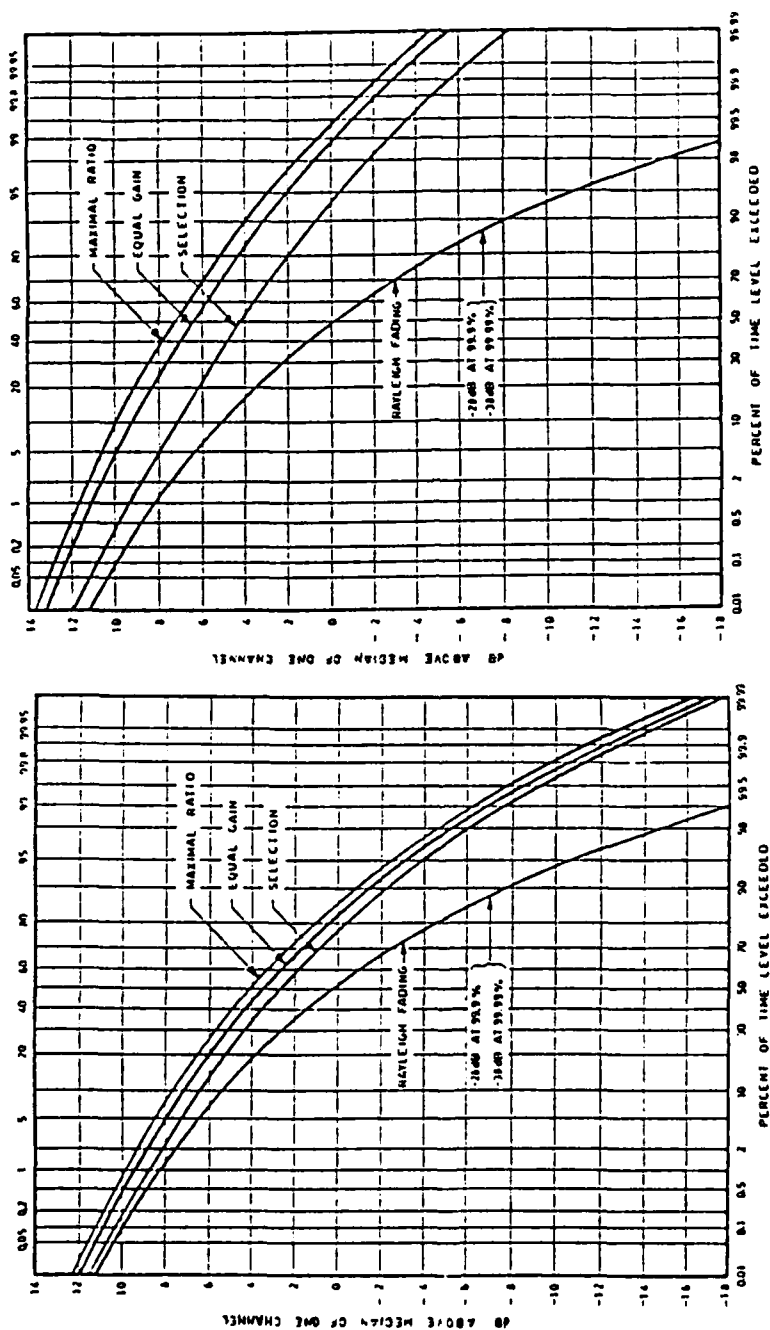
is used with f , being the operating frequency in MHz; θ , the scattering angle, in mrad; d , path length, in km; and l approximately 15 m in this case. Caution is advised in using these expressions below 1 GHz [CCIR, 1986, pp. 381,382]. As a general rule, a horizontal space separation of 100λ or a frequency separation of 2% or more suffices [Roda, 1988, p. 87].

The diversity improved RSL is realized through a *combiner* which can be of several configurations [*"Evaluation of FDM and FM Systems,"* 1983; *"Tropospheric Scatter,"* 1979].

- a. Simplest is the *selector* or *switching combiner* which selects then switches to the receiver having the best signal. Therefore, the selector method is not a combiner *per se*, and since it does not combine receiver outputs, it is the poorest performer of combining techniques.

- b. An *equal gain combiner* adds contributing signals to provide a single output. Provided individual signals are all within about 6 dB of one another, equal gain combiners outperform selector combiners. However, under deep fades (about 30% of the time) equal gain combiners are less effective unless the poorer performing path's receiver is squelched.
- c. Finally, the *optimum ratio, ratio squared, variable gain, or maximal ratio combiner* also adds individual signals but only after conditioning circuitry manipulates individual receiver inputs. The manipulation is in proportion to the noise contributions of separate signals. Ultimately, a portion of the weaker signal(s) is added to the strongest signal giving the best performance of all combining techniques.

Figure 45 compares the performance of these methods for (left) dual diversity and (right) quad diversity. Generally, dual diversity will yield 4 dB improvement 50% of the time and 17 dB, 0.1% of the time. Quad diversity improves performance to about 7 and 27 dB respectively under the same time



Source: Roda, G. Troposcatter Radio Links.
Norwood, Maine: Artech House, 1988, p. 94, 95.

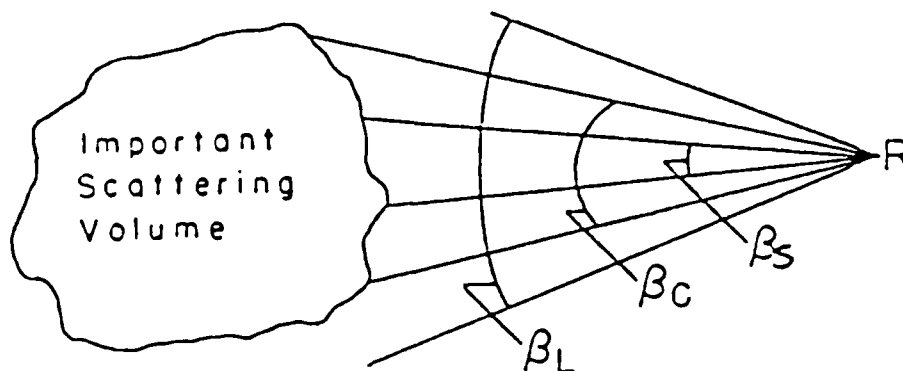
Figure 45. Diversity distribution curves: (left) Dual diversity, (right) Quad diversity

percentages [Panter, 1972, pp. 18,19]. Studies in diversity and combining techniques enjoy voluminous treatment; excellent initial sources include Roda [1988] and Panter [1972].

4.2.4 Aperture-to-Medium Coupling Loss

Completing the components that impact the RSL is *aperture-to-medium coupling loss* (coupling loss). This term, first coined by Booker and deBettencourt [1955], describes the apparent degradation of theoretical gain for large aperture, troposcatter antennas. Generally, this degradation occurs only for antennas with gains exceeding 30 dB, and shows little distance dependence between 150 to 500 km [Boithias and Battesti, 1983, p. 662]. Discovery of this oddity, unique to troposcatter, was comparatively recent since it becomes appreciable only at apertures exceeding a hundred wavelengths which are, currently, physically realizable at microwave frequencies or higher [Crawford, Hogg, and Kummer, 1959, p. 1080].

A widely accepted explanation of coupling loss is provided by Booker and deBettencourt [1955] with subsequent improvements by Boithias and Battesti [1983]. Figure 46 helps this discussion; however, a more realistic view incorporates a common volume full



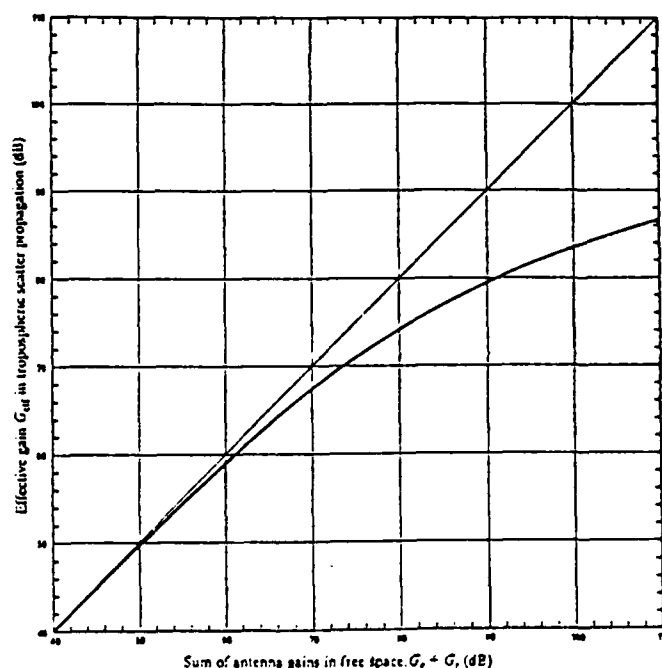
Source: Gordon, W.E. "A Simple Picture of Tropospheric Radio Scattering." *IRE Transactions on Communications Systems*, vol. CS-4, no.1 (March 1956), p. 99.

Figure 46. Coupling loss illustration

of scatters with the majority in the lower portion of the volume. Nevertheless, one would expect proportional gain at the receiver, R , as antenna beamwidths decrease from β_L to β_C . However, as β_C decreases to β_S , the antenna gain increase is countered by a decrease in scatterers. In essence, less scatterers are illuminated and therefore less scatterers participate in reradiation. Other explanations that focus on wavefront distortions due to antenna proximity to terrain and anisotropic turbulence have been discussed by Freeman [1987], Picquenard [1974], and Staras [1957]. Regardless, the work of Boithias and Battesti [1983], recognized in CCIR Report 238-5, provides predictions shown experimentally as quite adequate; however, when incorporated in overall link predictions, Parl [1979]

reveals substantial shortcomings in these empirically derived methods (see Section 5.3.6).

Sources use several techniques with which to calculate coupling loss. Two will be presented here. Boithias and Battesti [1983] conclude that Figure 47 (empirically derived) can be used for 150 to 500 km links. If, for example, transmit and receive



Source: Boithias, L. *Radio Wave Propagation*.
St. Louis: McGraw-Hill, 1967, p. 210.

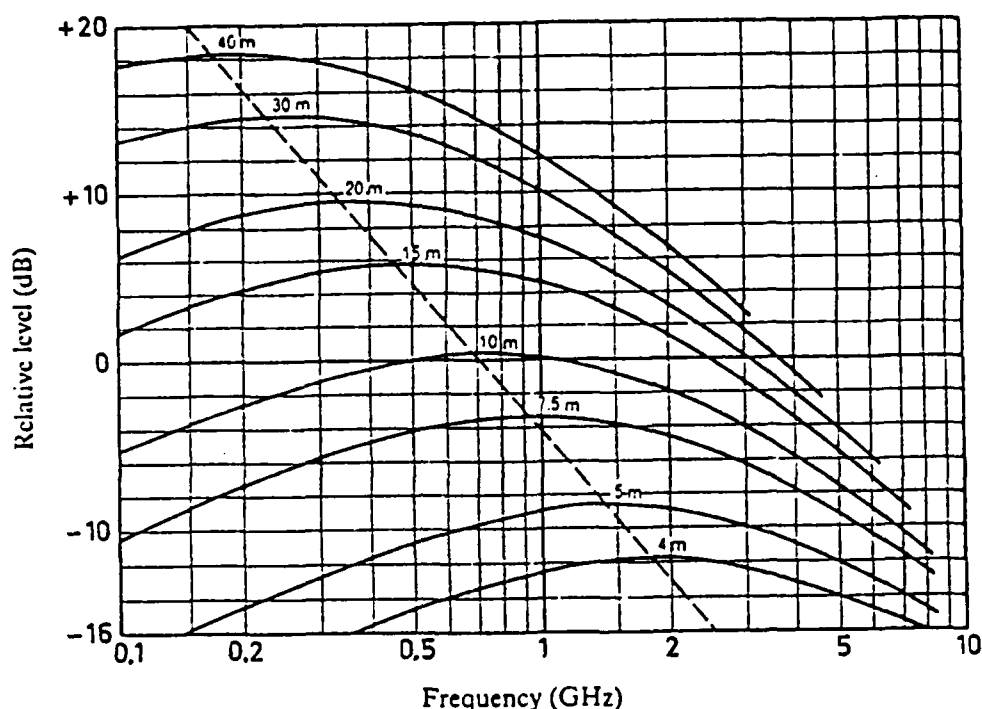
Figure 47. Graphic method for coupling loss calculation

antennas have a cumulative free space gain of 80 dB (40 dB for each antenna), the effective gain (G_{eff}) is about 74 dB representing a 6 dB coupling loss. Another method provides

$$\Delta g = 0.07 \exp\{0.055(G_t + G_r)\} \quad (4-3)$$

with transmit and receive antenna gains, G_t and G_r respectively, given in dB. For the same example mentioned above, coupling loss, Δg , computes to 5.7 dB. Expression 4-3 is limited to individual antenna gains of 55 dB, and both antennas should exhibit similar gain. Notably, coupling loss decreases above path lengths of 500 km, and vanishes above 1000 km [Roda, 1988, pp. 71,72].

An interesting comparison of practical importance results from discussion thus far. It is well known that there is a basic transmission loss between isotropic antennas in free space (see Appendix B); further, antennas exhibit a free space gain depending on aperture size. Finally, troposcatter coupling loss combines with these events, all of which show direct frequency relationships, to produce Figure 48. In this manner, optimum antenna selection for a chosen operating frequency is possible by weighing relative RSL benefits with the costs incurred by larger apertures [Boithias, 1987, pp. 212,213; Hall, 1979, pp. 138,139].



Source: Boithias, L. *Radio Wave Propagation*.
St. Louis: McGraw-Hill, 1987, p. 212.

Figure 48. Relative RSL comparison for antennas of different diameters for troposcatter links. Comparative reference set at 0 dB for two, 10 m antennas at 1 GHz.

4.3 Multipath Delay Spread

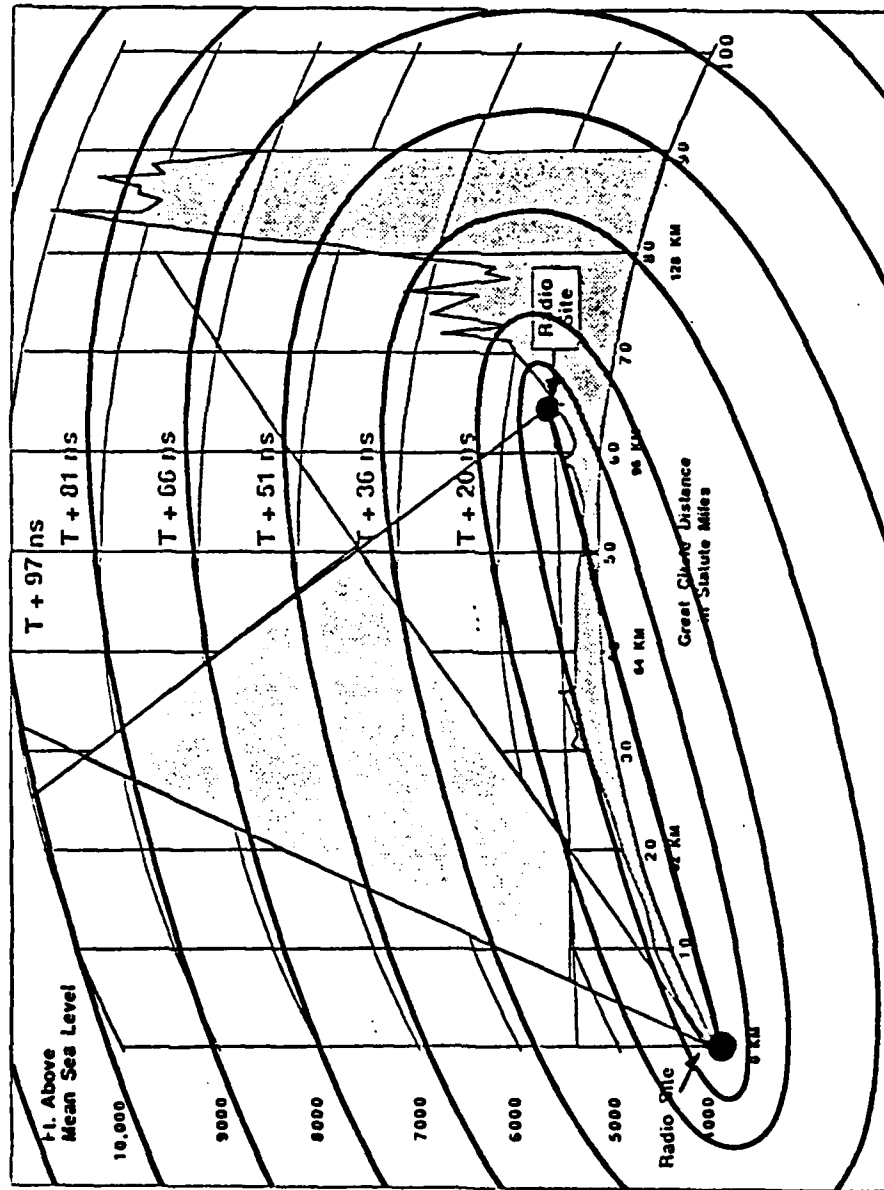
Multipath, which has been mentioned briefly several times, is the cause of many detrimental effects. These include fast fading or scintillation, bandwidth reduction (as will be discussed in Section 4.4), and *delay spread*. Multipath describes the slightly delayed arrival of portions of the transmitted wave. Therefore, individual rays of varying amplitude and phase arrive simultaneously and contribute in a positive manner, adding to the vector

sum of all arriving rays, or detrimentally, depending on phase relationships. They can be produced by partial reflection from refractivity gradient discontinuities, specular or diffuse ground reflections, and, always present in troposcatter, scattering from a number of randomly disposed inhomogeneities within the common volume (atmospheric multipath) [Freeman, 1987, p. 18]. In short,

the power scattered at different positions in space arrive at the receiving antenna at different times, due to the various path lengths involved. This can be detected as the broadening of a transmitting pulse [Gjessing and McCormick, 1974, p. 1330].

This broadening, termed delay spread, can catastrophically impact high speed digital transmission.

Delay spread, sometimes called *multipath-spread*, *differential-delay*, or *time-smear*, measures "the duration of the channel impulse response, or . . . the maximum delay difference between the first and last significant path" [Baghdady, 1970, p. 3]. It can be affected by frequency, antenna diameter, path length, and scattering angle [Monsen, et al., 1983, p. 6-11]. Representative values range from 50 to 370 ns although 1 μ s widths have been experimentally shown to occur [Lemmon, 1989, p. 30-6]. Figure 49 depicts typical delay scattering regions, note how

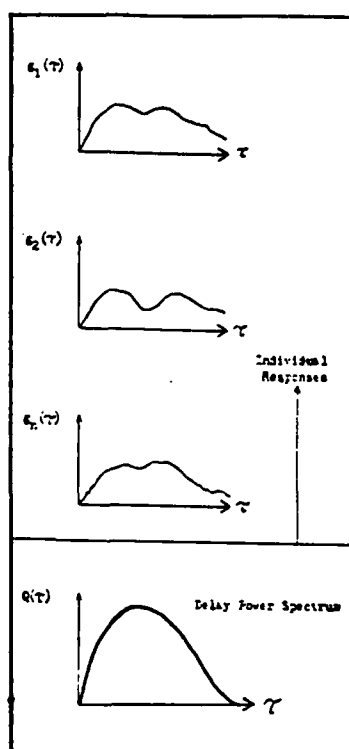


Source: Graham, J.W. "Troposcatter Transmission." Course notes from Session 7 of the MITRE Institute Course: Introduction to Digital Communication Systems, 20 October 1987, np.

Figure 49. Delay scattering regions

different portions of the common volume (shaded region) contribute different path delays. Notably, spread values exhibit seasonal variations due mainly to changes in the structure constant, C_N^2 (see Appendix C) [Monsen, et al., 1983, p. 6-11]. Measurement techniques for delay spread are discussed by Lemmon [1989].

The formation of delay spread in a troposcatter link is simplistically depicted in Figure 50. A short transmitted pulse (impulse)



Adapted From: Koda, G. *Troposcatter Radio Links*. Norwood, N.J.: Artech House, 1988, p. 74; Neuburger, A., Freyheit, P.J., Lertux, G., Livingston, D.C., and McLaughlin, K.P. "AM/TAC-170 Initial Link Engineering Manual." The MITRE Corporation Working Paper WP-25858, Bedford, Ma., 16 Jan 1985, p. 5.

Figure 50. Development of the delay power spectrum

scattered by the common volume will be received as $g_n(\tau)$ (the *power impulse response*) with a width much greater than that transmitted; amplitude will also be distorted. A subsequent pulse, transmitted shortly after the first, will exhibit a similar shape since high speed transmission rates greatly exceed short-term fading rates. However, additional received pulses will eventually change shape and the average, $Q(\tau)$, of all impulse responses establishes the *delay power spectrum*.

The spectrum width is commonly expressed as twice the rms spread, or the 2σ spread, of the delay power spectrum. Typical values were given previously; theoretical values incorporate formidable expressions rooted in the work of Bello [1969a] and well summarized by Freeman [1987] (see Section 5.3.10).⁸ Most importantly, however, the impact of delay spread is essentially the widening of received pulses. Thus, components which arrive late will spill over into adjacent time slots creating intersymbol interference (ISI), and, ultimately, degrading bit error rate (BER) [Freeman, 1987, p. 216]. It is significant to note that the delay power

⁸The interested reader would do well to reference *IEEE Transactions on Communications Technology*, vol. COM-17, no. 2 (April 1969) in which much of Bello's work is conveniently packaged.

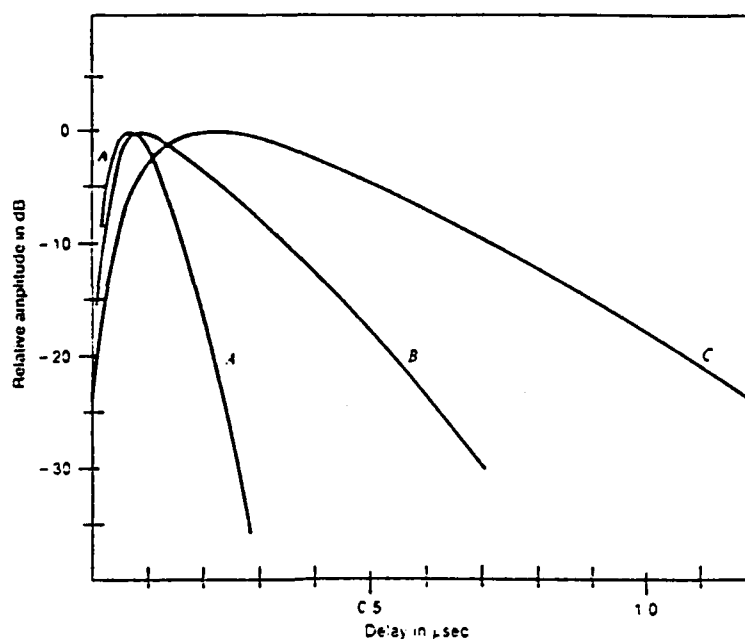
spectrum (a time domain representation) relates to the correlation bandwidth (a frequency domain expression) through Fourier transformation [Bello, 1969a, p. 130]. While the correlation bandwidth limits analog capabilities (see Sections 4.2.3.3 and 4.4), the delay power spectrum can be exploited by digital schemes in a unique way.

In Section 4.2.3.3 it was shown that FDM-FM systems which have RF bandwidths that exceed the medium's correlation bandwidth would experience frequency selective fades on certain subchannels. This can now be explained as due to multipath since multipath establishes the delay power spectrum which is known to be the Fourier transform of expressions for the correlation bandwidth. In this way, multipath is thought of as detrimental to troposcatter communications systems. However, if one were to take advantage of multipath in which different portions of the frequency band fade independently, a form of diversity, *implicit frequency diversity*, emerges. Similarly, since identical information will arrive over a spread in time, *implicit time diversity* is also possible [Monsen, 1980, p. 18; Roda, 1988, p. 101]. Hence, although multipath can induce severe problems in both

analog and digital transmission, it can, through rather clever techniques, be used to actually improve digital transmission.

A variety of techniques are available through which implicit diversity as well as ISI reduction is realized. Roda [1988, pp. 100-103] lists several. Additionally, Monsen [1980] provides a general description of probably the most widely used troposcatter technique, *adaptive processing*. The basic principle behind adaptive processing is that successive pulses differ very little from one another due to the relatively slow, short-term fading rates (slow with respect to transmitted data rates) of the medium. Incoming pulses are compared with previous ones through adaptive equalizers, correlation filters, or maximum likelihood detectors and pulse shapes are corrected as the processor "adapts" to fade induce distortions. The net effect is to minimize ISI while adding diversity improvement (implicit frequency and time). Roda [1988, p. 185] mentions that adaptive processors are available that can support up to 12 Mbps, exceeding typical correlation bandwidths; furthermore, although high in cost, the improvement is well worth the expense.

A preeminent example of the benefits gained through adaptive processing is given by the Raytheon distortion adaptive receiver (DAR) used on the transportable military AN/TRC-170 troposcatter terminal. Two time-gated information-bearing waveforms are transmitted on separate frequencies (subcarriers). Through time interleaving, the transmitted frequency is of nearly constant amplitude allowing 3 dB improvement over traditional, single-gated schemes. Distorted received pulse shapes are reformatted through the adaptive process described above and ISI can be circumvented up to a certain delay spread value, contingent on data rates. Finally, implicit diversity improvement is provided as multipath delay spread worsens (again, up to certain delay spread values). On Figure 51 three delay spread profiles are provided. The AN/TRC-170, operating between 4.4 and 5 GHz, 2 kW, quad explicit diversity, 1.024 Mbps, with 9.5 ft antennas will support total transmission losses of 237.4 dB for profile (A), 240 dB for (B), and 241.1 dB for (C) [Freeman, 1987, p. 218]. Discussion of the intricacies of the Raytheon DAR modem is provided by Monsen, et al. [1983].



Source: Freeman, R.L. *Radio System Design for Telecommunications (1-100 GHz)*. New York: John Wiley & Sons, 1987, p. 218.

Figure 51. Delay spread profiles. (A) 65 ns, (B) 190 ns, (C) 380 ns

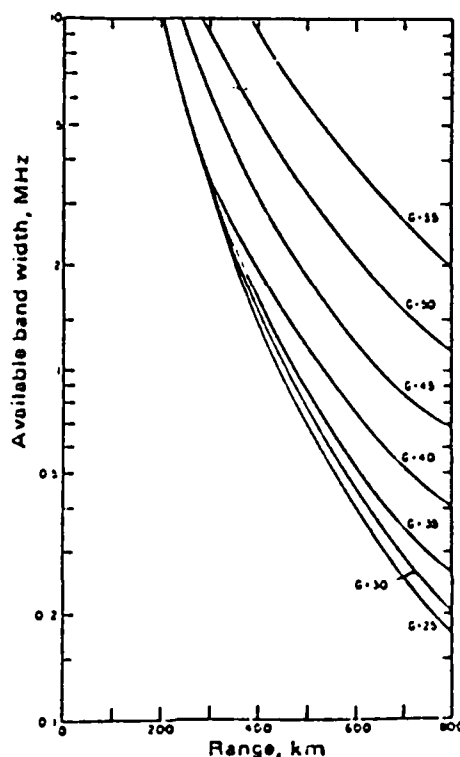
Current trends in communications systems probably dictate greater emphasis on digital performance. However, for digital troposcatter, sources are limited, consisting mainly of military sponsored research. Additionally, the in-place commercial communications infrastructure consists mainly of line-of-sight networks rapidly being augmented by fiber technology. For this reason, research material in troposcatter will probably never provide the multitude of documents typifying early work. Furthermore, with respect to troposcatter *propagation* (the thrust of this thesis), dated material maintains significance, regardless of the

transmission scheme. Simply, no matter how sophisticated terminal peripherals may be, systems will always require RSLs above threshold to operate.

Regardless, the impact of digital equipment peripherals, such as adaptive processors, has rejuvenated troposcatter systems through exploitation of otherwise detrimental propagation effects. The subsequent discussion on bandwidth will further amplify this assertion.

4.4 Bandwidth

Another parameter of interest is the capacity or bandwidth of troposcatter systems. Generally speaking, the transmittable bandwidth is related to climatology and distance [CCIR, 1986, p. 385]. Additionally, some original work by Booker and deBettencourt [1955] identified improved bandwidth performance with higher gain antennas. Figure 52 provides a broad look at bandwidth availability as a function of distance and free space antenna gain. Within several hundred kilometers, bandwidths of 3 to 4 MHz are typical; however, variability is noted. Although limited in capacity, analog troposcatter systems can provide multichannel operations, up to 120 commercial grade voice subchannels. Further, a demonstration of the ability of troposcatter to



Source: Hall, M.P.M. *Effects of the Troposphere on Radio Communication*. New York: Peter Peregrinus, 1979, p. 145.

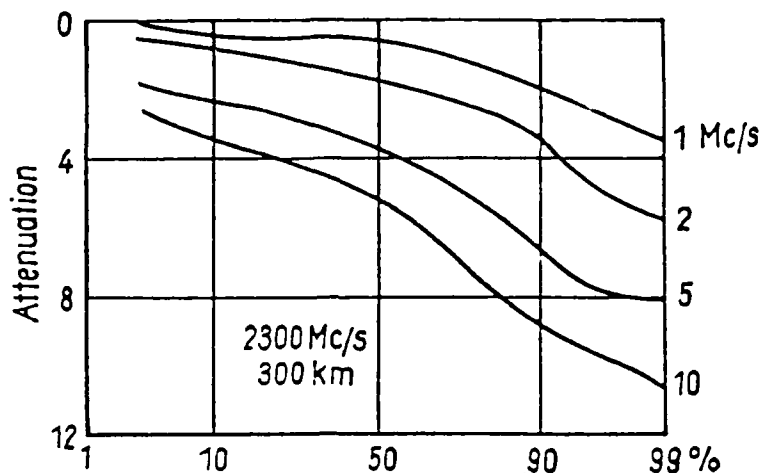
Figure 52. Useable bandwidth as a function of distance and antenna gain

support television transmission was provided as early as 1953 by Tidd [1955]. Adaptive processing has, on the other hand, diminished the limitations of bandwidth on digital troposcatter schemes allowing data rates exceeding 10 Mbps.

Explaining the comparatively small capacity of an analog troposcatter channel, one must again look at the propagation mechanism. Atmospheric multipath, produced by the random disposition of common volume scatterers, causes time variations in portions of the received signal. This, as mentioned,

introduces frequency selective fading in the frequency domain and delay spread in the time domain. Within the correlation bandwidth, frequency selective fading is not a concern since "all the frequency components of a signal would maintain substantially fixed relative amplitude and phase relationships and fluctuate practically in step" [Baghdady, 1970, p. 3]. This correlation bandwidth is an attribute of the propagation mechanism, and, as such, it is limited by the dimensions of the common volume.

If the transmitted bandwidth exceeds the correlation bandwidth, intermodulation noise on the analog baseband signal increases, decreasing system performance [Panter, 1972, p. 488]. Likewise, delay spread increases, and unless adaptive processing is used, ISI increases on digital systems. Either the correlation bandwidth or delay spread can therefore be used to determine bandwidth. Additionally, due to the volatile nature of the scatterers within the common volume, it should be evident that bandwidth will exhibit variability. This gives rise to the notion of an instantaneous bandwidth, and, therefore, a distribution of bandwidths as depicted in Figure 53 [du Castel, 1966, p. 72].



Source: du Castel, F. *Tropospheric Radiowave Propagation Beyond the Horizon*. New York: Pergamon, 1966, p. 71.

Figure 53. Distribution of bandwidths. (2.3 GHz, 300 km, 20 m Antennas)

Calculating bandwidth is a simple matter as Hall [1979, p. 144] and Picquenard [1974, p. 43] show. If Δt represents the difference in time between the arrival of the longest and shortest reradiated rays, the bandwidth is $1/\Delta t$. One can use the 2σ figure of the delay power spectrum as Δt and will get a worst case capacity of 2.7 MHz for 370 ns and a best case bandwidth of 20 MHz for 50 ns. Modern test equipment readily provides 2σ values; however, earlier techniques, such as that used by Crawford, Hogg, and Kummer [1959], relied on frequency-sweeps that provided frequency domain representations. Additionally, Gordon [1955] furnishes a way to theoretically calculate bandwidth through trigonometry.

Mentioned distance and antenna gain dependence also merit treatment. Distance dependence is easily explained: as path length increases, common volume dimensions increase, and, therefore, so does Δt (bandwidth decreases). For antenna gain, large beamwidth (low gain) antennas illuminate a large volume with numerous scatterers. As beamwidths decrease, less scatters participate and Δt therefore decreases (bandwidth increases). However, as Section 4.2.4 discusses, coupling loss develops for antennas with 30 dB or more gain; therefore, gain is sacrificed for bandwidth and the engineer must balance the two for an optimum mix [Booker and DeBettencourt, 1955, p. 289; Boithias, 1987, p. 213].

Concluding, it is interesting to note that bandwidth, once isolated as the major impediment to troposcatter applications, has diminished in significance for digital systems due to adaptive processing (see Section 4.3). Through adaptive equalization and implicit diversity, competitive data rates are available. The primary limiter now is power: energy-per-bit to noise power density ratios (E_b/N_0), critical in BER performance (see Section 5.3.11), is directly influenced by transmitter power

and this is physically limited by klystron capabilities [Monsen, 1980].

4.5 Diurnal, Seasonal, Climatic, and Meteorological Variables

This final section focuses on the conditions or variables under which propagation takes place and the impact of those variables on several of the previously mentioned parameters. It may help to define the variables to be discussed:

- a. *Diurnal* variations describe daily changes in link parameters.
- b. *Seasonal* variations describe seasonal (e.g. summer to winter) changes in link parameters.
- c. *Climatic* variations describe the regional differences in parameter values. These are provided in terms of geographical zones or latitude. Appendix F describes the climatic zones considered under troposcatter propagation.
- d. *Meteorological* variations describe weather's influence on link parameters.

Close relationships characterize several of these variations; for this reason, climatic variations are not discussed separately but are included with

diurnal and seasonal variations. Discussion will clarify this treatment.

Regardless of the variable considered, the cause of parameter variation is rooted in atmospheric phenomena. In general, three cases are cited:

- a. Propagation mechanisms may change. Depending on conditions, scatterers within the common volume may resemble small, random, turbulent eddies that produce incoherent scatter thereby increasing short-term fades while possibly lowering the median RSL.⁹ Conversely, under stratification, scatterers may arrange themselves into layers that promote quasi-coherent scatter which provides higher median RSLs and less scintillation.
- b. The entire path may be influenced by refractivity gradient changes which will, through wave bending, alter the position of the common volume. Since there are more scatterers at lower heights the median RSL may improve or degrade. Additionally, on shorter paths, multimode propagation

⁹From Figures 33 and 40 it is evident that incoherent scatter (dominant above about 2 GHz) fades more rapidly. Similarly, from Figure 34 and 40 it is evident that incoherent scatter provides lower RSLs below about 2 GHz.

(Appendix A) may occur or diffraction may dominate. Finally, the intensity of the scatterers within the common volume, as measured by the structure constant (C_N^2 , see Appendix C), will change as the gradient changes and RSL is effected.

- c. Substantial variations in the refractivity gradient may introduce anomalous propagation; while enhancements are possible, normally, RSL will degrade and short-term fading will increase.

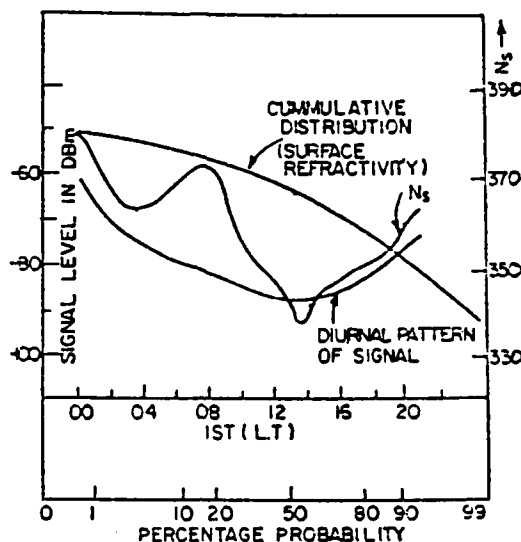
Discussion will show how variables can instigate these events during propagation. For consistency (and for ease of analysis), RSL deviations bear the brunt of parameter analysis. Literature more commonly uses long-term fading, transmission loss, or attenuation from a median value in similar studies.

4.5.1 Diurnal Variations

Daily variations in both RSL and short-term fading rates typify troposcatter links. Generally speaking, the RSL will be lowest in the afternoon and highest in the early morning. For desert climates, hourly median differences of 20 dB between these extremes are common. Temperate zones can show a 10 dB swing; however, equatorial regions exhibit nearly

insignificant changes [Bothias and Battesti, 1983, p. 658; CCIR, 1986, p. 377].

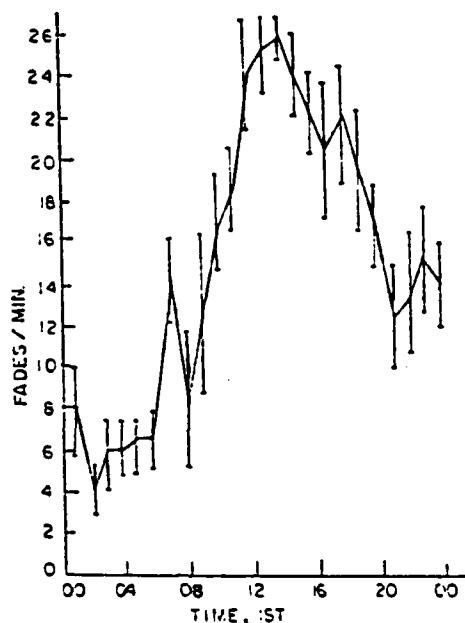
An example of diurnal RSL variation is provided in Figure 54. This link (2 GHz, 240 km in



Source: Sarkar, S.K., Dutta, H.N., and Reddy, B.M. "Development of a Prediction Technique for Tropo-Path Loss from Observed Transhorizon Propagation Characteristics over India." Third International Conference on Antennas and Propagation (ICAP 83), Part 2: Propagation, Institution of Electrical Engineers, London (1983), p. 231.

Figure 54. Diurnal RSL and surface refractivity, N_s , variation. (2 GHz, 240 km link in India)

India) shows swings of 30 dB. Fading rates are also known to vary diurnally, and this is illustrated in Figure 55. While RSLs are lower in the afternoon, fading rates are higher as expected for incoherent scatter dominance (see case (a) above) [Sarkar, Dutta, and Reddy, 1983].



Source: Sarkar, S.K., Dutta, H.N., and Reddy, B.M. "Development of a Prediction Technique for Tropo-Path Loss from Observed Transhorizon Propagation Characteristics over India." *Third International Conference on Antennas and Propagation (ICAP 83), Part 2: Propagation*, Institution of Electrical Engineers, London (1983), p. 232.

Figure 55. Diurnal fading rates. (2 GHz, 240 km link in India)

The causes of diurnal RSL and short-term fading deviations are explained mostly through case (a), with some contributions by case (b). Probably of greatest significance, as mentioned in Section 2.4.1, daily solar heating increases turbulent activity with convection currents bringing turbulent eddies to higher levels; therefore, incoherent scatter occurs. Nighttime movement is obviously reduced and this would increase the likelihood of quasi-coherent scatter. Case (b) is also likely to occur on a diurnal basis. It was demonstrated in Section 2.3.2.1 that daily K-factor (therefore,

refractivity gradient) variations are common. Therefore, the combination of cases (a) and (b), brought on by routine atmospheric phenomena (some of which are cited here), contribute to daily RSL and fading variations.

4.5.2 Seasonal Variations

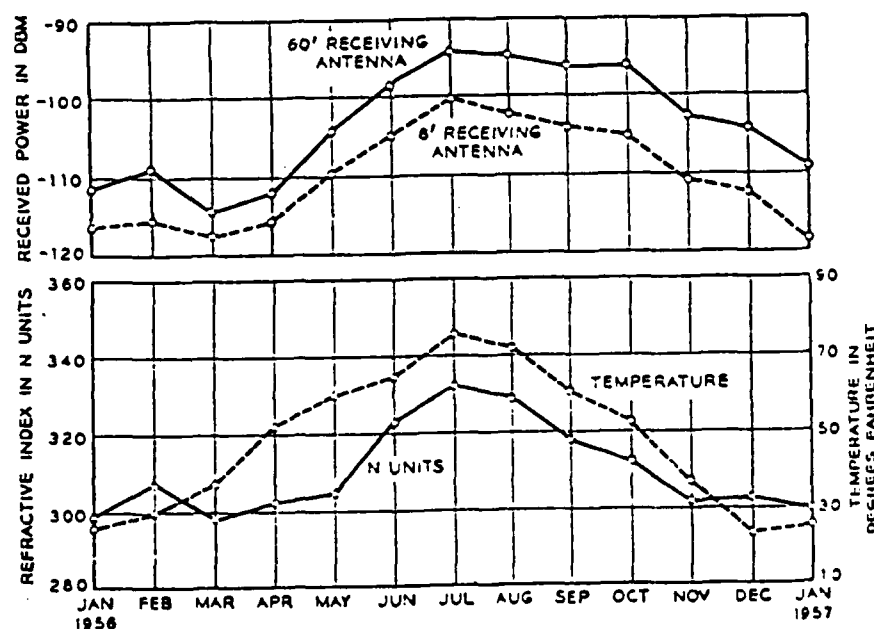
As with diurnal variations, seasonal variations in RSL vary with climate. In temperate zones, RSLs are lower by as much as 15 dB for 150 to 250 km paths in the winter than in the summer. (Notably, diurnal RSL variations are also lower in the winter [CCIR, 1986, p. 377].) The opposite is true for desert regions where RSLs are lowest during the hottest season. Tropical zones exhibit minimum RSLs during the rainy season, whereas monsoon climates provide lowest RSLs during the rainy and dry seasons. In all cases, the influence of seasonal variation diminishes with path distance [Boithias and Battesti, 1983, p. 658]. For purposes of analysis, seasonal variations are divided among eight time blocks as provided in Table 4; time block 2 is most often used as it provides worst case figures for temperate climates [Freeman, 1975, p. 267].

Table 4. Seasonal Variation Time Blocks

Number	Month	Hours
1	Nov-Apr	0600-1300
2	Nov-Apr	1300-1800
3	Nov-Apr	1800-2400
4	May-Oct	0600-1300
5	May-Oct	1300-1800
6	May-Oct	1800-2400
7	May-Oct	0000-0600
8	Nov-Apr	0000-0600

Source: Freeman, R.L. *Telecommunication Transmission Handbook*. New York: John Wiley & Sons, 1975, p. 267.

An example of seasonal RSL variation for a 4.1 GHz, 171 mile link in the northeastern portion of the U.S. is given in Figure 56. Also depicted is a



Source: Crawford, A.B., Hogg, D.C., and Kummer W.H. "Studies in Tropospheric Propagation Beyond the Horizon." *The Bell System Technical Journal*, vol. 38, no. 5 (September 1959), p. 1088.

Figure 56. Seasonal RSL, temperature, and surface refractivity variations. (4.1 GHz, 171 mile link in northeastern U.S.)

close correlation between RSL and surface refractivity, N_s . This analysis may be misleading since changes in the refractivity gradient along the entire path and within the common volume, as in case (b), explain seasonal variations.¹⁰

To clarify, one may analyze any region where certain months display higher humidity and temperature. Humidity (the measure of water vapor content) and temperature variations will effect refractivity as noted in expression (2-3). Water vapor variations are by far the largest contributor; therefore, during periods of high humidity refractivity will increase. Evidently, this increase (or a subsequent seasonal decrease) is not proportionally distributed with height and, therefore, the refractivity gradient, $\Delta N/\Delta h$, differs from its median (-40 N units/km for the first kilometer of height). Super-refraction will occur (displacing the common volume downward where more scatterers are found), and scatterer intensity as

¹⁰From Figures 54 and 55, one might conclude that surface refractivity is a reasonable indicator of RSL deviations. In numerous situations, it is [Bean and Dutton, 1966]. However, one must remember that troposcatter propagation is influenced by gradient changes along the path and within the common volume; therefore, the refractivity gradient and structure constant are the best measurable indicators of RSL deviations.

well as population will increase. The cumulative result of super-refraction and scatterer variations is improved RSLs during more humid periods. CCIR Report 563-3 [1986] provides evidence of seasonal gradient variation in Figures 5 through 8 of that report. In short, seasonal variations within the atmosphere alter the refractivity gradient generating a case (b) situation.

Finally, the distance dependence (less seasonal influence with longer path distance) is explained through the displacement of the common volume to greater heights as path distance increases [Boithias, 1987, p. 208]. Although gradient changes may reduce this height, less scatterers are present than for a comparable shorter link. In effect, a change in RSL will occur for both links (in this case, an increase) but will be proportionally less for the longer of the two.

4.5.3 Meteorological Variations

Research provided little material addressing the effects of weather on troposcatter performance. Most efforts concern the diurnal and seasonal deviations mentioned above. This is predictable; theoreticians and engineers are more concerned with

long-term performance. However, users express concern only when the system fails to support requirements. Assuming proper equipment maintenance, the engineer must be aware of the weather conditions sponsoring degradations, and, somehow, he must explain this to the user. This section will attempt to help the engineer in this unenviable position.

Discussion thus far has described typical diurnal and seasonal climatic variations. The introduction of temporary weather effects may, however, radically alter traditional performance. While there are a variety of weather phenomena, analysis boils down to refractivity; specifically, anomalous propagation. Section 2.3.2.2 discussed anomalous propagation, a brief summary follows:

- a. Subrefraction - When the refractivity gradient exceeds the norm (greater than -40 N units/km) wave bending is decreased.
- b. Super-refraction - When the refractivity gradient is less than the norm (less than -40 N units/km) wave bending is increased.
- c. Ducting - As gradient values less than -157 N units/km are encountered, surface or elevated ducting occurs.

Any one of these events will signal the onset of case (c) degradations (or possibly enhancements, but these will be ignored). The key is to determine the weather event(s) that produces these anomalies. Such events were also briefly discussed in Section 2.3.2.2. This treatment will include that information with some amplification.¹¹

4.5.3.1 Subrefraction

Under Type A conditions (surface temperatures exceeding 30° C and relative humidity below 40%), convection currents will raise layers of high humidity and, therefore, water vapor concentrates at increased heights. This most often occurs in the late afternoon. Type B conditions (surface temperature between 10° and 30° C and humidity exceeding 60%) will occur mostly in the early morning "in constant trade wind and sea breeze areas where differential heating of land and sea results in advection of air which is warmer and more humid than the normal surface layer" [Brauburger, 1979, p. 27].

¹¹The conditions producing super-refraction can, depending on severity, invoke surface ducts. Additionally, the simultaneous occurrence of sub- and super-refractive conditions may create elevated ducts. In both instances, propagation can deviate substantially and degrade troposcatter performance. Section 2.3.2.2 should be referenced for further information on ducting.

It's apparent that Type B conditions also occur when weather fronts are present. The net effect of Type A or B conditions is an increase in density, primarily water vapor content, with height producing an increase in the refractivity gradient. This action will redefine the common volume to higher levels where scatterer population decreases [Brauburger, 1979].

4.5.3.2 Super-Refraction

Figure 8 indicates that within the troposphere temperature normally decreases with height. If, however, "cooler air either passes over or develops over a warm body of water or over warm moist soil" a *temperature inversion* will occur [Brauburger, 1979, p. 24]. Hence, temperature rises with altitude producing large density decreases with height. This can occur at night as the water or ground cools faster than the air, or can occur anytime a cold front moves into an area. Another weather phenomenon, *subsidence*, develops when the dry air mass of a high pressure system slowly settles from high altitude. "This air mass is warmed by adiabatic compression, over-laying and trapping a cooler air mass saturated by surface moisture" [Brauburger, 1979, p. 25]. In both instances,

density decreases with height much more than normal. This will decrease the refractivity gradient, more bending will occur, and troposcatter propagation can be severely degraded. Clues toward recognizing super-refractive conditions include cold front activity and low altitude layering of smoke, haze, or mist [Brauburger, 1979].

From a more general perspective, it should be apparent that weather fronts can provide poor propagation conditions. Albrecht [1967] reports RSL decreases by as much as 24 dB with the passage of cold fronts (900 MHz, 278 km link). Occlusions, formed as a cold front overtakes a warm front, provide similar effects. Additionally, thunderstorms within the common volume produce results much like a cold front. Since rain attenuation at troposcatter frequencies is, for the most part, negligible, thunderstorm degradation is better described by case (b): as the storm moves through the common volume, gradient changes will alter the intensity of the scatterers. On the other hand, compared to cold fronts, warm fronts have a less pronounced influence. Speculatively, if a link is located on a slow moving or stationary front, prolonged degradation is likely.

Summarizing, a variety of weather effects influence troposcatter propagation; however, the key determinant is refractivity gradient changes. Thus, determining meteorological influences on troposcatter propagation is difficult. Accurate real-time analysis is hampered by the need to accumulate and correlate RSL and gradient data. Additionally, using visual or generalized indicators such as haze layers, fronts, costal breezes, and subsidence is, at best, guesswork. Finally, while surface refractivity measurements are easily obtained and known to correlate with RSL deviations, noted limitations (du Castel [1966, p. 80] and Hall [1979, p. 180]) introduce speculation that prohibits complete reliability (see also footnote 10, this chapter). The accumulation of more empirical studies, termed *radiometeorology*, is neatly summarized in CCIR Report 563-3; however, the focus is rather general, and not specific to troposcatter propagation.

The author has, on several occasions, experienced the frustrations of weather oriented degradations on tactical military systems. Links that normally performed well were degraded for periods of several days, and, at least from a military perspective, this is unacceptable. In this

situation, analysis is worthless: operations were conducted regardless of the predicament faced by communications personnel; furthermore, in austere locations, meteorological data giving gradient behavior is unobtainable. There is a need for the development of systems whose attributes mirror troposcatter (comparatively long range, high quality, multichannel, and cost effective). Although the AN/TRC-170 mentioned earlier offers improved capability, it cannot avoid the effects of extreme super-refraction or ducting. Until development of such a system, the user would be well advised to "wait until the weather changes."

CHAPTER 5

TROPOSCATTER PREDICTION TECHNIQUES

5.1 Introduction

Armed with the knowledge provided in preceding chapters, one might suspect that predicting troposcatter link performance is difficult. Due to atmospheric complexity, troposcatter propagation offers a variety of deviations through multipath, diurnal, seasonal, climatic, and meteorological conditions. On top of this, it is known that the mechanism for propagation can include a mix of diffraction, incoherent scatter, and quasi-coherent scatter depending on such variables as path distance, operating frequency, and atmospherics. However, certain situations dictate the use of troposcatter. Thus, the engineer must have a tool for analyzing the feasibility of the proposed link to support requirements.

Fortunately, there is a simple and quite reliable tool available. Unfortunately, the single variable needed to use this tool, the refractivity gradient within the common volume, is difficult to

obtain. (This technique, the Radiometeorological method, will be discussed later.) Therefore, an assortment of methods have been proposed, most of which rely on empirical, statistically oriented relationships established through a rather massive accumulation of data [Hall, 1979, p. 135].

The shortcomings of these experimentally derived techniques are readily apparent: no single method can encompass the multitude of variables impacting propagation in all areas of the world. Recognizing this problem, several techniques include uncertainty parameters which project the confidence which one can place in the prediction. Additionally, with the advantage of small, powerful computers one can provide these predictions rather rapidly, but, naturally, the product is only as good as the method employed and the data input. In short, the prediction must be viewed as an estimate, not absolute in accuracy since the result is rooted in statistical analysis [Military Handbook, 1977, p. 4-321].

5.2 Prediction Preparation

Assuming the selected technique provides suitable accuracy, one must be adequately prepared to begin the prediction. This first step, the

accumulation of data, is the most time consuming and critical step in troposcatter propagation prediction. An initial desktop analysis supplemented by an actual site survey provides inputs to include great circle calculations, path profiles, and, most importantly, antenna elevation angles. In addition, such variables as antenna height, sources of interference, location of the common volume, and typical meteorological conditions supplement the list of necessary data. In this treatment, it is assumed that this necessary first step is completed. An excellent document describing data accumulation is *Military Handbook, Facility Design for Tropospheric Scatter* [1977].

5.3 Prediction Techniques

The "granddaddy" of troposcatter prediction tools is *Transmission Loss Predictions for Tropospheric Communication Circuits* (Rice, P.L., et al. [1967]) commonly referred to as NBS Tech Note 101 (TN 101). This document, first published in 1965, accumulated data from many years and consolidated related studies (most notably Barsis, Norton and Rice [1961, 1962] and Gordon [1955]). Additionally, *Military Handbook, Facility Design for Tropospheric*

Scatter [1977] uses the same technique provided in TN 101.

CCIR Report 238-5 offers three techniques. Method I is a simplified version of TN 101. Method II reflects the work of Boithias and Battesti [1983]. Finally, the Chinese method appears in Annex II of the CCIR report. Notably, the earlier mentioned Radiometeorological method appears in Report 238-4 but not in the more recent, 238-5 version (it was moved to Report 718-2).

A newer technique, based on the ideas of Parl [1979] and Monsen, et al. [1983], still use portions of TN 101. However, whereas TN 101 is rather limited in application (explained in Section 5.4), this more contemporary approach incorporates variability through the spectrum function. Additionally, aperture-to-medium coupling loss is calculated in more precise terms. Finally, calculations emphasize the incoherent scatter mechanism as this provides worst case analysis. The brunt of this effort was funded through a military contract and focuses on military systems; however, the basic approach is applicable for all troposcatter systems. Although most work was done through contract with SIGNATRON, Inc., this tool is termed the Parl method in

deference to Dr. Steen A. Parl's [Parl, 1979] earlier efforts; note also that Parl co-authored the 1983 SIGNATRON document [Monsen, et al., 1983].

Additionally, the MITRE Corporation specialized the Parl method for the AN/TRC-170 military tactical LOS/troposcatter terminal. Hence the MITRE method is limited mostly by frequency (4.4 to 5 GHz) and equipment (the DAR modem).

A collection of other methods are available. These include the Yeh, Rider, Collins, Bullington, MIT, RCA, Page, ITT, and Longley-Rice models. The first four will be discussed. The remainder (except Longley-Rice which is a computerized version of TN 101) are briefly considered by du Castel [1966, pp. 209-213].

Before selecting a method, one must be aware that some techniques may exclude several important factors. These include atmospheric absorption, intermodulation noise, delay spread, aperture-to-medium coupling loss, diversity improvement, short-term fading, and diurnal and seasonal effects. As an example, the brief description of the system equation in Appendix B provides the essential ingredients of TN 101. After some scrutiny, the reader will observe the inclusion of coupling loss and absorption;

however, other factors such as diversity improvement and delay spread (if digital) are absent and can be overlooked. This is not a criticism of TN 101 since this technique is one of the most thorough offered. It is imperative, however, that the engineer be aware of the applicability of the selected method, making adjustments as needed. As a final word of caution, other techniques, not listed here, exist and perform well in specific situations; in short, beware of site specific tools.

The remainder of this section provides a brief look at most of the prediction methods listed above. It will highlight the concepts incorporated in several of these techniques and, for others, it will provide the actual calculation. This approach is taken for brevity and simplicity: TN 101 and the Parl methods are complex and rather intimidating whereas the others are easily understood.

5.3.1 TN 101

Using data accumulated in the 1950's and early 1960's, the authors of TN 101 developed empirical models "for the estimation of the cumulative distribution of annual hourly median transmission loss as a function of frequency and path geometry" [Crane, 1988, Appendix A, p. 3]. Critical

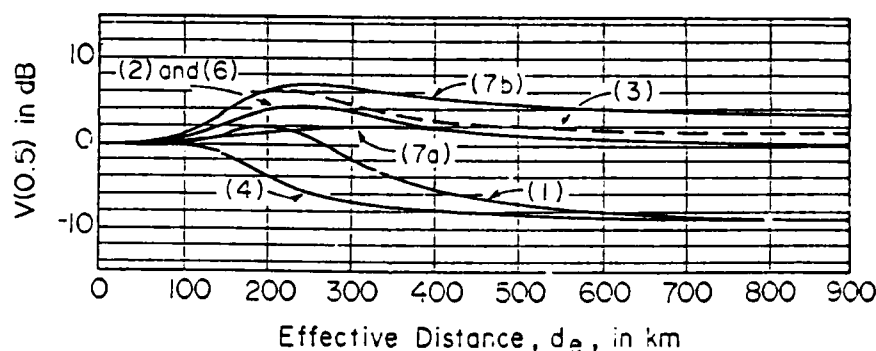
in this approach is the description of hourly, long-term median RSL which, as shown through long-term fading in Section 4.2.3.2, displays a log-normal power density function. A standard deviation of nearly 6 dB is noted, and this deviation gives cause for the development of confidence measures [Christopher and Debroux, 1987, p. 43.3.4]. Before the calculation of confidence measures, however, TN 101 considers the reference basic transmission loss (L_{bsr}) given in Appendix B, expression (B-6). Although simplistically presented, calculations for L_{bsr} entail much greater complexity. Regardless, for the pure troposcatter propagation mode (TN 101 also analyzes multimode and diffraction paths), the calculation is then extended to accommodate the desired *time availability* and *service probability*.¹

For simplicity, it is assumed that L_{bsr} is calculated as described in Appendix B. From there the following is applied:

$$L_n(0.5, 50) = L_{bsr} - V_n(0.5, 50) \quad (5-1)$$

¹When this is done, the system equation of Appendix B (equation (B-1)), which is an expression of the power required for a specified carrier-to-thermal noise ratio at *any instant in time*, is modified as described in *Military Handbook* [1977, pp. 4-174 to 4-177].

where $L_n(0.5, 50)$ describes the basic transmission loss with a service probability of $Q = 0.5$ and a time availability of $q = 50\%$. A time availability of 50% signifies that the path loss will meet or exceed L_n half of the time. A service probability of 0.5 indicates that half of a sample of links under identical conditions will meet the specified time availability. The term $V_n(0.5, 50)$ is a climate-variation factor. It is provided in Figure 57 for climate zones (subscript n) defined in Appendix F [Freeman, 1987, pp. 146-178].²

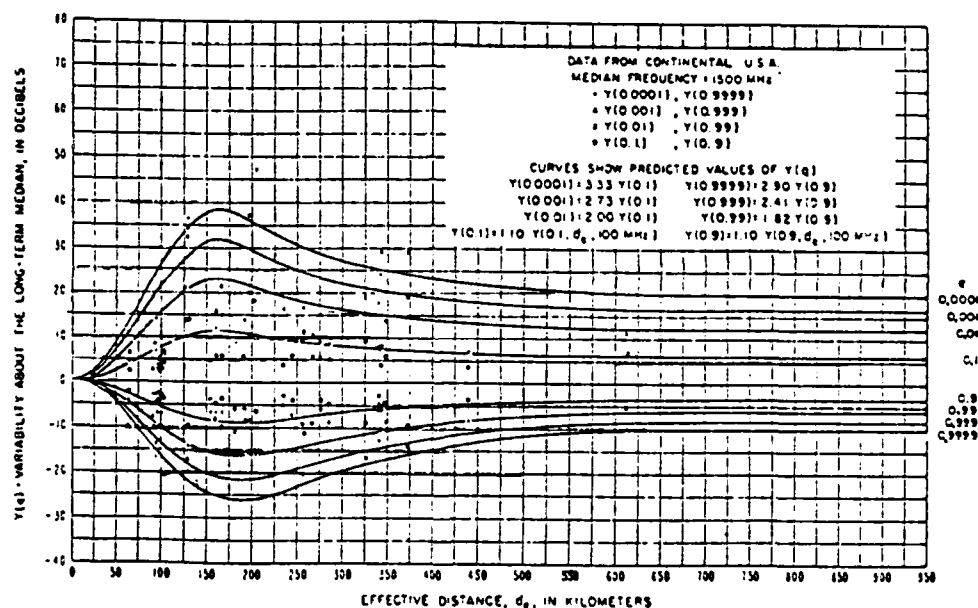


Source: Military Handbook, Facility Design for Tropospheric Scatter (Transhorizon Microwave System Design). MIL-HDBK-417, Department of Defense, Washington, DC, 25 November, 1977. Available through Navy Publications and Forms Center, ATTN: NPODS, Office of Navy Publications, 5801 Tabor Avenue, Philadelphia, Pa., 19120-5094, p. 4-154.

Figure 57. Climate-variation factor as a function of effective distance and climate type.
(Code numbers provided in Appendix F)

²Figure 57 uses different nomenclature for the climate-variation factor. This difference stems from terminology, and is not consequential in this analysis; therefore, consider $V_n(0.5, 50) = V(0.5)$ [Military Handbook, 1977 p. 4-151; Freeman, 1987, p. 178]. The effective distance, d_e , used in Figure 57 is simple to calculate; see Freeman [1987, p. 173].

With $L_n(0.5, 50)$ one now knows the basic troposcatter transmission loss exceeded 50% of the time for 50% of all links under similar conditions. This grade of service is unacceptable for most applications; therefore, time availability and service probability are scaled-up to desired levels. A simple approach to extend time availability is realized through curves similar to Figure 58. An



Source: Freeman, R.L. *Radio System Design for Telecommunications (1-100 GHz)*. New York: John Wiley & Sons, 1987, p. 183.

Figure 58. Long term power fading for continental temperate climate (Region 6), Frequency > 1 GHz

additional loss, $Y_n(q, d_e)$, is found through the curve corresponding to the desired time availability (q , on the far right) and is included in expression (5-1).

A family of such curves for different climates and frequency is available in TN 101; however, as more data accumulates, changes are made [*Military Handbook*, 1977, p. 4-153]. Furthermore, these curves are depicted for general frequency ranges; therefore, a more refined approach, as summarized by Freeman [1987, p. 178], uses a frequency correction factor that can improve accuracy by more than 2 dB.

The service probability, included since there are additional variations for which the model cannot account, is enhanced through the following semiempirical formulas:

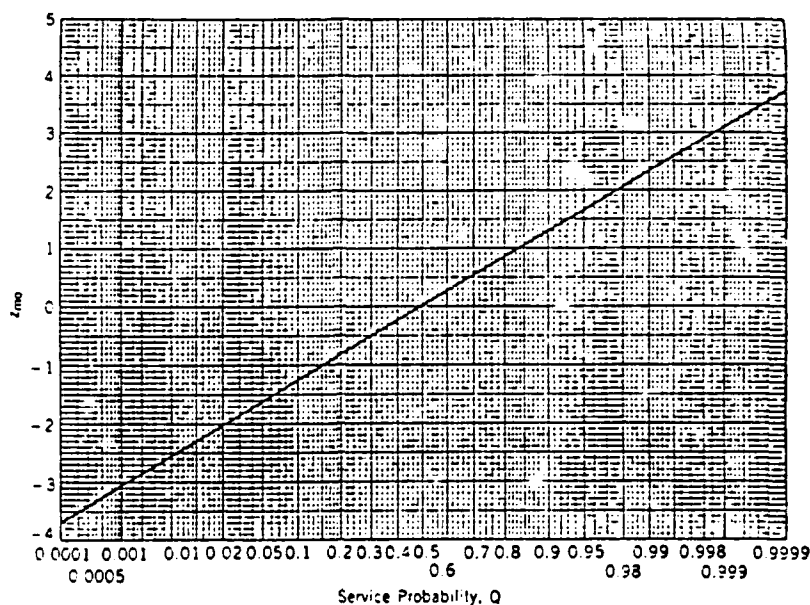
$$\sigma_c^2(q) = 12.73 + 0.12Y_n^2(q, d_e) \quad (5-2)$$

and

$$\sigma_{rc}(q) = (s_c^2(q) + s_r^2)^{1/2}. \quad (5-3)$$

The first step is to solve expression (5-2), using curves similar to Figure 58 for $Y_n(q, d_e)$, giving $\sigma_c^2(q)$, the path-to-path variance between predicted and actual median transmission loss. Next, equation (5-3) is used to find $\sigma_{rc}(q)$, the error between predicted and actual median transmission loss for q percentage of time. s_r^2 is 4 dB² for new links and 2 dB² for established ones.

Finally, $\sigma_{RC}(q)$ is multiplied by the standard normal deviate, $z_{mo}(Q)$, given in Figure 59. One



Source: Freeman, R.L. *Radio System Design for Telecommunications (1-100 GHz)*. New York: John Wiley & Sons, 1987, p. 195.

Figure 59. The standard normal deviate

simply selects the desired service probability, Q , finds the product $z_{mo}(Q)\sigma_{RC}(q)$, and gets a value in dB that must be included in expression (5-1) along with the scaled-up time availability factor $Y_n(q, d_e)$. The result is a prediction yielding the desired time availability, q , and service probability, Q .

Normally, $Q = 0.95$ and $q = 99.99\%$ for high quality transmission; obviously the transmission loss for $L_n(0.95, 99.99)$ will increase from the original $L_n(0.5, 50)$ [Freeman, 1987, pp. 193-197].

Despite this admittedly shallow treatment of TN 101, one should now understand the fundamental concept used in this prediction tool. That is, if enough data is accumulated on a variety of troposcatter links, empirically derived models will afford adequate prediction. Further, recognizing inherent shortcomings, estimates should include time availability and service probability to bolster the confidence of the prediction. Affirming this summary, a family of curves, similar to Figure 58, as well as a climate-variation factor (Figure 57) characterize TN 101's underlying approach.

5.3.2 CCIR Method I

A "short course" in TN 101 is offered by the first CCIR prediction technique, CCIR Method I. Although no match for TN 101's laborious calculations, resulting predictions are close enough to make it perhaps the most popular of all tools. If compared with expression (B-6) in Appendix B, one will note many similarities in this method's fundamental formula:

$$L(50) = 30 \log f - 20 \log d + F(qd) - G_t \\ - G_r + L_c - V(d_e) \text{ (dB)}. \quad (5-4)$$

For convenience, components are again delineated:

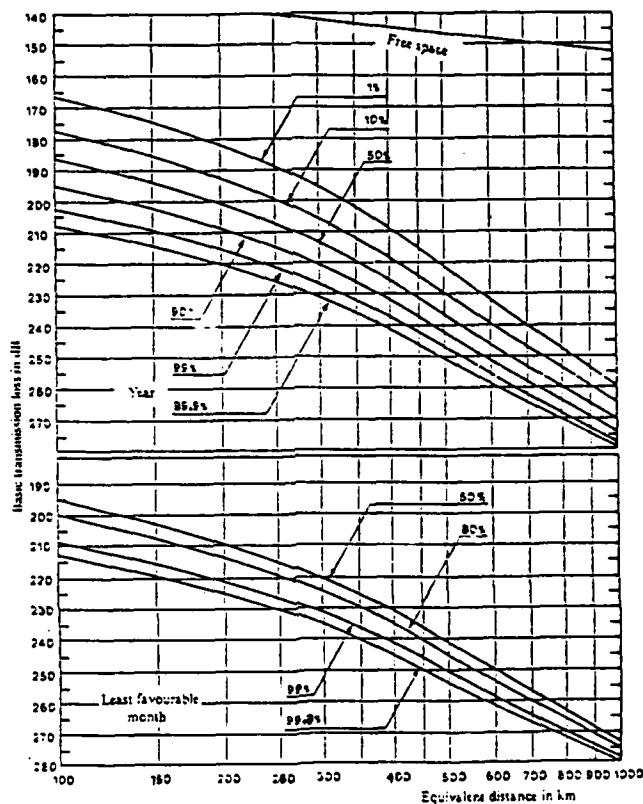
- f operating frequency in MHz,
- d path length (km),
- $F(qd)$ the attenuation function (see Appendix B, Figure B3),
- G_t, G_r transmit and receive antenna gains (dB),
- L_c aperture-to-medium coupling loss (see Section 4.2.4, expression {4-3}), and
- $V(d_e)$ the climate-variation factor (see Section 5.3.1, Figure 57).

After solving for $L(50)$, CCIR Method I uses a similar yet simpler time availability and service probability technique than TN 101 to establish prediction confidence.

5.3.3 CCIR Method II

At about the same time as the first publication of TN 101, Boithias and Battesti completed work on an easy-to-use technique based on worst month statistics. This graphical method requires knowledge of "the equivalent path distance. . . , the time percentage required, the type of climate, and the frequency" [Hall, 1979, p. 142]. CCIR Report 238-5 incorporates this tool as CCIR Method II.

Using Figure 60, the basic transmission loss ($L\{q\}$) for the least favorable month at a selected time availability is derived. There are three other



Source: Balmain, L. *Radio Wave Propagation*.
St. Louis: McGraw-Hill, 1987, p. 204.

Figure 60. Mean attenuation, overland path, temperate climate, 1 GHz

such curves, one each for humid tropical, equatorial, and desert climates. These curves are for a 1 GHz path with zero degree elevation angles. For other frequencies (less than 5 GHz), a factor of $30\log f$ (GHz) is added. In addition, the term $20\log(d/d_0)$ is included where

$$d_q = d + 8.5(\theta_1 + \theta_2). \quad (5-5)$$

d_q is the equivalent path distance (km), and, again, d is the path distance (km). θ_1 and θ_2 are the elevation angles of the transmit and receive antennas respectively. Summarizing, for calculation of the actual transmission loss

$$L(q) = l(q) + 30 \log f + 20 \log (d/d_q) - G_{\text{eff}} \quad (5-6)$$

where Figure 47 provides the effective gain (G_{eff}) which is the sum of both antenna gains and the coupling loss [Roda, 1988, pp. 125-129; CCIR, 1986, pp. 372-376].

5.3.4 The CCIR Chinese Method

Researchers in China have suggested use of the following empirical formula (in dB):

$$L(50\%) = 30 \log f + 30 \log \theta + 10 \log d - G_{\text{eff}} + 124.6 - 0.08(N_s - 320) + N(H). \quad (5-6)$$

Here, f is the operating frequency in MHz, θ is the scattering angle in radians, d is the path distance in km, G_{eff} is the effective gain from Figure 47, and N_s is the annual mean surface refractivity value. Additionally,

$$N(H) = 20 \log(5 + 0.3H) + 0.65H \quad (5-7a)$$

and

$$H = \theta d_1 d_2 / d \quad (5-7b)$$

with d_1 and d_2 being the distances from each antenna to the crosspoint of the radio horizon rays (at the lowest portion of the common volume). Additionally, this method calculates the variability of the hourly median losses. In this instance, these are also shown to be log-normally distributed but standard deviations, σ , are given through terminal location, radio horizon path distance (d_s), and the difference between mean summer and winter surface refractivity (ΔN_s) [Roda, 1988, pp. 132,133; CCIR, 1986, pp. 386,387] (in dB):

$$\sigma = 7.0 + 0.09\Delta N_s \exp(-0.003d_s) \text{ (flat areas)} \quad (5-8a)$$

$$\sigma = 4.6 + 0.06\Delta N_s \exp(-0.003d_s) \text{ (mountains)} \quad (5-8b)$$

$$\sigma = 8.8 + 0.11\Delta N_s \exp(-0.003d_s) \text{ (over the sea)} \quad (5-8c)$$

5.3.5 The Radiometeorological Method

The work of Battesti and Boithias, along with a third cohort (P. Misme), was again recognized by the CCIR in report 238-4 for efforts in troposcatter prediction. Recognizing that refractivity gradient changes will not only displace the position of the common volume but also alter the intensity of individual scatterers, their efforts produced an

exceptionally accurate technique termed the Radiometeorological method [CCIR, 1982, p. 137; Boithias and Battesti, 1983, pp. 659,660]. While it has been stressed that the best indicator of troposcatter performance loss is the gradient, this is a parameter of substantial variability and is, currently, impossible to model for every conceivable path. Regardless, if one knew the yearly gradient variations within the proposed link's common volume, he would apply

$$L(\text{dB}) = 30 \log f + 30 \log d + 102 + 1.5G_c \quad (5-9)$$

using f , the operating frequency in MHz; d , the path length, in km; and G_c , the common volume's gradient, in N units per km. Obviously, $L(\text{dB})$, the basic transmission loss, is only as accurate as the sounding data used for G_c .³

Sarma [1988] shows the criticality of this sounding data in the design of a 300 km, 2 GHz link with a common volume situated above Kanpur, India.

³CCIR Report 238-4 recommends referencing the original work of Battesti, Boithias, and Misme ("Calcul des Affaiblissements en Propagation Transhorizon à Partir des Paramètres Radiométéorologiques" {"Calculations of Attenuations in Trans-horizon Propagation from Radiometeorological Parameters"}) in volume 23, number 5-6, pages 129-140 of *Ann. des Télécomm.*) for discussion of gradient soundings.

Using a plane mounted, state-of-the-art refractometer, Sarma obtained accurate refractivity gradient data for winter (worst case) conditions. Then, employing the Radiometeorological method, he compared results obtained through both the airborne configuration and available radiosonde measurements. The result was a discrepancy of nearly 35 dB; the costs of several days of data collection (use of a Cessna 182 H Skylane) are probably going to be less than the savings in transmitter configuration. Thus the importance of sounding data is demonstrated, and the advantages of the Radiometeorological method are well represented.

5.3.6 The Parl Method

It has now been well established that prediction accuracy largely depends on knowledge of the refractivity gradient within the common volume. However, many techniques, such as TN 101, do not stress this parameter due to its variability and simply assume a specific value. This, according to Parl [1979], limits prediction reliability. However, if one were to focus on activity within the common volume, specifically, the spectrum function (see Appendix C), accuracy would improve. This is the feature of the Parl method since the structure

constant (C_N^2) is known to relate directly to changes in the refractive index, and, further, since values of the spectrum slope (m) indicate whether incoherent or quasi-coherent scatter dominates [Eklund and Wickerts, 1968; Sarker, Dutta, and Reddy, 1983].⁴

Noting variability in the spectrum function, Monsen, et al. [1983] overhauled portions of TN 101 to include values of the spectrum slope and structure constant that allow accurate predictions for virtually all types of troposcatter systems. Parl [1979] mentions that TN 101 uses a spectrum slope of $m = 5$ which corresponds to quasi-coherent modes, he then adds that at $m = 11/3$, incoherent scatter dominates. Incorporating this mechanism would yield *more accurate predictions*, since many systems use higher frequencies and incoherent scatter dominates above about 1 GHz; or *more conservative analysis*, since, even at lower frequencies, turbulent atmospheric conditions may temporarily foster the notably poorer performing incoherent scatter mechanism. Then, using $m = 11/3$, Monsen, et al.

⁴The MITRE method incorporates the Parl method for specific application to the military tactical AN/TRC-170 terminal. Documents explaining the MITRE method include Dube and Hotzel [1985], Coirin and Kessler [1987], and Neuburger, et al. [1985]; however, these publications are limited in distribution.

[1983] developed an expression for C_N^2 (see expression {C-2a} of Appendix C) that allows calculation of path loss in a manner similar to TN 101 (similar method, different results). Notably, however, the Parl method allows use of any spectrum slope value since it is available on a rather flexible computer program called TROPO.

Another concept introduced in the Parl method highlights aperture-to-medium coupling loss. Basically, Parl [1979] asserts that coupling loss has been incorporated in other techniques (TN 101 for example) as an "afterthought" when, in reality, volume integrations used to derive path loss calculations must also account for narrow beamwidths.⁵ This is because most initial calculations feature integrations for wide beamwidth antennas which illuminate more scatterers, then, if narrow beams are used, only antenna gain and empirically derived coupling loss formulas are manipulated without regard to the initial integration. The error of this approach is readily seen; furthermore, in the majority of situations,

⁵This thesis has purposely avoided integral formulas; however, the basic methodology of all techniques begins with an integration of the scatterers within the common volume.

this aspect is a more significant differentiator than the variability of the spectrum slope.

Along with the advantage of being computer based, the Parl method also includes:

- a. Calculations for a variety of climates to include those delineated in TN 101 or any user defined zones.
- b. Computations for horizon angles, antenna elevation angles, antenna heights, diversity separations, coherence bandwidth, and yearly path loss and RSL distributions.
- c. The ability to analyze multimode paths.
- d. Performance predictions for specific modems (DAR and the MD-918, used on military systems) as well as delay spread calculations.
- e. Time availability and service probability analysis.

Again, however, it bears mentioning that the accuracy of this method is only as good as the data input. Furthermore, the uncertainty of the values used for the spectrum slope, as highlighted in Appendix C, once more introduces prediction skepticism since the Parl method performs only singular calculations for specific spectrum slope values. Echoing this

concern, Crane [1981a, 1981b] projects that only when accurate C_N^2 profiles are available will prediction accuracies substantially improved.

5.3.7 The Yeh Method

In 1960, Dr. Luang P. Yeh offered a simple prediction tool (in dB):

$$L_{mp} = 30 \log f + 20 \log d + 10\theta + L_C - 0.2(N_S - 310) + 57. \quad (5-10)$$

The parameter breakout for this calculation of the median path loss, L_{mp} , follows: f , operating frequency, in MHz; d , path length in miles; θ , scattering angle, in degrees; L_C , coupling loss; and N_S , the surface refractivity [Panter, 1972, p. 393; Freeman, 1987, p. 268].

5.3.8 The Rider Method

C. C. Rider's 1962 solution for the median path loss is as follows:

$$L_{mp} = 30 \log f + 30 \log d + 50 \log \theta + L_C - 0.43(N_S - 330) + 49 \quad (5-11)$$

where f , d , θ , and N_S are the same as in Yeh's method. Rider did not initially include coupling

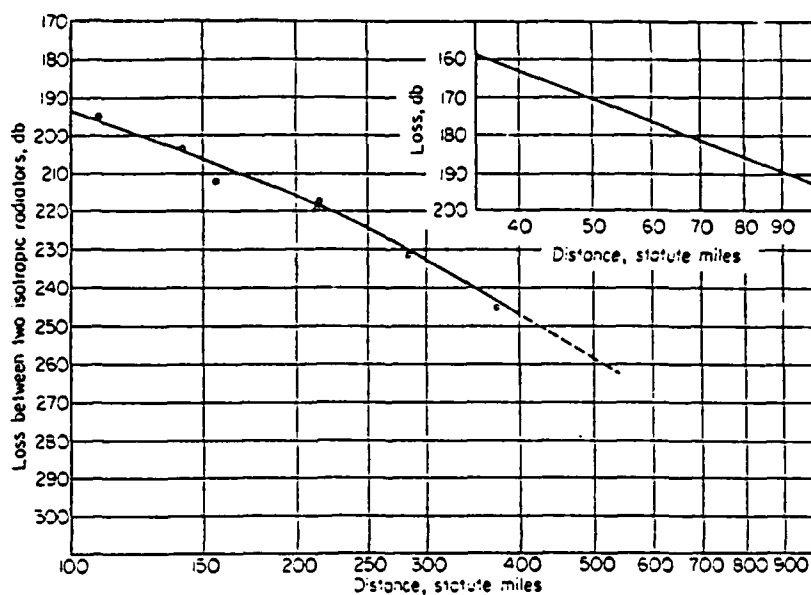
loss, L_C ; however, it is included here for comparative purposes [Panter, 1972, p. 394].

5.3.9 The Collins Method

Another prediction tool is the U.S. Army's quick and easy Collins method as developed by the Collins Radio Company. This totally graphical technique exhibits surprising accuracy through the use of four graphs (Figures 61 through 64). By adding the values obtained from all four graphs, Collins offers field expediency typifying tactical, on-the-move military communications [Panter, 1972, p. 394].

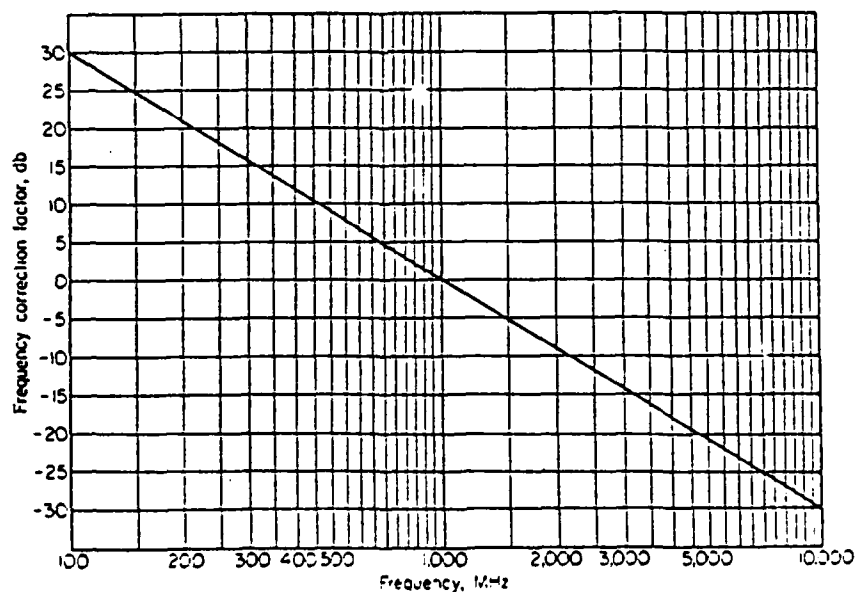
5.3.10 The New Bullington Model

The concept of using a combination of scatter and mode theories in predicting troposcatter propagation was offered by Bullington in 1963. This was discussed in Section 3.5 where it was pointed out that not much was done to further this idea. Two employees of the MITRE Corporation, Christopher and Debroux [1987], have reexamined Bullington's ideas, adding foreground reflection and diversity considerations to the hypothesis that predictions can be based on an exponentially varying refractivity profile. The result is a computer driven prediction



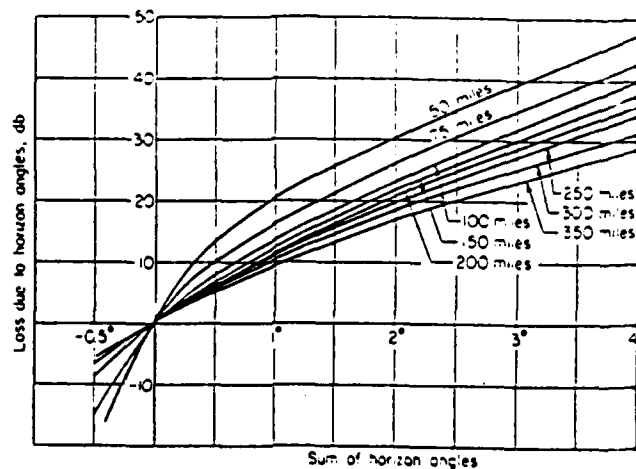
Source: Panter, P.F. *Communication Systems Design: Line-of-Sight and Tropo-Scatter Systems*. St. Louis: McGraw-Hill, 1972, p. 395.

Figure 61. Collins method: Basic propagation loss at 1 GHz



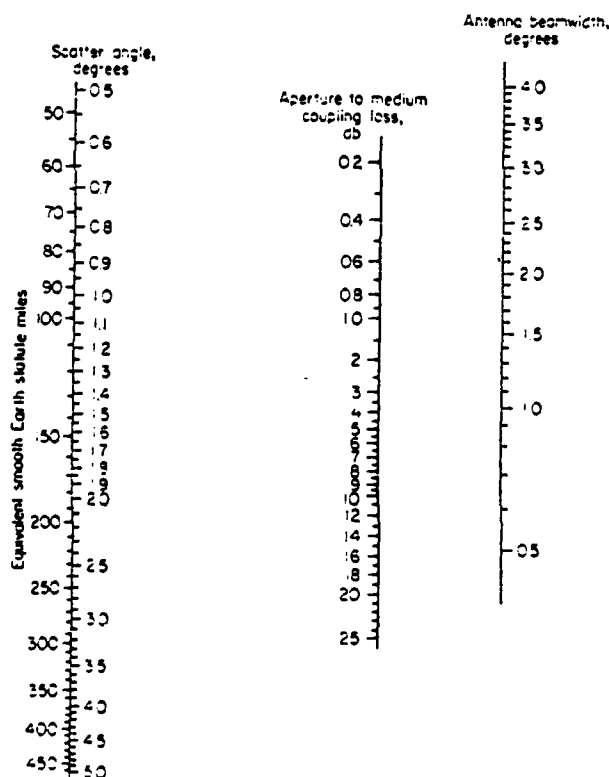
Source: Panter, P.F. *Communication Systems Design: Line-of-Sight and Tropo-Scatter Systems*. St. Louis: McGraw-Hill, 1972, p. 396.

Figure 62. Collins method: Frequency correction curve



Source: Panter, P.F. *Communication Systems Design: Line-of-Sight and Tropo-Scatter Systems*. St. Louis: McGraw-Hill, 1972, p. 396.

Figure 63. Collins method: Horizon angle loss



Source: Panter, P.F. *Communication Systems Design: Line-of-Sight and Tropo-Scatter Systems*. St. Louis: McGraw-Hill, 1972, p. 397.

Figure 64. Collins method: Coupling loss nomogram

tool, simple to use, yet rivaling the accuracy of more complex methods.

5.3.11 Digital Considerations

Completing this compendium of troposcatter prediction tools are digital transmission considerations. In many respects, digital troposcatter transmission systems use the same prediction tools as analog systems. Transmission loss (including coupling loss), path profiles, and antenna siting calculations can use any one of the described tools; however, delay spread and BER analysis, not included above, warrant consideration.

A method to calculate delay spread, as mentioned in Section 4.3, is offered by Freeman [1987, p. 205]:

$$\Delta = 5.21d(\Omega_t + \Omega_r)(4\alpha_o + 4\beta_o + \Omega_t + \Omega_r)10^{-8}. \quad (5-12)$$

Here, d is path length in km, α_o and β_o are the transmit and receive main beam angles corrected for above horizon elevation (α_{oo} and β_{oo} of Figure 5) in radians, and Ω_t and Ω_r are the transmit and receive antenna 3 dB beamwidths in radians. From this calculation one should ascertain the effects of delay spread as discussed in Section 4.3; adaptive processing considerations are essential.

To calculate the expected BER use the following:

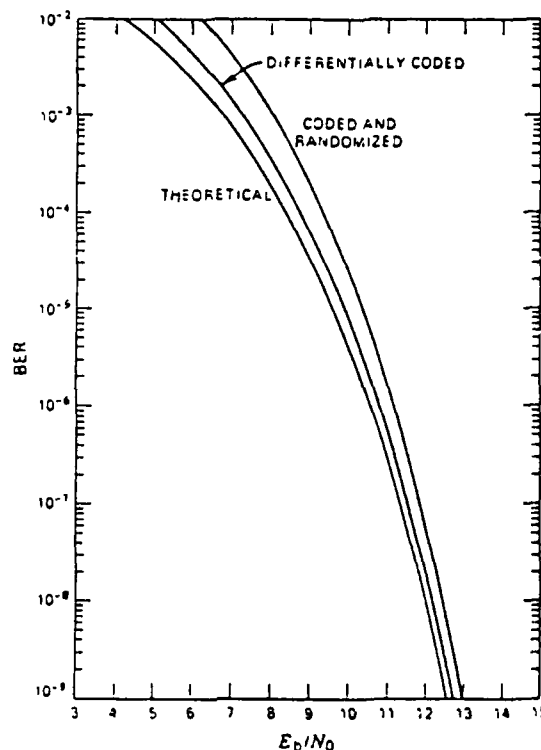
$$E_b/N_0 = RSL_{dBW} - 10 \log(BR) - (204 \text{ dBW} + NF_{dB}) \quad (5-13)$$

This expression for the energy-per-bit to noise power density ratio should be somewhat familiar: BR is the bit rate in bps, NF_{dB} is the noise figure of the receiver or low noise amplifier (LNA), and RSL is determinable through

$$RSL_{dBW} = EIRP_{dBW} - T_L + G_r - L_{Lr}. \quad (5-14)$$

For this equation, the effective isotropically radiated power (EIRP) includes the sum of transmitter power, antenna gain, and miscellaneous device losses (all in dB); T_L is the total transmission loss as determined by a prediction tool; G_r is the receive antenna gain; and L_{Lr} is the line loss to the LNA [Freeman, 1987, p. 214; Flock, 1987].

All that now remains is to find the BER using the calculated E_b/N_0 and Figure 65 (note the effect of different modulation schemes). One may see the importance of accurate prediction in the T_L term of expression (5-14); other factors remaining constant, the accuracy of the predicted BER is contingent on the accuracy of the prediction technique.



Source: Freeman, R.L. *Radio System Design for Telecommunications (1-100 GHz)*. New York: John Wiley & Sons, 1987, p. 215.

Figure 65. Determination of BER for coherent BPSK and QPSK

Furthermore, if delay spread is sufficiently neutralized, the BER is the single most important parameter in assessing digital system performance.

5.4 Comparison of Methods

Based on information presented thus far, it would seem prudent to choose a simple tool such as the Collins or Yeh method. However, simplicity smatters of shortcuts, shortcuts translate into a few dB, and these few dB can be critical in link prediction. A rigorous comparison of all techniques

is not available; furthermore, such an undertaking would be quite laborious and this, compounded with lack of commercial interest, means such comparisons are not likely. Some analysis exists, however, and these will be presented. The intent is to provide the engineer with enough information from which to choose an applicable method. A good way to begin is to analyze the advantages and limitations of proposed techniques.

Discussion will center on TN 101 as it forms the nucleus of many techniques including *Military Handbook, Facility Design for Tropospheric Scatter* [1977], CCIR Method I, the Parl, and the MITRE techniques. The primary advantage of TN 101 is its historical methodology. Years of empirical data are accumulated to provide prediction curves yielding accurate long term median path attenuation. This, however, can be a disadvantage since most data is gathered in temperate climates. Sarkar, Dutta, and Reddy [1983] report large discrepancies between TN 101 predictions and actual data for a link in the Indian sub-continent. Fitzsimons [1968] offers similar criticism with data gathered from an 87 km link in Cyprus.

Crane [1988] also notes that much of the data used in TN 101 is for lower (below 1 GHz) links. These frequency limitations were highlighted earlier: since TN 101 uses a spectrum slope of $m = 5$ and since this corresponds to quasi-coherent scatter which is dominant only at lower frequencies, TN 101 should be cautiously applied above 1 GHz [Parl, 1979]. This, as mentioned, is where the Parl and MITRE methods differ since the more conservative m value of $11/3$ is used (or any other value for the Parl method). Hence, the frequency limits of TN 101 are offset if one uses the similar Parl or MITRE methods. In addition, except for the Parl and MITRE models, all techniques incorporating aperture-to-medium coupling loss incorrectly embody this parameter and this can be exceptionally significant when narrow beamwidths are used. Unfortunately, subsequent calculations for modem performance in these methods are restricted to military systems; extending their use on a more general level would require alteration.

Simplicity is always a consideration and TN 101 and its derivatives (CCIR Method I excepted) do not offer this luxury. Notably, however, the Longley-Rice, Parl, and MITRE methods are available through computer applications. Further, there is no

reason why any of the models, with the exception of the Collins method, cannot be adapted for computer use. If, however, simplicity is crucial and computer programs are unavailable, any of the CCIR methods or the Yeh, Rider, or Collins techniques may be considered. These will not, however, offer comprehensive (or any) confidence measures typifying TN 101 and climate differentiation may not be incorporated.

Another limitation of many techniques, to include TN 101, is that they do not quantitatively embrace short-term Rayleigh fading characteristics. The new Bullington technique does; furthermore, this method offers simple, compact results through computer applications [Christopher and Debroux, 1987]. The newness of this technique may, however, generate skepticism; additionally, it is based, in part, on unaccepted mode reflection theories.

A final criticism of most methods is the dominating influence of surface refractivity, N_s , which has been shown fallacious in several instances. Methods that make this "mistake" include, to varying degrees, all TN 101 derivatives as well as the methods of Yeh and Rider. Neither the Collins, CCIR Method II, or the Radiometeorological method include

N_s . However, despite its simplicity, the Collins method exhibits limited application for long (greater than 400 mi) links. Furthermore, the Radiometeorological method is known to be quite accurate and simple only if refractivity gradient data within the common volume is available. Finally, CCIR Method II provides good "worst case" analysis, at least for temperate climates [Boithias and Battesti, 1983, p. 660; CCIR, 1986, p. 376].

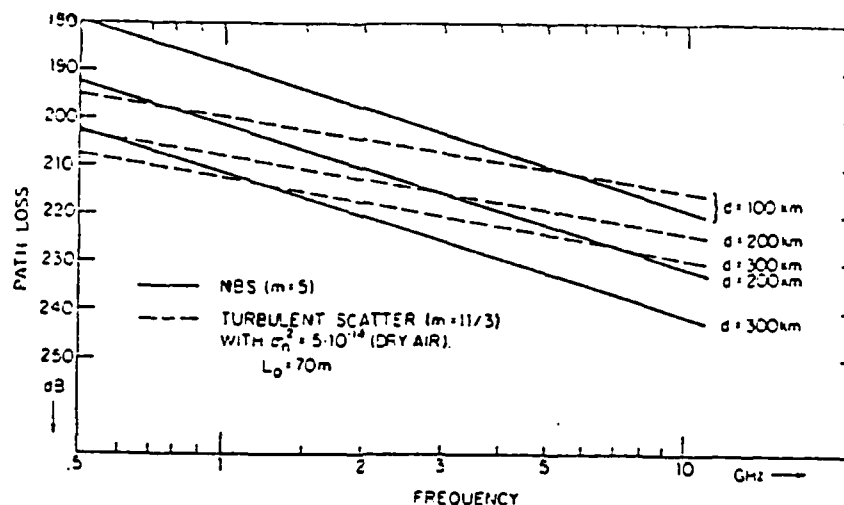
A 1968 comparison of several methods produced some surprising results [Larsen 1968]. Data from fifteen operational links in various regions were compared with predictions for those links using the techniques of TN 101, CCIR Method I, Yeh, Rider, and Collins. Notably, only two of the links had operating frequencies above 3 GHz and two more above 2 GHz. Despite several manipulations of results to provide equivalent solutions, Larsen states:

[t]he conclusions which may be drawn at this stage indicate that the N.B.S. [TN 101] and CCIR are almost equal in performance, although CCIR is much more convenient to use. The CCIR method provides important estimates of fading ranges, and a combination of CCIR and Yeh gives good estimates of median path loss. The Collins method suffers from having a restricted range of parameters, but gives very good results when used inside this range. All the calculation methods show remarkable failure to account satisfactorily for climate variation, and indicate the need for further investigation of this point [Larsen, 1968, p. 114].

Larsen's calculations indicated reasonable correlation for all methods except Rider's; it was considerably inferior. The Collins method outperformed all, with Yeh's being slightly better than TN 101 and CCIR Method I. However, Larsen cautions that his link sample could have significantly influenced results.

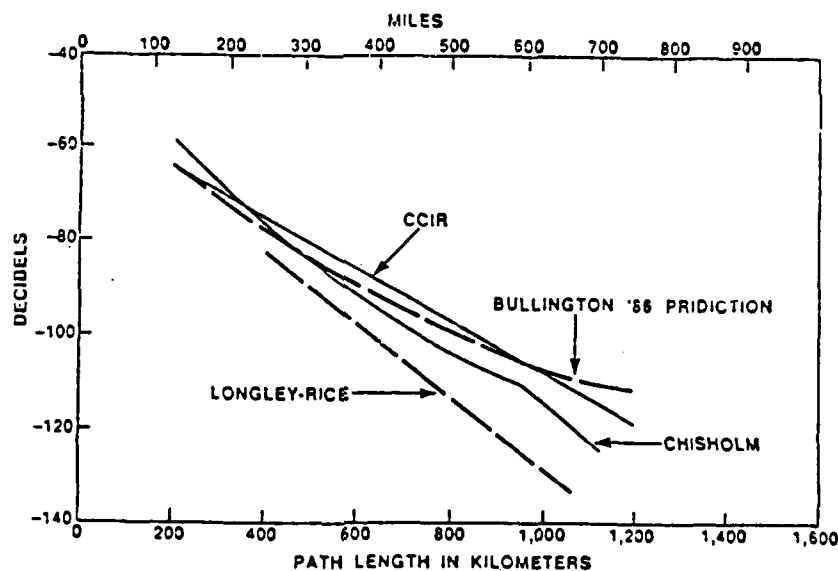
Fitzsimons [1968] may also be referenced for a comparison between actual data on an 87 km, 4.7 GHz link in Cyprus and the predictions of TN 101, Collins, Yeh, and an earlier CCIR model. Results were all on the pessimistic side: Yeh by 7 dB, Collins by 9 dB, and TN 101 by 11 dB.

Among the newer methods, Parl [1979] and Christopher and Debroux [1987] offer some comparisons. In Figure 66 a comparison of TN 101 (NBS) and the Parl (Turbulent Scatter) methods are given. The difference can be attributed to coupling loss calculations and the conservative approach of using incoherent scatter in all cases instead of quasi-coherent scatter as in TN 101's case. Figure 67 compares the scatter losses of the new Bullington method with an earlier (1962) CCIR method and TN 101 (Longley-Rice). As a reference, the "Chisholm" curve represents actual data for several links at 400 MHz.



Source: Parl, S. A. "New Formulas for Tropospheric Scatter Path Loss." *Radio Science*, vol. 14, no. 1 (January-February 1979), p. 53.

Figure 66. Comparison of TN 101 (NBS) and the Parl (Turbulent Scatter) methods



Source: Christopher, P.F., and Debroux, P.S. "New Applications of Bullington's Tropospheric Reflection Model." *MILCOM 87, IEEE Military Communications Conference*, vol. 3 (Oct 1987), p. 43.3.6.

Figure 67. Comparison of the CCIR (1962 Data), TN 101 (Longley-Rice), and Bullington methods. "Chisholm" represents actual data for several links at 400 MHz.

5.5 Conclusions

Conclusions are less than obvious. None of the techniques offer complete, "any situation" accuracy except the Radiometeorological method. Yet this statement is made with a notable absence of complete comparison. The poor performance of TN 101 in Larsen's analysis leads one to suspect similar performance in the *Military Handbook* [1977], CCIR Method I, Parl, and the MITRE methods.⁶ However, given Larsen's limited analysis, heavily favoring lower frequencies, it is erroneous to include the Parl and MITRE methods in this allegation since these contemporary approaches fundamentally differ from TN 101. Further, the limited samples used by Larsen and Fitzsimons nullify any conclusive arguments.

One should note that with respect to theoretical considerations, the Parl method stands out. Through computer flexibility, this method allows variable inputs, provides theoretically sound coupling loss calculations, and does not emphasize surface refractivity or singular spectrum slope values as does TN 101. CCIR Method I, the CCIR

⁶One must assume that Larsen correctly applied the techniques being compared for each of the 15 links analyzed.

Chinese method, and Yeh and Rider's techniques center on surface refractivity. The Collins method has limited application, CCIR Method II works best in temperate climates, and Bullington's treatment is untried and based, in part, on unaccepted mode theory.

To conclude, recognizing that the majority of prediction techniques are simply estimates based on empirical analysis, the best procedure would be to choose a variety of methods. Final analysis would include projections from several techniques, and a best case/worst case forecast would establish prediction confidence. This recommendation is based on the limitations presented; modifications to techniques such as the Radiometeorological or Parl methods supplemented with development of accurate methods to profile common volume gradient variations could allow significant improvement.

BIBLIOGRAPHY

- Albrecht, H.J. "Correlating Tropospheric Scatter Data and Cyclonic Parameters." *Proceedings of the IEEE*, vol. 55, no. 10 (October 1967): 1768-1769.
- Anthes, R.A., Cahir, J.J., Fraser A.B., and Panofsky, H.A. *The Atmosphere*. 3rd ed. Columbus, Ohio: Charles E. Merrill, 1981.
- Azurza, J.J. "Tropospheric Scatter Communications in the Oil Industry." MS thesis, Univ. of Colorado, 1975.
- Baghdady, E.J. "Performance Characteristics of Multipath Channels." The Electromagnetic Science Series of Short Courses Lecture Notes 5.2: Tropospheric Radio Propagation. Sponsored by the U.S. Department of Commerce, Environment Science Services Administration, Institute for Telecommunication Science and the University of Colorado, Electrical Engineering Department, 27 July - 7 August, 1970.
- Barrow, B.B., Abraham L.G., Cowan, W.M. Jr., and Gallant, R.M. "Indirect Atmospheric Measurements Utilizing Rake Tropospheric Scatter Techniques- Part I: The Rake Tropospheric Scatter Technique." *Proceedings of the IEEE*, vol. 57, no. 4 (April 1969): 537-551.
- Barsis, A.P., Norton, K.A., and Rice, P.L. *Performance Predictions for Single Tropospheric Communication Links and for Several Links in Tandem*. U.S. National Bureau of Standards, Technical Note, no. 102 (Aug 1961).
- Barsis, A.P., Norton, K.A., and Rice, P.L. "Predicting the Performance of Tropospheric Communication Links, Singly and in Tandem." *IRE Transactions on Communications Systems*, vol. CS-10, no. 1 (March 1962): 2-22.

- Barton, J.H. "A Selective Survey of Soviet Bloc Scatter Development." *IRE Transactions on Antennas and Propagation*, vol. AP-10, no. 3 (May 1962): 335-339.
- Bean, B.R. "Some Meteorological Effects on Scattered Radio Waves." *IRE Transactions on Communications Systems*, vol. CS-4, no. 1 (March 1956): 32-38.
- Bean, B.R., and Dutton, E.J. *Radio Meteorology*. National Bureau of Standards, U.S. Department of Commerce, Monograph 92, 1966.
- Bean, B.R., Horn, J.D., and Riggs, L.P. *Synoptic Radio Meteorology*. National U.S. Department of Commerce, Bureau of Standards Technical Note 98. Washington: Superintendent of Documents, U.S. Government Printing Office, 1962.
- Bello, P.A. "A Troposcatter Channel Model." *IEEE Transactions on Communications Technology*, vol. COM-17, no. 2 (April 1969a): 130-137.
- Bello, P.A. "Selection of Multichannel Digital Data systems for Troposcatter Channels." *IEEE Transactions on Communications Technology*, vol. COM-17, no. 2 (April 1969b): 138-161.
- Bello, P.A., and Ehrman L. "Error Rates in Diversity FDM-FM Digital Troposcatter Transmission." *IEEE Transactions on Communications Technology*, vol. COM-17, no. 2 (April 1969): 182-191.
- Birnbaum, G., and Bussey, H.E. "Amplitude, Scale, and Spectrum Refractive Index Inhomogeneities in the First 125 Meters of the Atmosphere." *Proceedings of the IRE*, vol. 42, no. 10 (October 1955): 1412+.
- Boithias, L. *Radio Wave Propagation*. St. Louis: McGraw-Hill, 1987.
- Boithias, L., and Battesti, J. "Propagation Due to Tropospheric Inhomogeneities." *IEE Proceedings*, vol. 130, part F, no. 7 (December 1983): 657-664.
- Bolgiano, R., Jr. "The Role of Turbulent Mixing in Scatter Propagation." *IRE Transactions on Antennas and Propagation*, vol. AP-6, no. 2 (April 1958): 161-168.

- Booker, H.G., and deBettencourt, J.T. "Theory of Radio Transmission by Tropospheric Scattering Using Very Narrow Beams." *Proceedings of the IRE*, vol. 43, no. 3 (March 1955): 281-290.
- Booker, H.G., and Gordon, W.E. "A Theory of Radio Scattering in the Troposphere." *Proceedings of the IRE*, vol. 38, no. 4 (April 1950): 401-412.
- Brauburger, G.H. Jr. (Capt, USAFR). "Meteorological Factors Affecting AN/TRC-97A Tropospheric Scatter Communications." Technical Report no. TACCA/XQT-TR-79-1, Langley AFB, Va, 1 August 1979.
- Bremmer, H. "The Propagation of Electromagnetic Waves Through a Stratified Medium and its WKB Approximation for Oblique Incidence." *Physica*, vol. 15 (August 1949): 593-608.
- Bullington, K. "Radio Propagation at Frequencies Above 30 Mc/s." *Proceedings of the IRE*, vol. 35 (1947): 1122+.
- Bullington, K. "Radio Transmission Beyond the Horizon in the 40- to 4,000-MC Band." *Proceedings of the IRE*, vol. 41, no. 1 (January 1953): 132-135.
- Bullington, K. "Characteristics of Beyond-the-Horizon Radio Transmission." *Proceedings of the IRE*, vol. 43, no. 10 (October 1955): 1175-1180.
- Bullington, K. "Status of Tropospheric Extended Range Transmission." *IRE Transactions on Antennas and Propagation*, vol. AP-7, no. 4 (October 1959): 439-440.
- Bullington, K. "Reflections from an Exponential Atmosphere." *The Bell System Technical Journal*, vol. XLII, no. 6 (November 1963): 2849-2867.
- Carroll, T.J. "Internal Reflections in the Troposphere and Propagation Beyond the Horizon." *Transactions of the IRE, Professional Group on Antennas and Propagation*, PGAP-2 (March 1952a): 9-27.

- Carroll, T.J. "Normal Tropospheric Propagation Deep into the Earth's Shadow: The Present Status of Suggested Explanations." *Transactions of the IRE, Professional Group on Antennas and Propagation*, PGAP-3 (August 1952b): 6-11.
- Carroll, T.J. "Tropospheric Propagation Well Beyond the Horizon." *Transactions of the IRE, Professional Group on Antennas and Propagation*, PGAP-3 (August 1952c): 84-100.
- Carroll, T.J. "Marconi's Last Paper, 'On the Propagation of Microwaves over Considerable Distances'." *Proceedings of the IRE*, vol. 44, no. 8 (August 1956): 1056-1057.
- Carroll, T.J., and Ring, R.M. "Propagation of Short Radio Waves in a Normally Stratified Troposphere." *Proceedings of the IRE*, vol. 43, no. 10 (October 1955): 1384-1390.
- CCIR. Volume V. *Propagation in Non-Ionized Media*. Geneva, 1982.
- CCIR. Volume V. *Propagation in Non-Ionized Media*. Dubrovnik, 1986.
- Chisholm, J. H. "Progress of Tropospheric Propagation Research Related to Communications Beyond the Horizon." *IRE Transactions on Communications Systems*, vol. CS-4, no.1 (March 1956): 6-16.
- Christopher, P.F., and Debroux, P.S. "New Applications of Bullington's Tropospheric Reflection Model." *MILCOM 87, IEEE Military Communications Conference*, vol. 3 (Oct 1987): 43.3.1-43.3.7.
- Clavier, A.G. "Microwave Communication Beyond the Horizon." *Electrical Communication*, vol. 33, no. 2 (June 1956): 108-116.
- Coirin, M.R., and Kessler, J.A. "User's Guide for the Personal Computer Version of the AN/TRC-170 Initial Link Engineering Manual." The MITRE Corporation Working Paper WP-25855, Supp. III, Fort Huachuca, Az, May 1987.

- Colwell, J.F., and Anderson, L.J. "Concerning the Radio Field Due to Internal Reflection in the Stratified Troposphere." *Transactions of the IRE, Professional Group on Antennas and Propagation*, PGAP-3 (August 1952): 117-125.
- Cox, D.C. "Review of Techniques in Transhorizon Propagation Research and their Relationship to Parameters of the Troposphere." *Radio Science*, vol. 4, no. 10 (October 1969): 905-925.
- Craig, K.H., and Levy, M.F. "The Modeling of Transhorizon Anomalous Propagation Conditions." *Fifth International Conference on Antennas and Propagation (ICAP 87) Part 2: Propagation*, Institution of Electrical Engineers, London (1987): 347-350.
- Crain, C.M. "Survey of Airborne Microwave Refractometer Measurements." *Proceedings of the IRE*, vol. 43, no. 10 (October 1955): 1405-1411.
- Crain, C.M., and Gerhardt, J.R. "Measurements of the Parameters Involved in the Theory of Radio Scattering in the Troposphere." *Proceedings of the IRE*, vol. 40, no. 1 (January 1952): 50-54.
- Crane, R.K. "Fundamental Limitations Caused by RF Propagation." *Proceedings of the IEEE*, vol. 69, no. 2 (February 1981a): 196-209.
- Crane, R.K. "A Review of Transhorizon Propagation Phenomena." *Radio Science*, vol. 16, no. 5 (September-October 1981b): 649-669.
- Crane, R.K. *Tropospheric Scatter Propagation at 5 and 15 GHz: Preliminary Results for a 161 km Path*. Interim Report on Research Conducted Under the Post-Doctoral Program, Rome Air Development Center, Hanscom AFB, Maine. Hanover, New Hampshire: Dartmouth College, 1988.
- Crawford, A.B., Hogg, D.C., and Kummer W.H. "Studies in Tropospheric Propagation Beyond the Horizon." *The Bell System Technical Journal*, vol. 38, no. 5 (September 1959): 1067-1178.
- David, P., and Voge, J. *Propagation of Waves*. New York: Pergamon, 1969.

- de Belatini, P.C.M. "Inadequacy of Scatter Mechanisms in Tropospheric Radio Propagation." *Nature*, vol. 184, no. 4698 (November 14, 1959): 1558-1559.
- Derr, V.E. *Remote Sensing of the Troposphere*. U.S. Department of Commerce, National Oceanic and Atmospheric Administration, Environmental Research Laboratories, and the University of Colorado. Washington: Superintendent of Documents, U.S. Government Printing Office, August 15, 1972.
- "Discussion on 'Tropospheric Propagation Beyond the Horizon--I'." *The Proceedings of the Institution of Electrical Engineers*, Pt. B, Supp. 8, vol. 105 (1958): 122-126.
- Doherty, L.H., and Stone, S.A. "Forward Scatter from Rain." *IRE Transactions on Antennas and Propagation*, vol. AP-8, no. 4 (July 1960): 414-418.
- Dougherty, H.T. "The Refractive Index Gradient and Surface Refractivity." *The Electromagnetic Science Series of Short Courses Lecture Notes 2.1: Tropospheric Radio Propagation*. Sponsored by the U.S. Department of Commerce, Environment Science Services Administration, Institute for Telecommunication Science and the University of Colorado, Electrical Engineering Department, 27 July -7 August, 1970.
- du Castel, F. *Tropospheric Radiowave Propagation Beyond the Horizon*. New York: Pergamon, 1966.
- du Castel, F., ed. *Progress in Radio Science 1960-1963, Volume II, Radio and Troposphere*. New York: Elsevier, 1965.
- Dube, R.J., and Hotzel, P.M. "TRI-TAC Equipment Interface Plan for AN/TRC-170." The MITRE Corporation MTR-85A00004, McLean, Virginia, May 1985.
- Eklund, F., and Wickerts, S. "Wavelength Dependence of Microwave Propagation Far Beyond the Radio Horizon." *Radio Science*, vol. 3 (New Series), no. 11 (November 1968): 1066-1074.

- Engineering Considerations for Microwave Communications Systems*. 2nd ed. San Carlos, California: GTE Lenkurt, 1972.
- Evaluation of FDM and FM Systems*. Air Force Communications Command (AFCC) textbook for AFCC 30000-1, Wright-Patterson AFB, Oh., January 1983.
- Fehlhaber, L. "Results of the Theory of Tropospheric Scattering, Derived from Propagation Measurements." *Conference on Tropospheric Wave Propagation*, 30 September - 2 October, IEE, 1968: 37-42.
- Feinstein, J. "Tropospheric Propagation Beyond the Horizon." *Journal of Applied Physics*, vol. 22, no. 10 (October 1951): 1292-1293.
- Feinstein, J. "The Role of Partial Reflections in Tropospheric Propagation Beyond the Horizon." *Transactions of the IRE, Professional Group on Antennas and Propagation*, PAGP-2 (March 1952a): 2-8.
- Feinstein, J. "Partial Reflections in Tropospheric Propagation." *Transactions of the IRE, Professional Group on Antennas and Propagation*, PGAP-3 (August 1952b): 101-111.
- Fitzsimmons, T.K. "Observations of Tropospheric Scatter Path Loss at C Band Frequencies and Meteorological Conditions in Cyprus." *Proceedings of the IEE*, vol. 115, no. 7 (July 7): 247-251.
- Flock, W.L. *Electromagnetics and the Environment: Remote Sensing and Telecommunications*. Englewood Cliffs, New Jersey: Prentice-Hall, 1979.
- Flock, W.L. *Propagation Effects on Satellite Systems at Frequencies Below 10 GHz*. Second Ed., NASA Reference Publication 1108(03), 1987.
- Freeman, R.L. *Telecommunication Transmission Handbook*. New York: John Wiley & Sons, 1975.
- Freeman, R.L. *Radio System Design for Telecommunications (1-100 GHz)*. New York: John Wiley & Sons, 1987.

- Friis, H.T., Crawford, A.B., and Hogg, D.C. "A Reflection Theory for Propagation Beyond the Horizon." *The Bell System Technical Journal*, vol. XXXVI, no. 3 (May 1957): 627-644.
- Gerlach, A.M., ed. "Objective Analysis and Prediction Techniques - 1984." Air Force Geophysics Lab Report No. AFGL-TR-84-0328, Hanscom AFB, Ma., (30 Nov 1984).
- Gjessing, D.T., and Irgens, F. "On the Scattering of Electromagnetic Waves by a Moving Tropospheric Layer Having Sinusoidal Boundaries." *IEEE Transactions on Antennas and Propagation*, vol. AP-12, no. 1 (January 1964): 51-64.
- Gjessing, D.T., and McCormick, K.S. "On the Prediction of the Characteristic Parameters of Long-Distance Tropospheric Communication Links." *IEEE Transactions On Communications*, vol. COM-22, no. 9 (September 1974): 1325-1331.
- Global Tropospheric Chemistry: A Plan for Action.* National Research Council, Global Tropospheric Chemistry Panel Board of Atmospheric Sciences and Climate Commission on Physical Sciences, Mathematics, and Resources. Washington: National Academy Press, 1984.
- Gordon, W.E. "Radio Scattering in the Troposphere." *Proceedings of the IRE*, vol. 43, no. 1 (January 1955): 23-28.
- Gordon, W.E. "A Simple Picture of Tropospheric Radio Scattering." *IRE Transactions on Communications Systems*, vol. CS-4, no.1 (March 1956): 97-101.
- Graham, J.W. "Troposcatter Transmission." Course notes from Session 7 of the MITRE Institute Course: Introduction to Digital Communication Systems, 20 October 1987.
- Gunther, F.A. "Tropospheric Scatter Communications (Past, Present, and Future)." *IEEE Spectrum*, vol. 3, no. 9 (September 1966): 81-100.
- Hall, M.P.M. *Effects of the Troposphere on Radio Communication.* New York: Peter Peregrinus, 1979.
- Hall, M.P.M., and Barclay, L.W., eds. *Radiowave Propagation.* London: Peter Peregrinus, 1989.

- Hall, M.P.M., and Dowling, G.R. "Effect of Rain on 4GHz Troposcatter Radio Paths." *Electronics Letters*, vol. 10, no. 11 (May 30, 1974): 210-212.
- Hooke, W.H., and Hardy, K.R. "Further Study of the Atmospheric Gravity Waves over the Eastern Seaboard on 18 March 1969." *Journal of Applied Meteorology*, vol. 14, no. 1 (February 1975): 31-38.
- Ippolito, L.J. Jr. *Radiowave Propagation in Satellite Communications*. New York: Van Nostrand Reinhold Co., 1986.
- Iribarne, J.V., and Cho, H.-R. *Atmospheric Physics*. Boston: D. Reidel, 1980.
- Isted, G.A. "Guglielmo Marconi and Communication Beyond the Horizon: A Short Historical Note." *The Proceedings of the Institution of Electrical Engineers*, Pt. B, Supp. 8, vol. 105 (1958): 79-83.
- Johnson, M.A. "A Review of Tropospheric Scatter Propagation Theory and its Application to Experiment." *The Proceedings of the Institution of Electrical Engineers*, Pt. B, Supp. 8, vol. 105 (1958): 165-176.
- Jowett, J.K.S. "The Measurement and Prediction of VHF Tropospheric Field Strengths at Distances Beyond the Horizon." *The Proceedings of the Institution of Electrical Engineers*, Pt. B, Supp. 8, vol. 105 (1958): 79-83.
- Katzin, M. "Tropospheric Propagation Beyond the Horizon." *Transactions of the IRE, Professional Group on Antennas and Propagation*, PGAP-3 (August 1952a): 112-116.
- Katzin, M. "The Insignificance of Continuous Internal Reflections in Tropospheric Propagation Beyond the Horizon" *Transactions of the IRE, Professional Group on Antennas and Propagation*, PGAP-4 (December 1952b): 14-18.
- Kerr, D.E. *Propagation of Short Radio Waves*. Rev. ed. London: Peter Peregrinus, 1987.

Khalil, M.A.K., and Rasmussen, R.A. "Carbon Monoxide in the Earth's Atmosphere: Indications of a Global Increase." *Nature*, vol. 332 (March 17, 1988): 242-244.

Lane, J.A. "Review of Tropospheric Propagation." The Electromagnetic Science Series of Short Courses Lecture Notes VI-1 and VI-2. Sponsored by the U.S. Department of Commerce, Environment Science Services Administration and the University of Colorado, Electrical Engineering Department, 17 June - 3 July, 1968.

Larsen, R. "A Comparison of Some Troposcatter Prediction Methods." *Conference on Tropospheric Wave Propagation*, 30 September - 2 October, IEE, 1968: 110-117

Lemmon, J.J. "Propagation and Performance Measurements Over a Digital Troposcatter Communications Link." A paper reprinted from Conference Proceedings No. 419, Advisory Group for Aerospace Research and Development (AGARD), (1989).

Livingston, D.C. *The Physics of Microwave Propagation*. Englewood Cliffs, New Jersey: Prentice-Hall, 1970.

Lutgens, F.K., and Tarbuck, E.J. *The Atmosphere: An Introduction to Meteorology*. 2nd ed. Englewood Cliffs, New Jersey: Prentice-Hall, 1982.

Martin, J. *Communications Satellite Systems*. Englewood Cliffs, N.J.: Prentice-Hall, Inc., 1978.

McGavin, R.E. *A Survey of the Techniques for Measuring the Radio Refraction Index*. National U.S. Department of Commerce, Bureau of Standards Technical Note 99. Washington: Superintendent of Documents, U.S. Government Printing Office, 1962.

McKay, L.R. *What Every Engineer Should Know about Electronic Communications Systems*. New York: Marcel Dekker, 1989.

Megaw, E.C.S. "Scattering of Electromagnetic Waves by Atmospheric Turbulence." *Nature*, vol. 166, no. 4235 (December 30, 1950): 1100-1104.

Megaw, E.C.S. "Fundamental Radio Scatter Propagation Theory." *The Proceedings of the Institution of Electrical Engineers*, Part C, vol. 104 (1957): 441-455.

Military Handbook, Facility Design for Tropospheric Scatter (Transhorizon Microwave System Design). MIL-HDBK-417, Department of Defense, Washington, DC, 25 November, 1977. Available through Navy Publications and Forms Center, ATTN: NPODS, Office of Navy Publications, 5801 Tabor Avenue, Philadelphia, Pa., 19120-5094.

Monsen, P. "Fading Channel Communications." *IEEE Communications Magazine*, vol. 18, no. 1 (January 1980): 16-25.

Monsen, P., Parl, S., Malaga, A., Tolman, S., and Fetteroll, J. *Digital Troposcatter Performance Model: Users Manual*. Lexington, Massachusetts: SIGNATRON, Inc. publication no. A288-15, November, 1983.

Neiburger, M., Edinger, J.G., Bonner, W.D. *Understanding our Atmospheric Environment*. San Francisco: W.H. Freeman, 1973.

Neuburger, A., Freyheit, P.J., Leroux, G., Livingston, D.C., and McLaughlin, K.P. "AN/TRC-170 Initial Link Engineering Manual." The MITRE Corporation Working Paper WP-25855, Bedford, Ma., 16 Jan 1985.

Norton, K.A., Rice, P.L., and Vogler, L.E. "The Use of Angular Distance Transmission Loss and Fading Range for Propagation through a Turbulent Atmosphere over Irregular Terrain." *Proceedings of the IRE*, vol. 43, no. 10 (October 1955): 1488-1526.

Norton, K.A. *Advances in Electronics*, Academic Press, New York, vol. 1 (1948): 381-423.

Ortusi, J. "The Various Theories on the Propagation of Ultra-Short Waves Beyond the Horizon." *IRE Transactions on Antennas and Propagation*, vol. AP-3, no. 2 (April 1955): 86-91.

- Ortwein, N.R., Hopkins, R.U.F., and Pohl, J.E.
 "Properties of Tropospheric Scattered Fields."
Proceedings of the IRE, vol. 49, no. 4 (April 1961): 788-802.
- Panter, P.F. *Communication Systems Design: Line-of-Sight and Tropo-Scatter Systems*. St. Louis: McGraw-Hill, 1972.
- Parl, S. A. "New Formulas for Tropospheric Scatter Path Loss." *Radio Science*, vol. 14, no. 1 (January-February 1979): 49-57.
- Pekeris, C.L. "Wave Theoretical Interpretation of Propagation of 10 cm and 3 cm Waves in Low-Level Ocean Ducts." *Proceedings of the IRE*, vol. 35 (1947): 453+.
- Penkett, S.A. "Increased Tropospheric Ozone." *Nature*, vol. 332 (March 17, 1988): 204-205.
- Peterson, C.F., Farrow, J.J., Capps, F.M., and Samson, C.A. *Propagation at 5GHz in Europe - A Comparison of Predictions and Measurements for Various Types of Paths*. U.S. Department of Commerce, Environmental Science Services Administration, Institutes for Environmental Research, ESSA Technical Report IER 2 ITSA 2. Boulder, Co: Institute for Telecommunication Sciences and Aeronomy, July 1966.
- Picquenard, A. *Radio Wave Propagation*. New York: Macmillan, 1974.
- "Radio Transmission By Ionospheric and Tropospheric Scatter." A report of the Joint Technical Advisory Committee (JTAC) in *Proceedings of the IRE*, vol. 48, no. 1 (January 1960): 4-44.
- Rice, P.L., Longley, A.G., Norton, K.A., and Barsis, A.P. *Transmission Loss Predictions for Tropospheric Communication Circuits*. Vols. I and II. Rev. ed. U.S. Department of Commerce, National Bureau of Standards Technical Note 101. Washington: Superintendent of Documents, U.S. Government Printing Office, 1967.
- Roda, G. *Troposcatter Radio Links*. Norwood, Maine: Artech House, 1988.

- Sarkar, S.K., Dutta, H.N., and Reddy, B.M.
"Development of a Prediction Technique for Tropo-Path Loss from Observed Transhorizon Propagation Characteristics over India." *Third International Conference on Antennas and Propagation (ICAP 83)*, Part 2: Propagation, Institution of Electrical Engineers, London (1983): 229-232.
- Sarma, S.B.S.S. "Troposcatter Link Design Using Airborne Microwave Refractometer Observations over Kanpur." *Indian Journal of Radio & Space Physics*, vol. 17 (June 1988): 103-107.
- Saxton, J.A. "Tropospheric Scatter Propagation." *Wireless World*, vol. 62, no. 12 (December 1956): 587-590.
- Silverman, R.A. "Fading of Radio Waves Scattered by Dielectric Turbulence." *Journal of Applied Physics*, vol. 28, no. 4 (April 1957): 506-511.
- Smith, E.K. "Introduction to the Physics of Media: The Atmosphere, The Ionosphere." The Electromagnetic Science Series of Short Courses Lecture Notes II-1 and II-4. Sponsored by the U.S. Department of Commerce, Environment Science Services Administration and the University of Colorado, Electrical Engineering Department, 17 June - 3 July, 1968.
- Smith, E.K., and Weintraub, S. "The Constants in the Equation for Atmospheric Refractive Index at Radio Frequencies." *Proceedings of the IRE*, vol. 41, no. 8 (August 1953): 1035-1037.
- Sommerfeld, A.N. "The Propagation of Waves in Wireless Telegraphy." *Ann. Phys.*, series 4, vol. 28 (1909): 665+.
- Staniforth, J.A. *Microwave Transmission*. New York: John Wiley & Sons, 1972.
- Staras, H. "Aperture-to-Medium Coupling Loss." *IRE Transactions on Antennas and Propagation*, vol. AP-5, no. 2 (April 1957): 228-232.
- Staras, H., and Wheelon, A.D. "Theoretical Research on Tropospheric Scatter Propagation in the United States, 1954-1957." *IRE Transactions on Antennas and Propagation*, vol. AP-7, no. 1 (January 1959): 80-87.

- Tatarski, V.I. *Wave Propagation in a Turbulent Medium*. New York: McGraw-Hill, 1961.
- Tidd, W.H. "Demonstration of Bandwidth Capabilities of Beyond-Horizon Tropospheric Radio Propagation." *Proceedings of the IRE*, vol. 43 no. 10 (October 1955): 1297-1299.
- "Tropospheric Scatter, Satellite, and VLF/LF Communications." USAF Technical Training School Study Guide and Workbook KEO 3000-119, Keesler AFB, Ms., June 1979.
- VanZandt, T.E., Green, J.L., Gage, K.S., and Clark, W.L.. "Vertical Profiles of Refractivity Turbulence Structure Constant: Comparison of Observations by the Sunset Radar with a new Theoretical Model." *Radio Science*, vol. 13, no. 5 (September-October 1978): 819-829.
- Volz, A., and Kley, D. "Evaluation of the Montsouris Series of Ozone Measurements made in the Nineteenth Century." *Nature*, vol. 332 (March 17, 1988): 240-242.
- Waterman, A.T. Jr. "Advanced Research in Propagation Techniques Quarterly Report: Transhorizon Propagation Techniques." U.S. Army sponsored Research and Development Technical Report ECOM-0138-2, October 1970.
- Weitzen, J.A., and Ralston, W.T. "Meteor Scatter: An Overview." *IEEE Transactions on Antennas and Propagation*, vol. 36, no. 12 (December 1988): 1813-1819.
- Wheelon, A.D. "Radio Scattering by Tropospheric Irregularities." *Journal of Atmospheric and Terrestrial Physics*, vol. 15, nos. 3/4 (October 1959): 185-205.
- Wiesner, Jerome B. "New Methods of Radio Transmission." *Scientific American*, vol. 196, no. 1 (January 1957): 46-41.

APPENDIX A

MULTIMODE PROPAGATION

Two modes for terrestrial, beyond the horizon propagation are diffraction and troposcatter. While most troposcatter paths are engineered to avoid diffracting obstacles (unless diffraction is desired), situations may dictate otherwise. Roda [1988, p. 142] notes that at small scatter angles (less than about one degree) diffraction can, for a certain time percentage, dominate.

For short periods (minutes) the mechanism with the lower loss is dominant if the two losses differ by 6 dB or more. For longer periods (days, months), in view of the variability of the signals, the dominant mechanism is definitely that with the lower loss if the median path losses differ by more than 20 dB [Roda, 1988, p. 142].

While troposcatter signals exhibit deep fades, diffracted signals remain comparatively stable therefore limiting the effects of fading on some links.

Freeman [1987, pp. 145,146] discusses two ways to differentiate dominant propagation modes.

- a. Assuming low (ground level) antenna height, the transition distance (d) at which distances exceeding d is predominantly troposcatter (less than d

implies diffraction) is given in kilometers by

$$d = 65(100/f)^{1/3}, \quad (\text{A-1})$$

where f is the operating frequency (MHz).

- b. If the scatter angle exceeds 20 mrad (about 1.1 degrees), diffraction effects cease to be important.

Using (A-1) for small scatter angles, Table A.1 is developed:

Table A.1. Mode Transition Distances		
Frequency (MHz)	Distance (km)	Distance (mi)
500	38	24
1000	30	19
3000	21	13
5000	18	11

Other situations may allow diffraction contributions to be disregarded. If more than three diffracting obstacles are in the path, troposcatter is the dominant mode. Also, at microwave frequencies over a somewhat smooth earth, diffraction losses are large enough to allow consideration of troposcatter only [Monsen, et al., 1983, p. 2-55].

APPENDIX B

THE SYSTEM EQUATION

The troposcatter system equation, as provided by *Military Handbook, Facility Design for Tropospheric Scatter* [1977] (which borrows from Rice, P.L., et al., [1967]), is used for path predictions and can also serve to illustrate the impact of the earth's atmosphere on troposcatter propagation. This equation,

$$P_t = R + B + L_l - G_p - 204 + F + L_{bcr} \text{ (dBW)}, \quad (B-1)$$

specifies the required transmitter power, P_t , to provide a specific carrier-to-noise ratio, R , at any instant in time. Assume, for this example, that R and the following parameters are fixed:

- B bandwidth (dB);
- L_l the sum of waveguide, duplexer, and other system element losses (dB); and
- G_p effective antenna gain (dB), this parameter will also include degradations introduced by aperture-to-medium coupling loss described in Chapter 4.

The constant -204, termed Johnson noise power per hertz, is found through $(-10 \log kT)$ with k being Boltzman's constant and T as the ambient reference

temperature, usually 288.5 K. The remaining parameters of (B-1), F and L_{bcr} , are of particular interest since these include the uncontrollable effects of the atmosphere.

F , the effective noise factor in dB, is found through

$$F = 10 \log f \text{ (dB)} \quad (B-2)$$

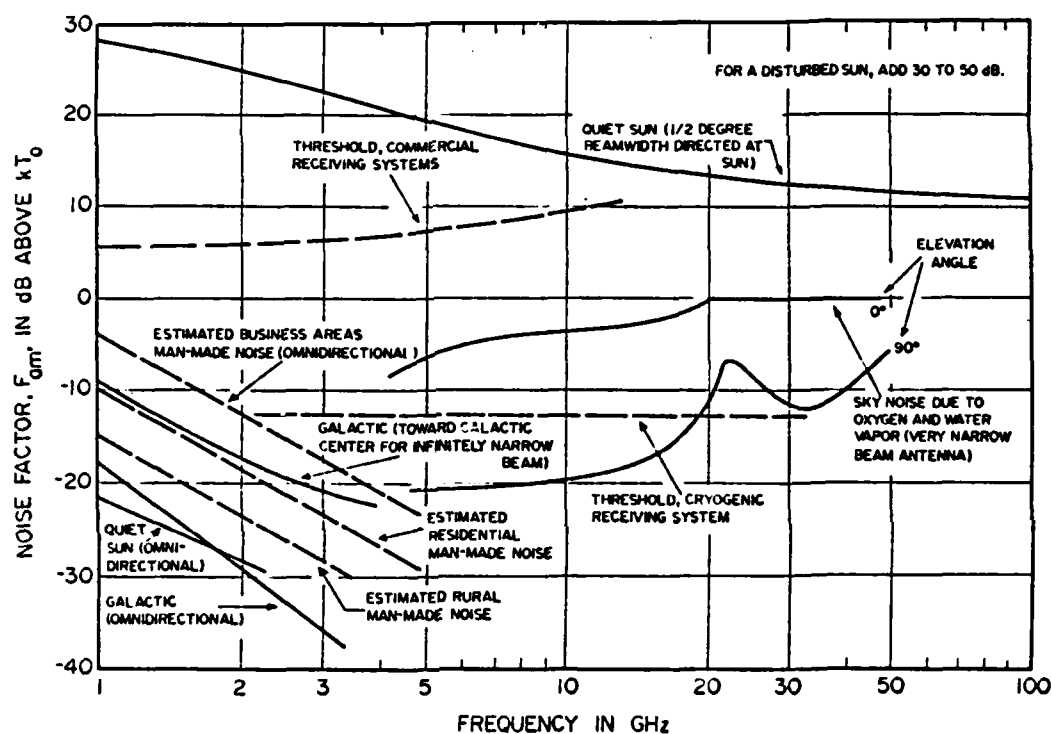
and

$$f = f_{am} - 1 + l_c l_l f_r \quad (B-3)$$

where

f_{am} is the external noise factor,
 l_c is antenna circuit loss,
 l_l is transmission line loss, and
 f_r is the receiver noise.

All constituents of (B-3) are expressed in power units. Critical in this analysis is f_{am} which is depicted on Figure B1 in dB as F_{am} . While a variety of noise sources factor into F_{am} , note the contributions of sky noise due to oxygen and water vapor. These atmospheric related contributors appear negligible at troposcatter frequencies. However, the sun, although not considered an atmospheric component, merits mention since its effect can be substantial (25 dB at 2 GHz) when it passes through



Source: *Military Handbook, Facility Design for Tropospheric Scatter (Transhorizon Microwave System Design)*. MIL-HDBK-417, Department of Defense, Washington, DC, 25 November, 1977. Available through Navy Publications and Forms Center, ATTN: NPODS, Office of Navy Publications, 5801 Tabor Avenue, Philadelphia, Pa., 19120-5094, p. 4-205.

Figure B1: External Noise Sources

antenna beams. Therefore, although atmospheric noise contributions are insignificant for troposcatter, certain circumstances (direct solar noise) preclude complete disregard of all external noise contributors.

While external noise sources are, for the most part, nominal, the atmosphere's effect on the calculated reference basic transmission loss, L_{bcr} , is more severe. For any instant in time, this loss is expressed as

$$L_{bcr} = L_{bf} + A_a + A_{Cr} \text{ (dB)} \quad (B-4)$$

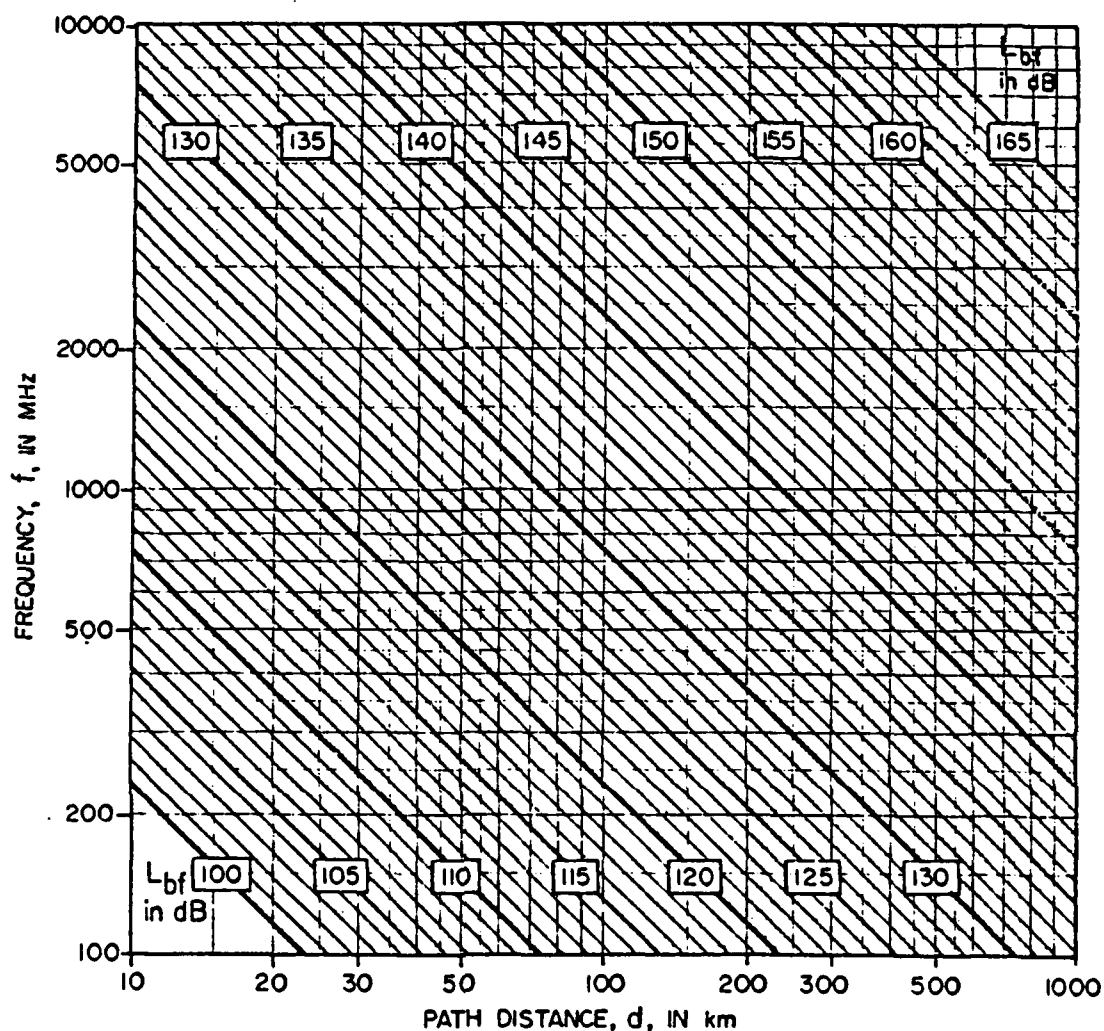
where

L_{bf} is basic free space loss in dB (Figure B2),

A_a is oxygen and water vapor absorption in dB (Figure 20), and

A_{Cr} is attenuation below that of free space due to atmospheric and terrain features in dB.

A_{Cr} is a rather versatile figure contingent on the mode of propagation. Ignoring pure diffraction and multimode possibilities, focus is on pure



Source: *Military Handbook, Facility Design for Tropospheric Scatter (Transhorizon Microwave System Design)*. MIL-HDBK-417, Department of Defense, Washington, DC, 25 November, 1977. Available through Navy Publications and Forms Center, ATTN: NPODS, Office of Navy Publications, 5801 T bor Avenue, Philidelphia, Pa., 19120-5094, p. 4-27.

Figure B2: Basic Free Space Transmission Loss

troposcatter and A_{cr} is then developed.¹

To conform with cited work, A_{cr} is renamed as A_s (scatter loss) for a pure troposcatter path, and is the attenuation relative to free space in dB:

$$A_s = L_{bsr} - L_{bf} \text{ (dB)}. \quad (B-5)$$

Note that the basic free space loss, L_{bf} , will drop from (B-4) when used with (B-5). For typical troposcatter links (exceptions as noted in *Military Handbook*, 1977, p. 4-142) the reference basic transmission loss, L_{bsr} , is

$$L_{bsr} = 30 \log f - 20 \log d + H_0 + F(\theta d) \text{ (dB)}, \quad (B-6)$$

with f as frequency in MHz and d as path distance in km. H_0 , the frequency gain function is significant only for low effective antenna heights and will be ignored for this analysis. (*Military Handbook*, 1977, pp. 4-144, 4-145 describes H_0 for these rare instances.)

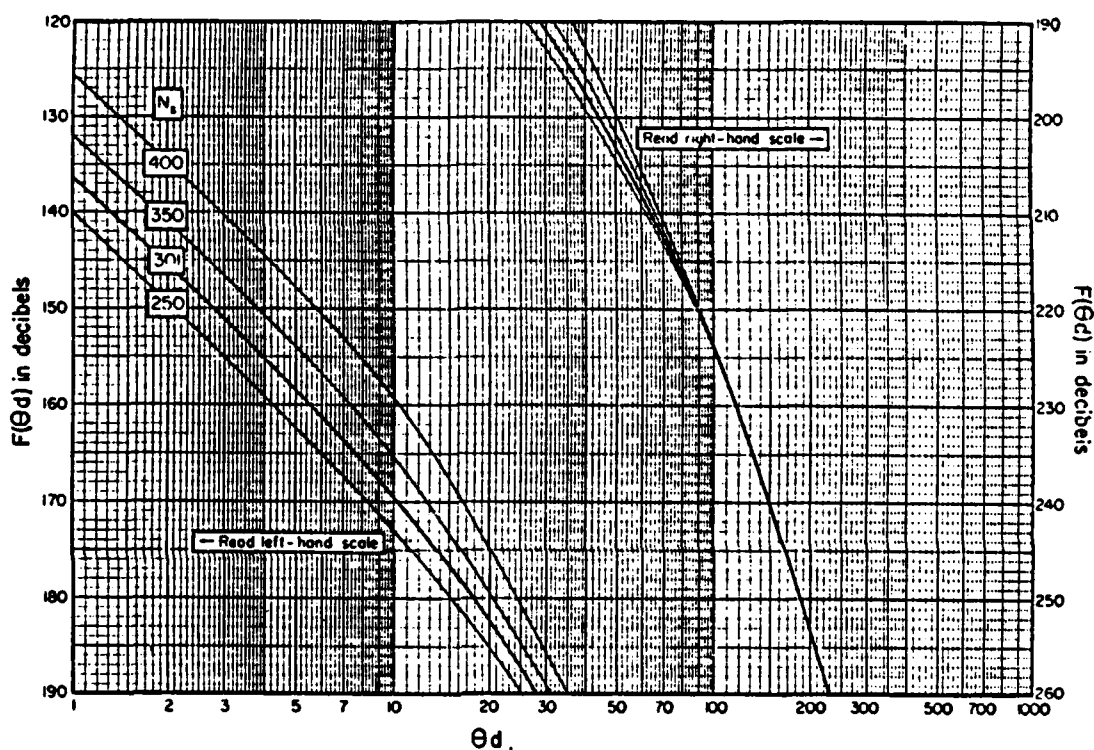
The attenuation function, $F(\theta d)$ is plotted as a function of the product of the scatter angle, θ in

¹By ignoring diffraction and multimode a substantial portion of the path prediction tools provided by *Military Handbook, Facility Design for Tropospheric Scatter* [1977] and Rice, P.L. et al. [1967] is neglected. This is more in line with the thrust of this thesis (pure troposcatter); however, the engineer cannot neglect other mechanisms unless profile data dictate otherwise.

radians, and d (Figure B3). The scatter angle was described in Section 1.3. Note the influence of N_s , surface refractivity, a parameter described in Section 2.3.1 and dependent on atmospheric conditions.

As an example of atmospheric effects on the calculated reference basic transmission loss, L_{bcr} , consider a 200 km link, operating at 4.4 GHz, with a scatter angle of 0.039 radians. Clear sky atmospheric absorption, A_a , would cause about 1.5 dB loss (see Figure 20) with rain adding no more than 2 dB (see Figure 23). However, $F(\theta d)$ would range from about 155 to 169 dB, depending on N_s , which in turn forces variations of 3 to 17 dB for A_s . Overall, L_{bcr} might vary from 4.5 dB (best case) to 20.5 dB (worst case) for this example.

Concluding, while several parameters in (B-1) are manageable, two parameters, F and L_{bcr} , exhibit uncontrollable and, at times, damaging traits contingent on atmospheric conditions. Fortunately, both F and L_{bcr} are predictable and can be nearly circumvented through engineered margins. It remains, however, that atmospheric phenomena emerge as a crucial consideration in troposcatter link design.



Source: *Military Handbook, Facility Design for Tropospheric Scatter (Transhorizon Microwave System Design)*. MIL-HDBK-417, Department of Defense, Washington, DC, 25 November, 1977. Available through Navy Publications and Forms Center, ATTN: NPODS, Office of Navy Publications, 5801 Tabor Avenue, Philadelphia, Pa., 19120-5094, p. 4-143.

Figure B3: $F(\theta_d)$ Versus the Product θ_d

APPENDIX C

THE SPECTRUM OF IRREGULARITIES

Referring to Figure 15, the equation for the spectrum function, $S(k)$, often shown as $\Phi(k)$, is of the general form

$$S(k) = bC_N^2 k^{-m} \quad (C-1)$$

within the inertial subrange. Discerning individual parameter values is difficult as references provide several variations [CCIR Report 563-3, 1986; Crane, 1988; Derr, 1972; Eklund and Wickerts, 1968; Flock, 1979; Hall, 1979; and Parl, 1979]; however, sources are in general agreement with the following:

- b - a constant, typically 0.033;
- k - wavenumber, $2\pi/\lambda$;
- m - the slope of the spectrum;
- C_N^2 - The structure constant.

C_N^2 indicates the variability of amplitude fluctuations of the refractive index. Its value, valid below 2 km, ranges from 10^{-15} to 10^{-10} ($m^{-2/3}$) [Boithias, 1987, p. 108; Hall, 1979, p. 44]. Several formulas are available [Monsen, et al., 1983, p. 2-19; Gerlach, 1984, p. 49]:

$$C_N^2 = 8 \times 10^{-14} h^{-1/3} \exp(-h/3200) \quad (C-2a)$$

for $m = 11/3$, and, more generally,

$$\{N(X_1) - N(X_2)\}^2 = C_N^2 r^{2/3}. \quad (C-2b)$$

In expression (C-2a), h is the height above the earth's surface to a scatterer in meters, and in expression (C-2b) " N is the fluctuating refractive index at two points X_1 and X_2 separated by distance r " [Gerlach, 1984, p. 49]. VanZandt, et al. [1978] explore the structure function from a practical perspective.

The spectrum slope, m , is a figure of considerable uncertainty, values of which have engendered much of the controversy in predicting troposcatter paths. An often used figure of $11/3$ originates by assuming an isotropic homogeneous atmosphere applied to the turbulence theories of Kolmogorov and Obukhov [Fehlhaber, 1968, p. 38; Lane, 1968, p. 10].¹ However, Rice, et al. [1967, p. IV-7] note shortcomings in the use of the $11/3$ spectrum, although Parl [1979] reaffirms otherwise. Most

¹Immediately apparent is the error in assuming isotropic scatterers; however, ease of calculation forced this initial assumption and consequences were felt negligible. Note that Figure 27 more realistically shows anisotropic scattering.

realistically, Gjessing and McCormick [1974] show m as quite variable:

$$m = 40.6 + 708v^2 \quad (C-3)$$

where

$$v^2 = g/T(dT/dz + g/c_p). \quad (C-4)$$

Here v^2 is the Väisälä-Brunt frequency used to designate atmospheric stability, g indicates gravity, T shows temperature, dT/dz is the temperature lapse rate, and c_p is specific heat at constant pressure. On several links in Norway and Denmark, Gjessing and McCormick's findings relate values ranging from about $5/3$ to $20/3$ with a mean near $11/3$. Similar findings are reported in Bolgiano [1958], du Castel [ed., 1965], Cox [1969], and Sarkar, Dutta, and Reddy [1983].

Referring again to Figure 15, a specific value defined by

$$k = (4\pi/\lambda)\sin(\theta/2) \quad (C-5)$$

is used (θ is the scattering angle). It is at this value (wavenumber) that the spectrum must be evaluated for troposcatter paths since it gives the "intensity of the vertical spectrum" at the operating

wavelength [Lane, 1968, p. 9; Ortwein, Hopkins, and Pohl, 1961, p. 789].

Finally, a summary of the features of the spectrum is provided:

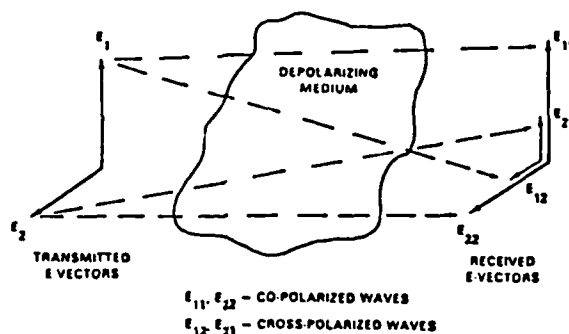
1. Variability of the form with time (hour to hour and season) especially at low heights of the common volume.
2. Variability of the slope of the spectrum with wave-number range within the inertial subrange.
3. Increased constancy with height [du Castel, ed., 1965, p. 73].

Thus, *variability* is the key term describing atmospheric turbulence.

APPENDIX D

DEPOLARIZATION

The depolarization mechanism, as depicted in Figure D1, results in received, copolarized (E_{11} and E_{22}) and crosspolarized waves (E_{21} and E_{12}). "The



Source: Ippolito, L.J. Jr. *Radiowave Propagation in Satellite Communications*. New York: Van Nostrand Reinhold Co., 1986, p. 94.

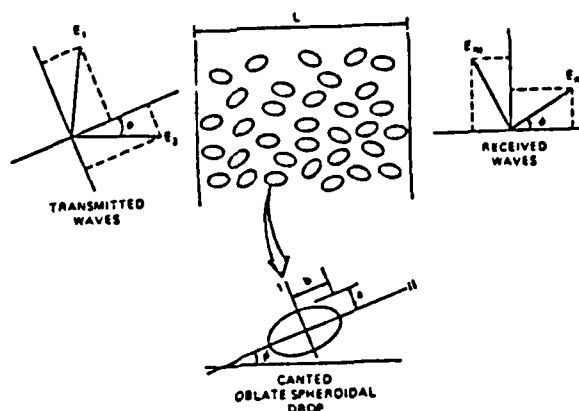
Figure D1: The Depolarization Mechanism

ratio of the power of the wanted or copolarized wave to the power of the unwanted or crosspolarized wave" is termed cross polarization discrimination (XPD) [Flock, 1987, p. 4-42]:

$$\text{XPD} = 20 \log (E_{11}/E_{12}) \quad (\text{dB}) \quad (\text{D-1})$$

This equation is applicable to the other fields (E_{22} and E_{21}) in a similar manner. Additionally, higher XPD values (such as 25 dB) are desirable.

Figure D2 shows depolarization due to rain. Drop canting results from wind forces and "normally

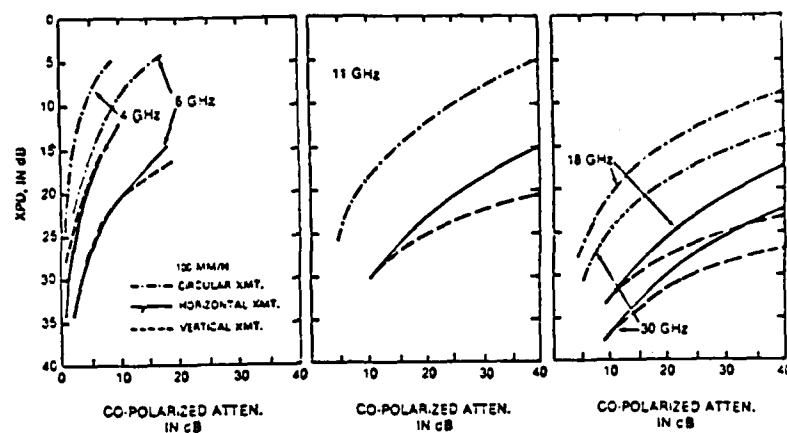


Source: Ippolito, L.J. Jr. *Radiowave Propagation in Satellite Communications*. New York: Van Nostrand Reinhold Co., 1986, p. 96.

Figure D2: Depolarization Due to Rain

exhibit a distribution of canting angles" [Flock, 1987, p. 4-43]. Basically, the received waves consist of vertical and horizontal components (co- and cross- polarized waves) which sum to give E_{R1} and E_{R11} . Rain depolarization produces both attenuation and phase differences which depend on droplet size and shape. Furthermore, at decreasing frequencies (below 10 GHz) depolarization remains a factor as the phase difference remains high at low frequencies [Flock, 1987, p. 9-33].

Figure D3 shows XPD changes on earth-space paths with respect to copolarized attenuation due to rain. Notably, troposcatter links, which normally



Source: Ippolito, L.J. Jr. *Radiowave Propagation in Satellite Communications*. New York: Van Nostrand Reinhold Co., 1986, p. 99.

Figure D3: Depolarization Effects Due to Rain

operate below 5 GHz, will experience negligible XPD degradation.

APPENDIX E

THE REFLECTION COEFFICIENT

Determining the reflection coefficient, ρ , for tropospheric layers offers unique complexities due to variability of the atmosphere. Rather than presenting a smooth, flat surface, atmospheric layers exhibit dimensional irregularity and constant motion which compound normally simple calculations.

It can be shown that for an abrupt change in the atmosphere's refractive index, Δn , Fresnel's equation for reflection can be reduced to

$$\rho_0 = \Delta n / 2\alpha^2 \quad (\text{E-1})$$

for $2\Delta n \ll \alpha^2$ [Picquenard, 1974, p. 49]. Here, α is the grazing angle. More often, however, layers can be formed by less abrupt changes in refractivity and ρ_0 will be reduced by a *form function*,

$$F_\rho = \sin(4\pi\alpha\Delta h/\lambda) / 4\pi\alpha\Delta h/\lambda, \quad (\text{E-2})$$

provided $\Delta n \ll \pi\alpha^3\Delta h/\lambda$ and layer thickness $\ll \lambda/(4\alpha)$ [Hall, 1979, p. 39]. This gives:

$$\rho = \rho_0 F_\rho \quad (\text{E-3})$$

which is normally much less than unity [Hall and Barclay, 1989, p. 168].

Exceptionally important for purposes of differentiating troposcatter propagation mechanisms: "[b]ecause the magnitude of F_p is inversely proportional to $\Delta h/\lambda$, layer reflection is not of much consequence above UHF" [Hall, 1979, p. 40, emphasis mine]. Finally, Hall [1979, p. 40] shows that for troposcatter paths where there are a number of reflecting surfaces, N:

$$\rho = \{2N/\alpha\lambda \int \rho_o^2 F_p^2 l_2^2 \alpha^2 dV\}^{1/2} \quad (E-4)$$

where l_2 is the shorter length of the Fresnel ellipsoid illuminating the reflecting layer and V is the common volume.

APPENDIX F

CLIMATIC REGIONS

Troposcatter link performance varies considerably in different parts of the world. For this reason, some prediction techniques have divided the planet into various regions depending on climatology. From there, analysis is made for the specific region in question. Analysis in *NBS Tech Note 101* [Rice, et al, 1967] provided the first consolidated effort to categorize according to climate. Since then, changes have been made as empirical studies demanded modification. Both *Military Handbook, Facility Design for Tropospheric Scatter (Transhorizon Microwave System Design)* [1977] and CCIR Report 238-5 [CCIR, 1986] provide agreement on a current division scheme. The following bullet summary is extracted directly from the CCIR report, all divisions are by latitude in both hemispheres unless indicated otherwise.

1. EQUITORIAL:
 - Between 10° N and 10° S.
 - Slightly varying high temperature.
 - Monotonous heavy rain.
 - Permanent humidity.
2. CONTINENTAL SUB-TROPICAL:
 - Between 10° and 20° .
 - Dry winter.
 - Rainy summer.

3. MARITIME SUB-TROPICAL:
 - Between 10° and 20° .
 - Lowland areas near the sea.
 - Influenced by the monsoon.
4. DESERT:
 - Two land areas roughly between 20° and 30° .
 - Yearly, semi-arid conditions.
 - Extreme diurnal and seasonal temperature variations.
5. MEDITERRANEAN:
 - On desert zone fringes, near the sea, between 30° and 40° .
 - Fairly high temperature.
 - Marked influence by the sea.
 - Nearly no rain in summer months.
6. CONTINENTAL TEMPERATE:
 - Between 30° and 60° .
 - Pronounced diurnal and seasonal variations.
 - Western portion:
 - Strongly influenced by sea.
 - More moderate temperature variations.
 - Year round rain.
 - Eastern portion:
 - More temperature variation.
 - Less rain in winter.
 - Can include Japan.
- 7a. MARITIME TEMPERATE, OVERLAND:
 - Between 30° and 60° where prevailing winds are unobstructed by mountains bringing moist maritime air inland.
 - Typical regions:
 - U.K.
 - North American west coast.
 - European west coast.
 - African northwest coast.
- 7b. MARITIME TEMPERATE, OVERSEA:
 - Similar to 7a, focus on costal and oversea areas.
 - Propagation path oversea although terminals inland.
8. POLAR:
 - Between 60° to poles.
 - Low temperature.
 - Low humidity.